A FAST-TIME STUDY ON INCREASING THE CAPACITY OF CONTINUOUS DESCENT APPROACHES THROUGH AIRBORNE PRECISION SPACING

A Thesis

by

LESLEY ANNE WEITZ

Submitted to the Office of Graduate Studies of
Texas A&M University
in partial fulfillment of the requirements for the degree of

MASTER OF SCIENCE

August 2005

Major Subject: Aerospace Engineering

A FAST-TIME STUDY ON INCREASING THE CAPACITY OF CONTINUOUS DESCENT APPROACHES THROUGH AIRBORNE PRECISION SPACING

A Thesis

by

LESLEY ANNE WEITZ

Submitted to the Office of Graduate Studies of
Texas A&M University
in partial fulfillment of the requirements for the degree of

MASTER OF SCIENCE

Approved by:

Chair of Committee,	John E. Hurtado
Committee Members,	John L. Junkins
	Srinivas R. Vadali
	Aniruddha Datta
Head of Department,	Helen L. Reed

August 2005

Major Subject: Aerospace Engineering

ABSTRACT

A Fast-time Study on Increasing the Capacity of
Continuous Descent Approaches Through
Airborne Precision Spacing. (August 2005)
Lesley Anne Weitz, B.S., The State University of New York at Buffalo
Chair of Advisory Committee: Dr. John E. Hurtado

Due to projected increases in air traffic, there are several research efforts underway to evaluate ways to safely increase the capacity of the National Airspace System (NAS), improve operational efficiency, and reduce aircraft noise. At NASA Langley Research Center (LaRC) in Hampton, Virginia, two parallel research efforts have focused on terminal area research: one is Airborne Precision Spacing (APS), and the other is the Quiet Aircraft Technologies (QAT) project. The APS objective is to increase terminal-area capacity without adversely affecting safety, whereas the QAT project objective is to develop noise- and fuel-efficient approach trajectories.

The APS project developed a cockpit tool, called Airborne Merging and Spacing for Terminal Arrivals (AMSTAR), that issues speed commands to aircraft to maintain desired spacing between aircraft pairs. The APS studies showed an ability to increase runway capacity; however, capacity increases may negatively impact noise and emission levels in airport areas. The QAT project created efficient Continuous Descent Approaches (CDAs), which showed reductions in aircraft ground noise and fuel consumption. Previous research has shown that CDA trajectories have adverse effects on runway capacity because aircraft must be spaced further apart at long distances from the runway to prevent separation losses at the runway threshold. To date, the APS and CDA concepts have been evaluated independently at LaRC.

In this study, three different approaches to combining APS and CDA operations were evaluated to determine the feasibility and benefits of combining these concepts. These methods combined AMSTAR with 3°-flight-path-angle-CDA approach routes, 3°-CDA routes with spoilers, and 2°-CDA routes without spoilers. Adding the use of spoilers allowed faster responses to large speed reductions issued by AMSTAR. This improvement was contrasted with the effects of a shallower flight-path angle for greater deceleration capabilities.

This research indicated that AMSTAR improved the performance of CDA operations, although full capacity improvements were not achieved. Whereas the 2°-CDA routes were expected to show the best results, the 3°-CDA case with spoilers showed the least variability in threshold spacing errors. All of the CDA routes were more noise, fuel, and time efficient than traditional step-descent routes that are commonly used today.

To Walter Pawlowski, who inspired me to become an engineer.

ACKNOWLEDGMENTS

First and foremost, I would like to thank my advisor, Dr. John E. Hurtado, for his encouragement and support over the last two years. I look forward to working with him over the next several years while I pursue a doctoral degree. Thank you to my committee members: Dr. John L. Junkins, Dr. Srinivas R. Vadali, and Dr. Aniruddha Datta. I am grateful to the National Science Foundation Graduate Research Fellowship and the Zonta International Amelia Earhart Fellowship for their financial support of this research. Any opinions, findings, conclusions, or recommendations expressed in this document are those of the author and do not necessarily reflect the views of the National Science Foundation.

I would like to acknowledge my colleagues and mentors at the NASA Langley Research Center for their much-appreciated support and patience, specifically Terry Abbott, Mark Ballin, Dr. Bryan Barmore, Jim Hull, Dr. Karthik Krishnamurthy (a fellow Aggie), Tod Lewis, Rosa Oseguera-Lohr (another fellow Aggie), and Dave Williams. I especially want to thank Frank Bussink for the time that he dedicated to reading this document and all of the support that he has given me over the past year. Thanks to Dr. Robert Lindberg and the National Institute of Aerospace (NIA) for facilitating my visits to Langley. Special thanks to Jacco Hoekstra, at the NLR in the Netherlands, for permission to use his amazing research tool, TMX.

This would not be complete without thanking my colleagues from Moog Inc. who took the time to write many graduate-school and fellowship recommendation letters: Brian Barker, Jim Czodli, Dudley Humphreys, Joe McKlemurry (Lockheed Martin), Jim Silliman, and Sal Socci. I would like to acknowledge my mentors at the University at Buffalo, Drs. John Crassidis, D. Joseph Mook, and Tarunraj Singh, for their encouragement and guidance in selecting a graduate institution. Special thanks to

Dr. Singh for the many recommendation letters that he has written for me over the years.

Thanks to my two best friends, Stephanie (Rabczak) Guize and Devonie (Vona) Lorigo, who have been huge parts of my life. I would like to thank all of my friends at A&M that enhanced my graduate-school experience: Roshawn Bowers, Eddie Caicedo, Steve Chambers, Thomas Elsom, Paul Gesting, Bjoern Kiefer, Tucker Lavin, Joe O'Neil, Josh O'Neil, Gary Seidel, Andy Sinclair, Mike Sovinsky, Theresa Spaeth, and Brian Wood.

Finally, I would like to acknowledge my loving family: my parents, William and Debra Weitz, and my brother, Jeffrey Weitz. Their support has been much appreciated.

TABLE OF CONTENTS

CHAPTER		Page
I	INTRODUCTION	1
II	CURRENT AIR TRAFFIC CONTROL APPROACH PROCEDURES	4
III	AIRBORNE PRECISION SPACING	7
	A. Distance-based Spacing	9
	B. Time-based Spacing	10
	1. ATAAS	12
	2. AMSTAR	14
IV	NOISE AND FUEL EFFICIENT APPROACHES	19
	A. Continuous Descent Approaches	19
	B. Low Noise Guidance System	22
V	EXPERIMENT DESIGN	25
	A. Baseline Simulations	25
	B. Research Approaches	26
	C. Performance Metrics	28
	D. Research Airspace	30
	E. Experiment Design Criteria and Assumptions	31
	F. Research-Scenario Summary	34
VI	SIMULATION ENVIRONMENT	35
	A. Flight Research Simulation System	35
	1. TMX Aircraft Performance Models	35
	2. Integration of AMSTAR in TMX	36
	3. CDA Trajectories in TMX and AMSTAR	37
	4. Model Improvements	38
	5. Spoiler Model	47
	B. Scenario Generator	48
VII	NOMINAL TRAJECTORIES	50

CHAPTER Page

A. Nominal Altitude and Speed Profiles 50
B. Nominal Transit Times 53
C. Nominal Fuel Consumption 53

VIII BASELINE RESULTS FOR STEP DESCENTS WITH AMSTAR 55

A. ±15-second RTA Error Case 55
1. Spacing Errors and Schedule Deviation 55
2. Losses of Separation 59
3. Speed Changes 63
4. Transit Times 65
5. Fuel Consumption 66
B. ±60-second RTA Error Case 68
1. Spacing Errors and Schedule Deviation 68
2. Losses of Separation 71
3. Speed Changes 73
4. Transit Times 75
5. Fuel Consumption 76
C. Summary of Results for Step Descents with AMSTAR . . . 76

IX BASELINE RESULTS FOR 3°-CDAS WITHOUT AMSTAR . . 78

A. ±15-second-RTA Error Case 78
1. Spacing Errors and Schedule Deviation 78
2. Losses of Separation 79
B. ±60-second-RTA Error Case 87
1. Spacing Errors and Schedule Deviation 87
2. Losses of Separation 88
C. Summary of Results for 3°-CDAs without AMSTAR 89

X APPROACHES TO COMBINING APS AND CDAS 91

A. 3°-CDAs with AMSTAR 91
1. ±15-second RTA Error Case 91
2. ±60-second RTA Error Case 103
3. Summary of Results for the 3°-CDAs with AMSTAR . 106
B. 3°-CDAs with AMSTAR and Spoilers 108
1. ±15-second RTA Error Case 108
2. ±60-second RTA Error Case 115
3. Summary of Results for the 3°-CDAs with AMSTAR and Spoilers 118

CHAPTER Page

C. 2°-CDAs with AMSTAR 119
1. ±15-second RTA Error Case 119
2. ±60-second RTA Error Case 128
3. Summary of Results for the 2°-CDAs with AMSTAR . 131

XI DISCUSSION OF RESULTS 132

XII CONCLUSIONS AND FUTURE WORK 138

REFERENCES 140

APPENDIX A 143

APPENDIX B 144

VITA 146

LIST OF TABLES

TABLE		Page
I	Flap and Gear Constraints for Experimental Routes.	47
II	Nominal Transit Times.	53
III	Mean Fuel Consumption for Nominal Trajectories.	54
IV	Spacing Errors for Step Descents with AMSTAR (±15-second Case).	59
V	Minimum Lateral Separation for Aircraft with 3-second LoS.	61
VI	Fuel Consumption for Step Descents with AMSTAR (±15-second Case).	67
VII	Spacing Errors for Step Descents with AMSTAR (±60-second Case).	71
VIII	Fuel Consumption for Step Descents with AMSTAR (±60-second Case).	77
IX	Aircraft That Lost Separation for More than 10 seconds.	81
X	Spacing Errors and LoS for 100-second Metering-Fix Spacing (±15-second Case).	85
XI	Comparison of Fix Spacing for ±15-second-RTA-Error Case.	86
XII	Spacing Errors and LoS for 100-second Metering-Fix Spacing (±60-second Case).	89
XIII	Fix-Spacing Comparison for ±60-second-RTA-Error Case.	90
XIV	Spacing Errors for 3°-CDAs with AMSTAR (±15-second Case).	94
XV	Fuel Consumption for 3°-CDAs with AMSTAR (±15-second Case).	102
XVI	Spacing Errors for 3°-CDAs with AMSTAR (±60-second Case).	105
XVII	Fuel Consumption for 3°-CDAs with AMSTAR (±60-second Case).	107

TABLE Page

XVIII Spacing Errors for 3°-CDAs with AMSTAR and Spoilers (±15-second Case). 109

XIX Fuel Consumption for 3°-CDAs with AMSTAR and Spoilers (±15-second Case). 114

XX Spacing Errors for 3°-CDAs with AMSTAR and Spoilers (±60-second Case). 117

XXI Fuel Consumption for 3°-CDAs with AMSTAR and Spoilers (±60-second Case). 118

XXII Spacing Errors for 2°-CDAs with AMSTAR (±15-second Case). . . . 121

XXIII Fuel Consumption for 2°-CDAs with AMSTAR (±15-second Case). . 127

XXIV Spacing Errors for 2°-CDAs with AMSTAR (±60-second Case). . . . 129

XXV Fuel Consumption for 2°-CDAs with AMSTAR (±60-second Case). . 131

XXVI Comparison of Spacing Errors and Standard Deviations. 133

XXVII Comparison of Separation Losses. 134

XXVIII Comparison of AMSTAR-Induced Speed Changes. 136

XXIX Comparison of Fuel Consumption Means and Standard Deviations. . 137

LIST OF FIGURES

FIGURE		Page
1	Normal arrival routes and possible path changes.	5
2	Effect of capacity increase on mean delay.	8
3	Typical and reduced-variability spacing error distributions.	9
4	Time-delay spacing concept	11
5	Speed control law.	12
6	AMSTAR range-error filtering.	15
7	AMSTAR operational example.	16
8	Comparison of CDAs and step descents.	20
9	LNG altitude and speed profiles.	23
10	Three approaches to combining AMSTAR and CDA operations.	27
11	Expected correlation between noise efficiency and capacity.	28
12	DFW TRACON.	31
13	TMX and FastWin comparison prior to model improvements (3°-CDA).	39
14	TMX and FastWin comparison after model improvements (3°-CDA).	43
15	FMS-type comparison	44
16	TMX and FastWin comparison prior to model improvements (step descents).	45
17	TMX and FastWin comparison after model improvements (step descents).	46
18	Nominal Bambe altitude and speed profiles.	51

FIGURE Page

19 Nominal Fever altitude and speed profiles. 51

20 Nominal Howdy altitude and speed profiles. 52

21 Differences in CDA altitudes compared to step-descent altitudes. . . 52

22 ±15-second-RTA-error distribution. 56

23 ±15-second-RTA-error distribution over 40 simulations. 56

24 Spacing errors and schedule deviation for the step descents with AMSTAR (±15-second case). 57

25 Mean spacing errors for the step descents with AMSTAR (±15-second case). 58

26 Mean schedule deviation for the step descents with AMSTAR (±15-second case). 60

27 Losses of separation for the step descents with AMSTAR (±15-second case). 61

28 Maximum time in LoS for the step descents with AMSTAR (±15-second case). 62

29 Additional speed changes for the step descents with AMSTAR (±15-second case). 63

30 Speed changes for the 57th and 80th aircraft flying step descents with AMSTAR (±15-second case). 64

31 Mean additional speed changes for the step descents with AMSTAR (±15-second case). 65

32 Mean transit-time differences for the step descents with AMSTAR (±15-second case). 66

33 Mean fuel consumption for the step descents with AMSTAR (±15-second case). 67

34 ±60-second-RTA-error distribution. 68

FIGURE Page

35 ±60-second-RTA-error distribution over 40 simulations. 69

36 Spacing errors and schedule deviation for the step descents with AMSTAR (±60-second case). 70

37 Mean spacing errors for the step descents with AMSTAR (±60-second case). 70

38 Losses of separation for the step descents with AMSTAR (±60-second case). 72

39 Maximum time in LoS for the step descents with AMSTAR (±60-second case). 72

40 Speed time histories for aircraft that lost separation flying step descents with AMSTAR. 74

41 Mean additional speed changes for the step descents with AMSTAR (±60-second case). 75

42 Mean transit-time differences for the step descents with AMSTAR (±60-second case). 76

43 Spacing errors and schedule deviation for the 3°-CDAs without AMSTAR (±15-second case). 79

44 Losses of separation for the 3°-CDAs without AMSTAR (±15-second case). 80

45 Relationship between losses of separation and fix spacing. 82

46 Maximum time in LoS for the 3°-CDAs without AMSTAR (±15-second case). 83

47 Minimum distance relationship to LoS time and threshold spacing. . 84

48 Spacing errors for the CDAs without AMSTAR (110-second spacing at fix). 87

49 Spacing errors and schedule deviation for the 3°-CDAs without AMSTAR (±60-second case). 88

FIGURE Page

50 Spacing errors and schedule deviation for the 3°-CDAs with AMSTAR (±15-second case). 92

51 Mean spacing errors for the 3°-CDAs with AMSTAR (±15-second case). 93

52 Mean schedule deviation for the 3°-CDAs with AMSTAR (±15-second case). 94

53 Losses of separation for the 3°-CDAs with AMSTAR (±15-second case). 95

54 Relationship between LoS time and the "expected" initial spacing when AMSTAR was used. 96

55 Maximum time in a LoS for the 3°-CDAs with AMSTAR (±15-second case). 97

56 Additional speed changes for the 3°-CDAs with AMSTAR (±15-second case). 97

57 Speed time-histories and speed change magnitudes for the 24th and 28th aircraft (3°-CDAs with AMSTAR). 98

58 Mean additional speed changes for the 3°-CDAs with AMSTAR (±15-second case). 100

59 Mean transit-time differences for the 3°-CDAs with AMSTAR (±15-second case). 100

60 Mean fuel consumption for the 3°-CDAs with AMSTAR (±15-second case). 101

61 Spacing errors and schedule deviation for the 3°-CDAs with AMSTAR (±60-second case). 103

62 Mean spacing errors for the 3°-CDAs with AMSTAR (±60-second case).104

63 Maximum time in a LoS for the 3°-CDAs with AMSTAR (±60-second case). 106

64 Spacing errors and schedule deviation for the 3°-CDAs with AMSTAR and spoilers (±15-second case). 109

FIGURE Page

65 Mean spacing errors for the 3°-CDAs with AMSTAR and spoilers (±15-second case). 110

66 Losses of separation for the 3°-CDAs with AMSTAR and spoilers (±15-seconds). 111

67 Total time that spoilers were used by each aircraft (±15-second case). 112

68 Speed time history of 45th aircraft. 113

69 Additional speed changes for the 3°-CDAs with AMSTAR and spoilers (±15-second case). 113

70 Spacing errors and schedule deviation for the 3°-CDAs with AMSTAR and spoilers (±60-second case). 115

71 Mean spacing errors for the 3°-CDAs with AMSTAR and spoilers (±60-second case). 116

72 Spacing errors and schedule deviation for the 2°-CDAs with AMSTAR (±15-second case). 120

73 Mean spacing errors for the 2°-CDAs with AMSTAR (±15-second case).121

74 Losses of separation for the 2°-CDAs with AMSTAR (±15-second case).122

75 Maximum time in a LoS for the 2°-CDAs with AMSTAR (±15-second case). 123

76 Additional speed changes for the 2°-CDAs with AMSTAR (±15-second case). 124

77 Speed time histories and speed-change magnitudes for the 52nd and the 66th aircraft (2°-CDAs with AMSTAR). 125

78 Mean additional speed changes for the 2°-CDAs with AMSTAR (±15-second case). 126

79 Mean transit-time differences for the 2°-CDAs with AMSTAR (±15-second case). 126

FIGURE Page

80 Spacing errors and schedule deviation for the 2°-CDAs with AMSTAR (±60-second case). 128

81 Mean spacing errors for the 2°-CDAs with AMSTAR (±60-second case).129

CHAPTER I

INTRODUCTION

Projected increases in air travel are placing strain on the National Airspace System (NAS)[1]. There are currently several government and industry efforts underway in the United States and Europe to examine ways to alleviate the pressure on the NAS, and some of the attention is on terminal-area operations. The capacity demand on major commercial airports is rapidly growing, even returning to, or exceeding, pre-September 11th levels [1]. The Federal Aviation Administration (FAA) has projected that several major hubs in the continental United States will be unable to meet capacity increases with their current operations. The global understanding is that without new Air Traffic Management (ATM) concepts, it will be difficult to safely meet future increases in air traffic. Building additional runways only is not a feasible solution due to high costs, construction time, space limitations, and environmental concerns.

Several research institutions are focusing on new terminal-area sequencing and merging concepts in order to safely increase runway arrival capacity. One such effort at the National Aeronautics and Space Administration (NASA) Langley Research Center (LaRC), is Airborne Precision Spacing (APS). The APS objective is to precisely space aircraft in terminal areas to reduce the variability in runway threshold[2] crossing times. This can be accomplished through the use of cockpit avionics tools that provide speed commands to aircraft that are following other aircraft in the approach sequence.

The journal model is *IEEE Transactions on Automatic Control*.

[1]The NAS is the common network of airspace, airports, navigation aids, and air traffic control equipment across the continental United States.

[2]The runway threshold is defined as the beginning of the runway that is available for landing.

With more accurate aircraft spacing, excess spacing buffers between aircraft can be safely reduced, thus increasing the runway capacity. As airport runways are expected to handle a higher volume of traffic however, aircraft noise becomes a concern for residents living in areas surrounding airports. Currently, noise restrictions are often placed on airports, which can limit daily operations.

New noise-efficient operations, such as Continuous Descent Approaches (CDAs), can significantly reduce the noise impact of landing aircraft by keeping aircraft at higher altitudes on approach to the airport and by reducing power during descent, thus alleviating some of the engine noise heard in residential areas. In addition, previous CDA research has shown the added benefit of fuel efficiency, which results in a reduction of aircraft emissions. Although CDAs are beneficial for noise and fuel savings, the uncertainties associated with these operations cause runway capacity to be sacrificed. CDA routes have been implemented at some airports during low-density traffic operations only. The Quiet Aircraft Technologies (QAT) project at NASA LaRC has been developing a tool to generate noise-optimal CDA trajectories that are aircraft-type specific. This tool was designed to improve CDA operations for both pilots and Air Traffic Controllers (ATC).

The objective of this thesis research has been to explore the feasibility and benefits of combining APS and CDA operations with the goal of improving airport capacity for quieter, more efficient terminal approaches. Fully retaining the benefits of both techniques was unachievable, but improvements were achieved in both capacity over current-day CDA operations and efficiency over traditional approach methods.

Chapters II, III, and IV will provide background on current ATC terminal-area procedures, APS concepts, and noise- and fuel-efficient descent methods, respectively. Chapter V discusses the experiment design, and Chapter VI describes the fast-time simulation environment. The nominal descent trajectories that were used for this

research are presented in Chapter VII. Chapters VIII, IX, and X present the fast-time simulation results. These results are discussed in Chapter XI, and conclusions and future work are summarized in Chapter XII. Commonly used acronyms are listed in Appendix A.

CHAPTER II

CURRENT AIR TRAFFIC CONTROL APPROACH PROCEDURES

Terminal-area-ATC towers are operated by both the FAA and non-federal organizations to provide adequate airborne separation to aircraft that are utilizing the airport. The primary ATC responsibility is to ensure sufficient runway separation between departing and arriving aircraft [2]. In addition to that responsibility, controllers also monitor and control airborne separation of departing and arriving aircraft, separate aircraft within those flows, and make the best use of available runways. Once an arriving aircraft enters a Terminal Radar Approach Control (TRACON) area[1], ATC must monitor that aircraft's spacing with surrounding aircraft along its route to the runway, while ensuring that the aircraft lands on schedule.

Late runway arrivals can severely impact efficient airport operation by affecting gate arrival times. Late arrivals at the gate can delay fuelers, baggage handlers, caterers, and ultimately other aircraft. To prevent late runway arrivals, arrival flow must be controlled.

Controllers have three methods to control separation and sequencing: lateral path changes, vertical (altitude) changes, and speed changes, which together are referred to as vectoring techniques [3]. Lateral path changes can be used to shorten or lengthen an aircraft's arrival route to position it in the desired location in the arrival flow. These changes are achieved by extending flight legs, cutting corners, flying holding patterns, and diverting aircraft to alternate runways. Common lateral-path-change methods are illustrated in Figure 1, where the solid lines represent the nominal approach routes, and the dashed lines depict possible path changes. Vertical

[1]The TRACON is a facility that uses radar to provide approach information to the air traffic control tower.

separation techniques are often used in combination with the aforementioned lateral techniques to ensure separation limits. However, speed increases and decreases are the most common method of controlling flow.

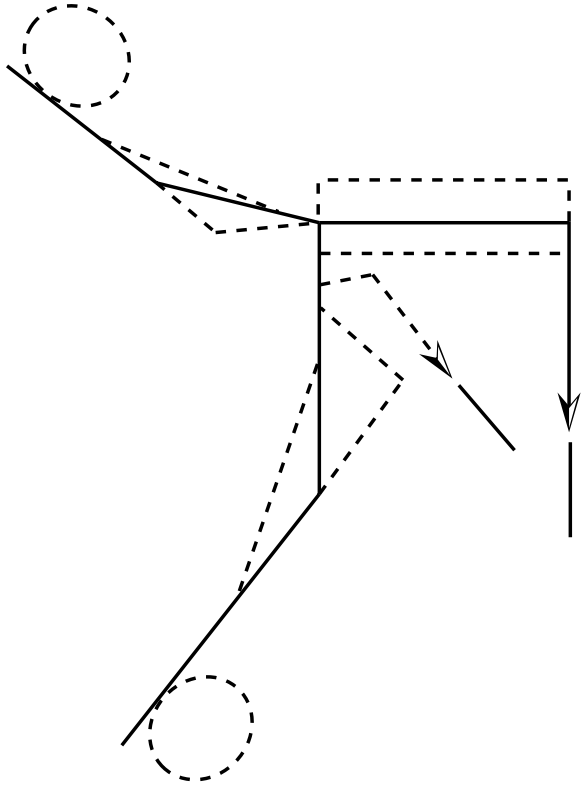

Fig. 1. Normal arrival routes and possible path changes [3].

Using vectoring techniques to control arrival flow poses two problems. Firstly, before vectoring techniques can be employed, meteorological conditions, aircraft performance limitations, and surrounding aircraft states must be taken into consideration. Vectoring an aircraft off of its nominal lateral path will require additional changes to return the aircraft to the nominal path at an appropriate time. Secondly, vectoring techniques are usually less fuel and noise efficient than the nominal paths, and these changes add to the workload of both the flight crews and the controllers. Us-

ing these techniques to achieve optimal arrival flow is highly dependent on controller experience.

Merging arrival streams is one of the most challenging ATC tasks. Controllers must understand wind-field effects and the performance characteristics of the different merging aircraft. Some decision support tools have been developed to aid controllers in managing merge operations; however, these tools are limited by current radar-surveillance systems.

Currently, controllers need years of experience to become efficient at merging and spacing aircraft in terminal areas. New ATM methods, such as APS, can assist controllers by providing them with the necessary tools to optimally and safely space aircraft in terminal areas.

CHAPTER III

AIRBORNE PRECISION SPACING

NASA LaRC has been researching APS, which is a part of the Distributed Air/Ground Traffic Management (DAG-TM) concept. The DAG-TM goal is to distribute decision making and increase collaboration between airborne and ground-based resources for more efficient aircraft operation throughout all phases of flight. Recent technological advances in communication, navigation, and surveillance (CNS) systems have made this goal possible. The FAA is developing standards for the Automatic Dependent Surveillance-Broadcast (ADS-B) system, which broadcasts an aircraft's current position (latitude, longitude, and altitude), velocity, and possibly other information. Other ADS-B equipped aircraft and ground-based resources may receive this data for a variety of applications [4]. ADS-B enables new and innovative flight-operation concepts, and LaRC has used ADS-B to develop airborne systems that help increase terminal area capacity through precise approach spacing.

Research has shown that a small increase in runway throughput[1] can have a significant effect on mean delay time (Figure 2) [5]. In the APS concept, aircraft in terminal areas will space themselves with an assigned lead aircraft by using cockpit systems that enable precision spacing. This concept is also known as self-spacing.

NASA has been evaluating in-trail[2] self-spacing in terminal areas since the 1970's. Accurate self-spacing can reduce the variability of threshold spacing errors, which are defined as the differences in actual spacing between aircraft pairs and the desired

[1]Runway throughput is defined as the maximum number of arrivals that a runway can accept based upon inter-aircraft spacing, and it can be measured in terms of aircraft per hour. APS aims to increase throughput through an increased arrival capacity.

[2]In-trail spacing is spacing along a common path, i.e., all aircraft are flying the same lateral route to the runway.

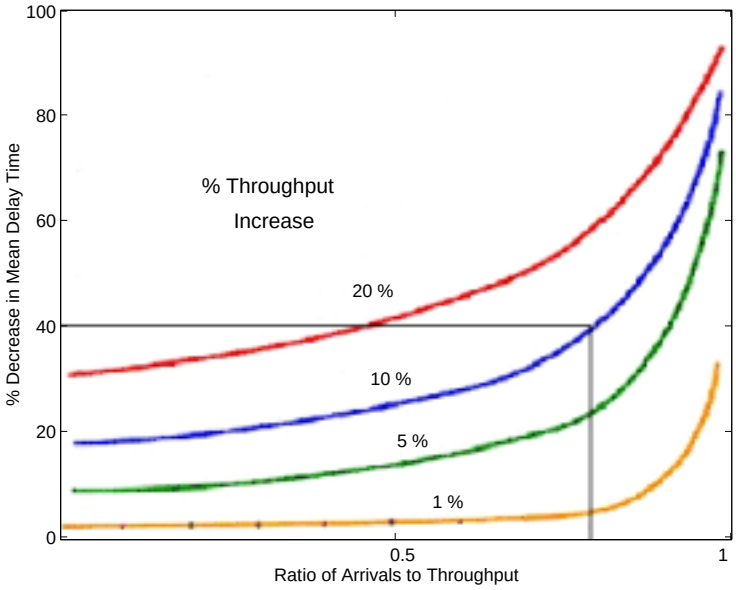

Fig. 2. Effect of capacity increase on mean delay. The ratio of arrivals to throughput is a measure of how many aircraft are landing on a runway relative to the total throughput. A ratio of 0.5 indicates that the runway is accepting only half of the possible arrivals [5].

spacing [6]. A positive spacing error indicates that the spacing between an aircraft pair was greater than desired, whereas a negative spacing error indicates that an aircraft pair was too close. If a trailing aircraft is too close to its lead aircraft, it may violate wake-vortex minimum-separation standards and it will be directed to leave the approach sequence to reenter at another point in the arrival pattern. Figure 3 compares a typical spacing-error distribution to a reduced-variability distribution. The mean of the spacing-error distribution will be positive due to additional spacing buffers between aircraft that are used to prevent separation losses. If the variability of the runway spacing error can be reduced, excess spacing buffers between aircraft pairs can be decreased, and the runway capacity will increase. Therefore, the maximum capacity of a runway is determined by both the maximum number of aircraft that

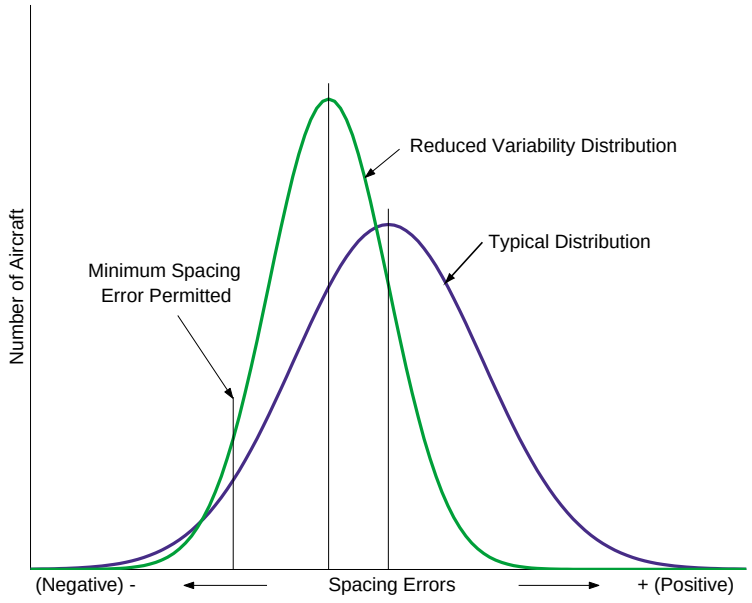

Fig. 3. Typical and reduced-variability spacing error distributions. The minimum spacing error permitted is a measure of wake-vortex minimum-separation limits.

can leave and reenter the arrival stream without resulting in schedule delays and the variability of the threshold spacing errors.

Precision self-spacing research includes distance- and time-based spacing concepts. In these concepts, aircraft maintain specific distance- or time-based spacing with lead aircraft. NASA has previously researched distance-based spacing concepts, however time-based spacing is the foundation of the APS concept.

A. Distance-based Spacing

The fixed-distance concept is the simplest in-trail spacing concept, where each aircraft in the approach sequence maintains a constant distance behind its lead aircraft [6]. However, when the lead aircraft begins to decelerate for its runway approach, the

trailing aircraft must also decrease its speed to match that of the lead aircraft. This can be fuel inefficient and noisy for long sequences of aircraft. When there are a mix of aircraft types in the approach, dissimilar approach speeds can lead to instabilities or create an accordion-like effect. The fixed-distance concept can be improved by incorporating speed scheduling, where speed constraints are satisfied at prescribed distances from the runway threshold. In the speed-scheduling concept, the spacing between aircraft at the original merge point is carefully designed so that although the interspacing between aircraft is compressed as the runway draws near, the spacing at the runway threshold will not exceed minimum wake-vortex separation standards.

B. Time-based Spacing

In the time-delay or time-history spacing concept, all in-trail aircraft fly the exact same speed profile to maintain a desired time-based spacing between aircraft. Figure 4 illustrates this concept for 90-second spacing between an aircraft pair, where speed histories are shown for both the lead and the trailing aircraft. The trailing-aircraft speed is less than the lead aircraft's speed, thus the trailing aircraft does not travel the same distance as the lead in the same amount of time. This will result in a positive spacing error between the two aircraft, which indicates that the pair-spacing is greater than desired. To decrease the spacing error, the trailing aircraft should increase its speed appropriately.

NASA LaRC has developed a closed-loop control law that is based upon the time-delay spacing concept, but is an implementation of a *nominal speed profile* technique. This control law, shown in Figure 5, was designed to generate speed commands for trailing aircraft to reduce spacing errors with their lead aircraft [6]. Two of the inputs to the control law are the trailing aircraft distance to the runway threshold

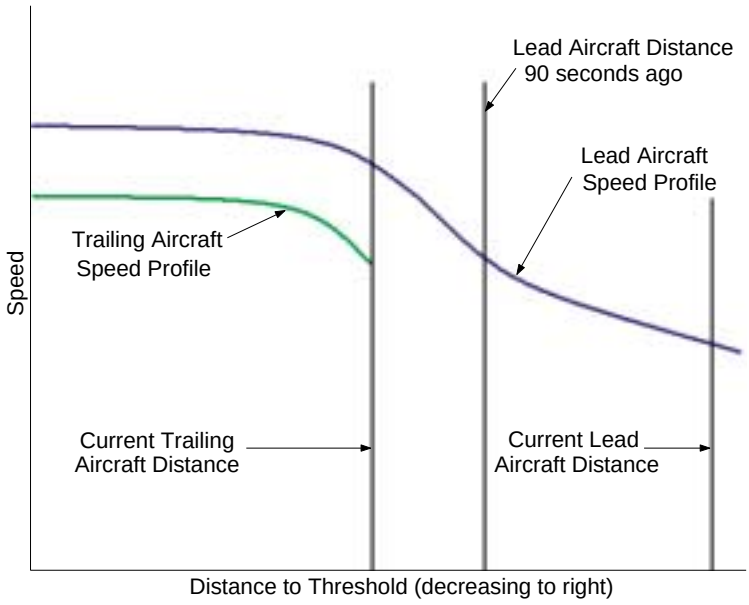

Fig. 4. Time-delay spacing concept. This example is for a 90-second desired spacing.

and the leading aircraft distance to the threshold at the goal-time, where the goal-time is the desired time-based spacing between the two aircraft. For example, if a 90-second spacing is desired between an aircraft pair, the leading aircraft distance at the goal-time would be the distance of the leading aircraft 90 seconds in the past. The difference in the distances, also called the range error, is multiplied by the gain, G1, which was set equal to 2.5 inverse seconds. The third input to the control law is the profile ground speed, which is calculated from a pre-defined nominal speed profile and wind-field information. This input limits the speed error to prevent excessive acceleration or deceleration; research at LaRC has limited the speed commands to $\pm 10\%$ of the nominal profile. The speed error is added to the profile ground speed, and the control law output is the trailing-aircraft speed command. This control law forms the basis of two precision spacing tools developed at NASA LaRC, which are ATAAS and AMSTAR.

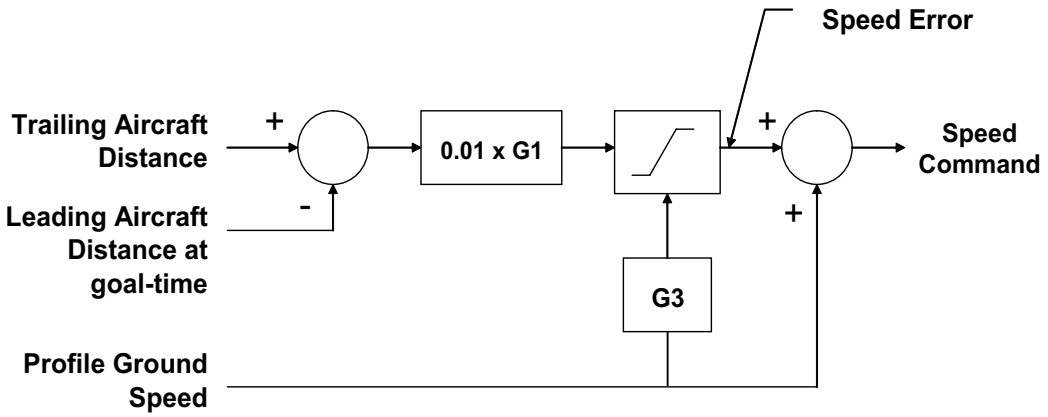

Fig. 5. Speed control law.

1. ATAAS

NASA LaRC developed a cockpit avionics system called the Advanced Terminal Area Approach Spacing (ATAAS) tool to enable precise in-trail spacing in terminal areas. ATAAS uses the control law, shown in Figure 5, to precisely space aircraft pairs along a common lateral path to the runway. Standard Terminal Arrival Routes (STARs), which are similar to approach routes that are in use today, have both altitude and speed constraints defined at specific distances to the runway. These STARs were used as a basis to create the nominal speed profiles that are used in ATAAS, though aircraft using the tool are not limited to these specific routes. All aircraft using ATAAS must have the capability to fly the common profiles. If a lead aircraft is not trailing another aircraft, ATAAS will command the speed of the nominal speed profile. ATAAS uses the speed control law to precisely space aircraft, but it is also able to compensate for dissimilar final approach speeds[3] and to determine if minimum in-trail separation

[3]The final approach speed is the speed that an aircraft maintains during the final segment of the approach and is the planned final, stable speed. These speeds are dependent on aircraft type and weight.

will be lost [6] .

ATAAS was designed to provide a constant speed segment prior to the threshold. At the point of deceleration to their final speeds, aircraft using ATAAS transition from actively spacing with their leads to flying their final approach speeds. ATAAS calculates the time from the final deceleration point to the runway for both the lead and trailing aircraft by using the nominal ground speed profiles. To account for dissimilar final approach speeds, ATAAS adjusts the desired time-based spacing interval that is used in the speed control law by using the difference in the time from the deceleration point to the runway for both the lead and trailing aircraft.

To determine if minimum separation limits will be breached, ATAAS evaluates distance and speed test conditions. The distance test condition evaluates the closure distance to minimum separation, and a speed test condition evaluates the rate of closure. If a loss of separation is likely to occur, the speed command is reset to a speed that will not result in a loss of separation.

NASA LaRC has evaluated ATAAS performance, operational procedures, and crew workload in both simulation and actual flight environments. ATAAS and proposed operational procedures were tested in a high-fidelity simulator with active-airline test pilots [7]. That study showed that the aircraft were able to meet the desired spacing intervals within one second when the speed-command tool was coupled to the autothrottles. The subject pilots rated the ATAAS workload as acceptable with no noticeable difference from standard procedures. A flight evaluation and demonstration of the ATAAS tool was conducted by NASA at the Chicago O'Hare International Airport, with three aircraft participating [8]. ATAAS evaluation included the ability to provide spacing in a vectored environment. Overall, the mean delivery precision was comparable to the simulation study, but with a higher standard deviation. Improvements in the accuracy of the ADS-B and wind forecast data, and

in the display and training for pilots were identified as factors that could improve the system's performance.

2. AMSTAR

The second-generation precision spacing tool developed by NASA LaRC is the Airborne Merging and Spacing for Terminal Arrivals (AMSTAR) system. AMSTAR is an enhanced version of ATAAS designed to precisely space aircraft that are flying dissimilar lateral routes prior to a merge point. AMSTAR's merge capability can increase the time for precision spacing to the entire terminal area, rather than just common approach paths, and it can enhance controller productivity by automatically merging arrival streams [9].

AMSTAR trajectories are generated using the STARs that were described in the previous section, though the STARs were modified to include lateral constraints to define a specific path to the runway. The altitude and speed constraints, or Trajectory Change Points (TCPs), in the STAR are used to create a four-dimensional trajectory. AMSTAR uses along-trajectory states and aircraft-to-aircraft trajectory states to calculate the relative spacing between aircraft pairs along the 4D trajectories [10].

The along-trajectory state calculation determines the location of both the leading and trailing aircraft relative to their own paths to the runway. Using the 4D trajectory defined by TCPs and current aircraft positions, AMSTAR determines both the lead and trailing aircraft estimated times of arrival (ETAs) at the runway threshold. The aircraft-to-aircraft trajectory state is the difference in the ETAs. This difference, along with the adjusted threshold crossing time for dissimilar final approach speeds, is the error term that is sent to the control law.

The AMSTAR error term is the difference between the aircraft-to-aircraft trajectory error and the desired spacing time, whereas the speed control law in ATAAS uses

the range error as an input. To create an equivalent range-error term, the AMSTAR time error is multiplied by the trailing aircraft's trajectory ground speed. This range error is then filtered as a function of the trailing aircraft's distance from the runway, and the filtered range error is the input to the control law. Range errors less than 0.5

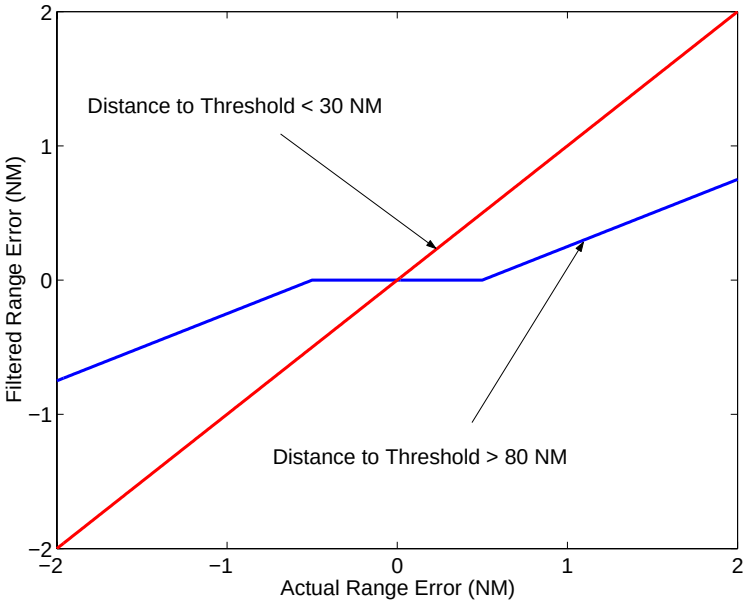

Fig. 6. AMSTAR range-error filtering.

nautical miles (NM) are disregarded if the trailing aircraft is more than 80 NM from the threshold, thus the notch value is equal to 0.5 NM. If the range error is greater than 0.5 NM, the gain is set to 0.5. If the aircraft is less than 30 NM to the threshold, no range errors are filtered (notch value is equal to 0.0) and the gain is set to 1.0. Between 30 and 80 NM to the threshold, the notch values and gain values are linearly interpolated. Based upon this filtering technique, the control law more aggressively spaces aircraft pairs as the trailing aircraft nears the threshold, and AMSTAR is most aggressive between 30 and 0 NM to the runway. These gains are illustrated in Figure 6 for the cases where the distance to the threshold is less than 30 NM and greater

than 80 NM.

To use the AMSTAR system, ATC would issue a lead-aircraft call sign and a desired spacing to an aircraft when it enters the terminal area. This information would be entered into the AMSTAR module in the flight computer. Using the ADS-B system, the lead aircraft's position, velocity, weight class, route, and final approach speed information would be broadcast and received by the trailing aircraft. AMSTAR would use this information to calculate the ETA at the runway for both the lead and trailing aircraft. Using the difference in ETAs and the desired spacing as the error term, AMSTAR would command an appropriate speed change to the trailing aircraft to decrease the spacing error. This concept is illustrated in Figure 7, where a 90-

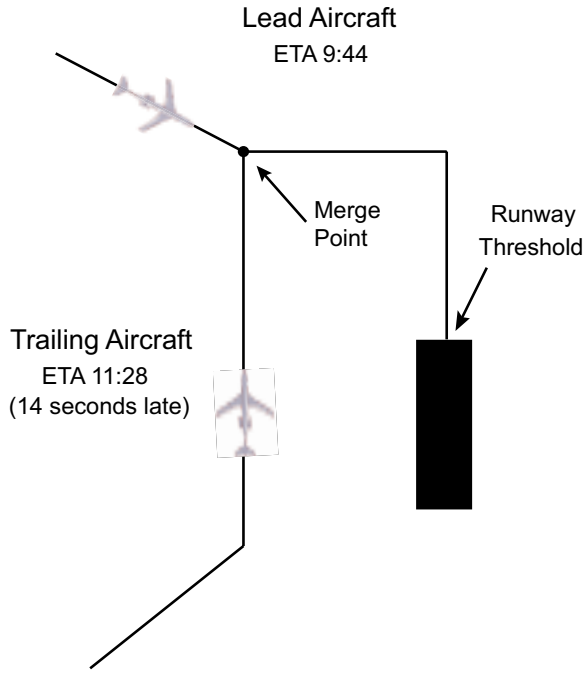

Fig. 7. AMSTAR operational example.

second spacing between the two aircraft is desired. In this case, the ETA of the trailing aircraft was 104 seconds later than the ETA of the lead aircraft, which is 14

seconds greater than the desired 90-second spacing. AMSTAR would issue a speed increase to the trailing aircraft to reduce the positive spacing error.

NASA LaRC has recently completed fast-time simulation studies to evaluate AMSTAR robustness and stability to variations in environmental and operational variables. That study evaluated AMSTAR performance for typical step-descent routes, which are approach methods commonly used today (step descents will be described in more detail in Chapter IV). The research variables in that study were:

- **ADS-B Range**

  The transmission range of ADS-B data was evaluated for its effect on pairwise spacing errors at the threshold. The research studied whether trailing aircraft could accurately space if state information from the lead aircraft was not received early in the approach.

- **Metering Accuracy**

  AMSTAR operations were started at the TRACON boundary. Aircraft were issued a time to enter the TRACON or a required time of arrival (RTA)[4]. AMSTAR performance was evaluated for RTA errors of ± 15 and ± 60 seconds.

- **Wind Prediction Error Effects**

  Wind prediction errors were evaluated to determine system performance when AMSTAR used incorrect wind fields to calculate ETAs at the runway threshold. A combination of wind magnitude and direction errors were studied.

[4]Aircraft entering a controlled airspace can be assigned RTAs to facilitate proper runway sequencing or optimized flow. The RTA error is a measure of how late or early an aircraft arrived relative to its assigned RTA.

- **Aircraft Type Mix**

  Different aircraft classes (small, large, heavy, and Boeing 757) were mixed to determine their combined effect on threshold spacing and system performance. These aircraft classes have differing performance characteristics and dissimilar final approach speeds. Different wake classes also have variable time-based spacing between aircraft pairs; therefore non-uniform spacing was also tested.

- **Merge Complexity**

  AMSTAR is designed for aircraft on merging routes; the effect of merge frequency was evaluated to determine its effect on system stability and performance.

The fast-time study demonstrated that AMSTAR and its onboard systems are highly robust to moderate variations in operational and environmental variables [11]. The system performance showed no noticeable impact for wind-direction prediction errors averaging up to 20 degrees or for RTA errors up to ± 60 seconds. AMSTAR operations may be affected by large errors in predicted wind magnitude, but errors of 10 knots only had a slight effect on AMSTAR performance. The spacing-error variability was greater for a mix of aircraft types in the arrival stream than when only a single aircraft type was used (Boeing 757s), but the magnitude of errors was still determined to be acceptable and did not impact overall system performance.

CHAPTER IV

NOISE AND FUEL EFFICIENT APPROACHES

Researchers have been evaluating ways to alleviate noise problems associated with increases in air traffic. Jet engine noise has led to restrictions on the number and type of operations at several airports. Continuous descent approaches are noise- and fuel-efficient terminal approaches that have been a research topic for many years. CDA research is being explored by several government, industry, and academic institutions because the concept is a proposed procedural change to reduce noise under the flight path.[1]

A. Continuous Descent Approaches

A continuous descent is defined as a descent with no level altitude segments, which are common in traditional step-descent approaches. The goal of developing a CDA is to keep the aircraft thrust as low as possible and the aircraft at higher altitudes for as long as possible. An ideal CDA allows the engines to be at idle thrust during most of the descent. Figure 8 shows an example of CDA altitude and speed profiles in comparison to a more traditional step-descent approach, which is the type of approach that was used in the AMSTAR fast-time simulation studies. The CDA in Figure 8 is called a 3°-CDA because of its 3° flight-path angle.[2]

Lower thrust, fuel consumption, and noise are a result of eliminating level altitude segments after the aircraft begins to descend; however, CDAs have diminished

[1]Procedural changes are ideal because no changes to the airframe or the engines are required for implementation.

[2]The flight-path angle is the angle between the flight-path and the ground. It can be found by calculating the inverse tangent of the change in vertical distance (altitude) divided by the change in lateral distance.

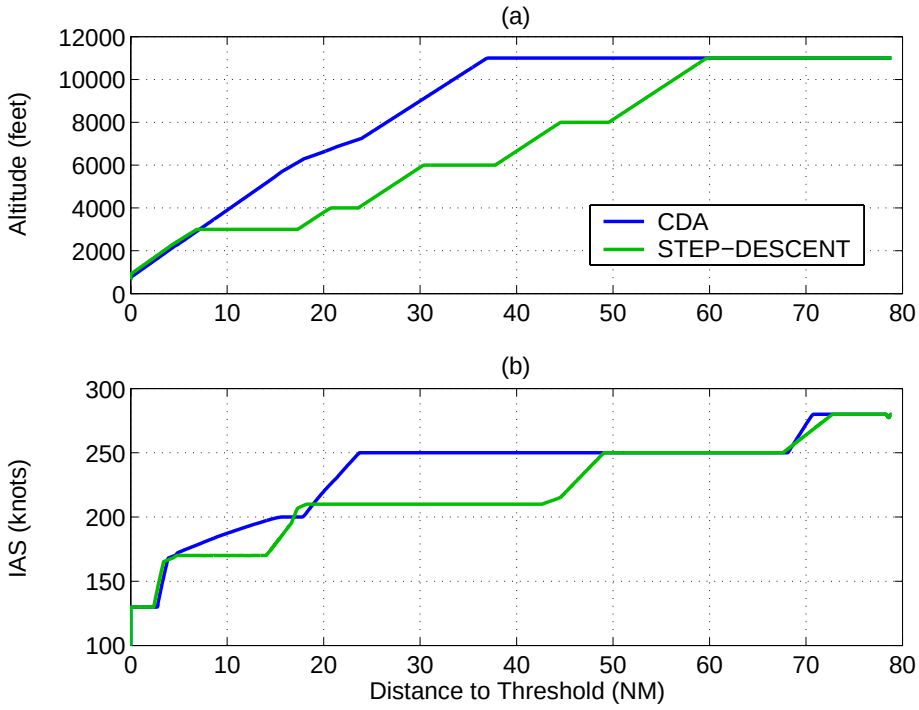

Fig. 8. Comparison of CDAs and step descents. Plots (a) and (b) show the altitude and speed profiles, respectively.

deceleration capabilities. Speed can be decreased by reducing power when aircraft are flying at level altitudes. In CDA operations, the thrust is near idle during most of the descent; therefore significant deceleration is achieved by using flaps. If the aircraft is above the speed threshold for different flap configurations, spoilers (speed brakes) can be used to increase drag. As a result of the inability to quickly decelerate during descent, aircraft flying CDAs are spaced further apart in terminal areas to ensure that separation limits are maintained throughout the approach and at the runway threshold. The adverse effect on runway capacity is one of the major setbacks of current CDA operations. In a study by Ho and Clarke [12], it was demonstrated that in the case of a Boeing 747-400 following a Boeing 737-300, an initial separation of up to three times the current-day separation was required to provide the minimum

separation at the runway threshold. Later research by Ren *et al.* proposed a modified descent approach where the aircraft does not reduce the thrust to idle when it begins to descend [13]. Combined with closed-loop control, i.e., descent-path tracking, their proposed descent approach can ensure 98% of current runway capacity.

While lower capacity is a disadvantage of CDA operations, the noise under the flight path is less than traditional descent methods. This is due to the differences in altitude between the CDA and step-descent trajectories, as well as lower thrust levels. Furthermore, CDA operations are more time efficient because aircraft remain at higher speeds during most of the approach in comparison to aircraft flying step descents.

CDA flight tests at Louisville International Airport have shown a 50% reduction in acoustic energy versus traditional approach routes, which is a noticeable difference to the human ear. A significant fuel savings was also shown, which over time would greatly benefit both the environment and the airlines [14]. CDA operations have been implemented at some airports, such as Heathrow in London and Schiphol in Amsterdam, during low-density traffic operations.

Other CDA research includes a study by Haraldsdottir *et al.*, which simulated CDA operations mixed with step descents to evaluate final approach spacing, runway throughput, time and fuel efficiency, and noise impacts [15]. These simulations included controller procedures, and results showed that CDAs could be used in high-density traffic conditions by controlling the scheduled times of arrival at a final approach fix in the terminal area. The simulated CDAs were optimized for time savings.

The Quiet Aircraft Technologies (QAT) project at NASA LaRC has been evaluating CDA operations with the objective to minimize the noise levels under the flight path. They have developed and implemented the Low Noise Guidance (LNG) system in a simulator environment with the goal of improving CDA operations for more

wide-spread use.

B. Low Noise Guidance System

The QAT project has designed the LNG system to predict and guide an aircraft along a lateral path to the runway using the most efficient vertical path, which minimizes power and maximizes altitude. QAT has defined two obstacles to implementing CDAs regularly in higher-density operations. One obstacle is the lack of a guidance tool to assist pilots in achieving the most optimal, fuel-efficient approach to the runway. The second obstacle is the lack of integration with current ATC procedures. The LNG system has been developed to offer solutions to these problems [16].

The LNG system was developed with consideration for future integration with Flight Management Systems (FMS). The LNG avionics system provides real-time, system-energy feedback to assist the pilot in maintaining the optimal energy along an ideal trajectory in the presence of winds and other environmental disturbances. To accommodate for real-time updates to the lateral path, the LNG system will output a new vertical path with new TCPs that are clearly indicated on cockpit displays. This feature was designed with consideration for current ATC operations where vectoring is used to maintain required separation limits between aircraft and to control flow. Because the altitudes and speeds of CDA operations are higher than the traditional approaches during much of the routes, more energy must be dissipated prior to landing. For this reason, some lateral routes may be unacceptable, or too short, for CDAs. The LNG system can calculate the desired and actual energy along lateral paths to the runway and determine whether the path is acceptable for the current states of the aircraft.

Each LNG trajectory is specific to the aircraft type (airframe and flap drag

characteristics), weight, lateral path, and wind field. The trajectories are designed for idle or near-idle descent from the top-of-descent (TOD) to a shallow deceleration segment. Following the deceleration segment, aircraft descend at a specified flight-path angle to a 3° angle to intercept the Instrument Landing System (ILS) glide slope.[3] Figure 9 shows an example of an LNG-generated trajectory that was designed for a 3°-flight-path angle following the deceleration segment. Changes in altitude, speed, and aircraft configuration are marked by TCPs.

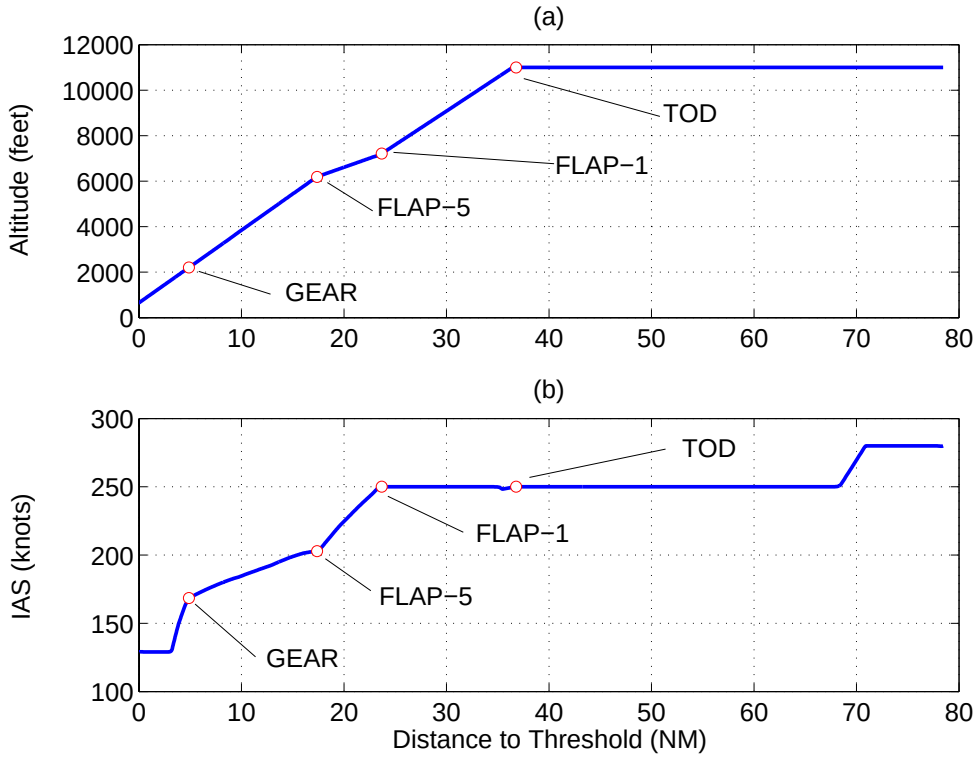

Fig. 9. LNG altitude and speed profiles (note: these profiles are the same as the CDA profiles shown in Figure 8).

[3]The ILS is a precision approach aid for landing operations that includes, but is not limited to, a localizer and a glide slope. The localizer provides lateral guidance to the runway, and the glide slope provides vertical guidance.

The LNG system was implemented in a high-fidelity motion simulator and a study was performed using commercial airline pilots. Fuel consumption was decreased by approximately 17% and the greatest noise reduction was 8.5 decibels at about 10.5 NM from the runway. While the QAT study evaluated the implementation of the LNG concept in a high fidelity environment, runway capacity effects were not studied.

CHAPTER V

EXPERIMENT DESIGN

The objective of this research was to evaluate the feasibility of using AMSTAR to precisely space aircraft flying CDA trajectories in terminal areas. This research addresses the following questions:

> ***Will combining CDA routes with the AMSTAR system provide improved throughput that is justified by acceptable spacing errors and schedule deviation at the runway threshold, while providing noise and fuel benefits over traditional step descents? How can these results be combined for the best throughput, noise, and fuel benefits?***

All research was performed in a fast-time simulation environment to evaluate overall system performance and stability. The simulation environment is described in more detail in the next chapter. To explore how to optimally combine APS with CDA trajectories, baselines for comparison were established and three approaches to combining the two concepts were evaluated. The baselines, research approaches, performance metrics, research airspace, and experiment-design assumptions are discussed in more detail below.

A. Baseline Simulations

Baseline simulations using step descents with AMSTAR and 3°-CDAs without AMSTAR were run. RTA metering errors were used to perturb the initial spacing errors between the aircraft pairs in the fast-time simulations. The RTA errors were randomly assigned using a 3σ-Gaussian distribution with limits of ± 15 and ± 60 seconds. These

baseline scenarios were simulated for the maximum runway capacity, which was based upon minimum-wake-vortex-separation distances. The baseline simulations are detailed below:

- **Step descents with AMSTAR**

  AMSTAR was developed and tested using step-descent routes that are representative of current-day operations. These routes were not optimized for noise and fuel efficiency. Step descents with AMSTAR were used to establish throughput, noise, and fuel consumption baselines.

- **3°-CDAs without AMSTAR**

  The 3°-CDAs were simulated without AMSTAR; therefore there was no interaction between aircraft. Subjecting the aircraft to RTA errors resulted in unacceptable spacing between aircraft pairs at the runway threshold. The runway capacity was then decreased until acceptable pair spacing was achieved at the threshold. This will serve as the baseline for the noise-optimal, 3°-CDA capacity when no precision spacing tool is used.

B. Research Approaches

The performance metrics were evaluated for three different approaches to combining AMSTAR with CDA trajectories. The first approach was to use AMSTAR to precisely space noise-optimal, 3°-CDA trajectories. Due to the diminished deceleration capabilities of aircraft flying CDA trajectories, significant speed decreases could not be achieved once the aircraft began their descents. The second approach included the use of spoilers to permit greater deceleration rates when AMSTAR commanded speed decreases. Spoiler use was expected to reduce the optimality of the CDA routes, but

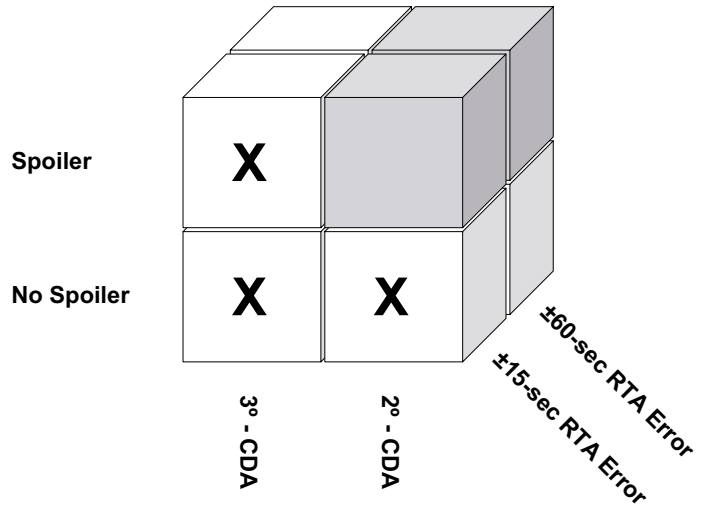

Fig. 10. Three approaches to combining AMSTAR and CDA operations.

these costs were evaluated to determine to what extent the spoilers positively impacted throughput and negatively impacted noise and fuel use. Improvements seen with the second approach were contrasted with the third approach, which was using AMSTAR to space 2°-CDAs without spoilers. While the 2°-CDAs were less noise optimal (their altitudes were lower), the shallower flight-path angle permitted greater deceleration rates than the 3°-CDAs did during the descent.

The three approaches to combining AMSTAR and CDA operations are shown in Figure 10. These approaches were also subjected to RTA errors limited by ±15 and ±60 seconds. The aircraft in these simulations were evaluated and compared for the maximum runway capacity.

Figure 11 shows each approach's relation to noise efficiency and capacity to illustrate the expected correlation between the different approaches to combining APS and CDA operations. This expected relationship was the motivation for choosing the three research approaches that were evaluated in this study.

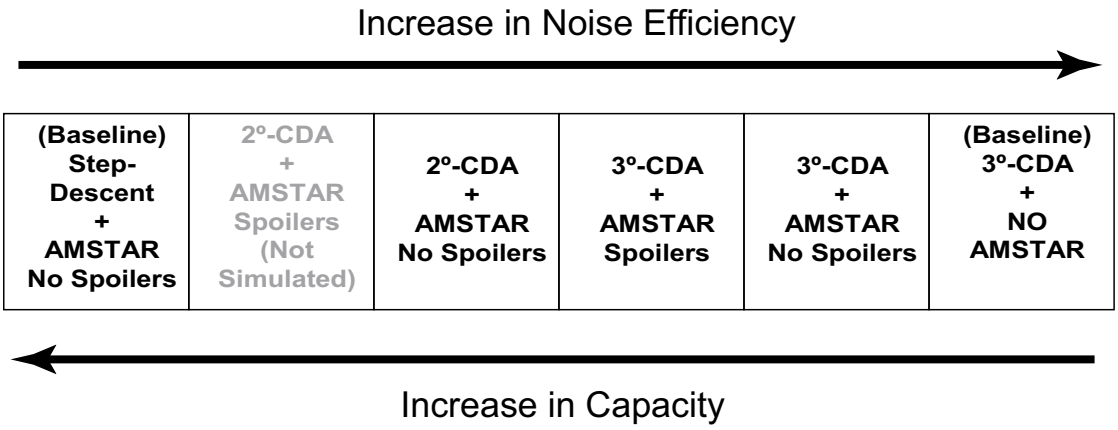

Fig. 11. Expected correlation between noise efficiency and capacity.

C. Performance Metrics

The performance metrics used to analyze the research results included:

- **Threshold Spacing Errors**

  This is the spacing error between an aircraft pair or the difference between the desired pair-wise spacing and the actual spacing at the runway threshold. For this research, a positive spacing error indicated that the pair-spacing was greater than desired at the threshold.

- **Schedule Deviation**

  This is a measure of how far the actual runway arrival schedule deviated from the expected schedule after each aircraft crossed the threshold. An unstable system would have a schedule deviation that grows without bound. If the average spacing error is approximately zero with a normal distribution, the schedule deviation will not grow unbounded.

- **Time in Loss of Separation**

  A loss of separation (LoS) in the terminal area occurred when two aircraft were closer than the minimum required separation limits. In this experiment, the separation limits are defined as 3 NM laterally or 1,000 feet vertically.[1] The amount of time that two aircraft were in a LoS situation was used to determine how well the precision spacing system was able to prevent separation losses for the different approaches.

- **Additional Speed Changes**

  The number of speed changes (both acceleration and deceleration) were counted to determine the effect of precision spacing on the nominal speed profile. Speed changes intrinsic to each route were subtracted from the total number of speed changes that each aircraft experienced to determine the number of AMSTAR-induced changes. Multiple speed changes, specifically speed increases near the end of approach, are not ideal for noise and fuel efficiency or from a pilot acceptability standpoint.

- **Transit Time**

  The transit time is defined as the total time to fly the approach route. The changes in transit time were evaluated to determine how AMSTAR-induced speed changes affect the overall time to fly the routes.

[1]These are separation limits defined for this study, and are not necessarily representative of FAA requirements.

- **Fuel Consumption**

  The fuel consumed along the approach route to the runway was calculated for each aircraft and these statistics were used to determine AMSTAR's cost to the CDA fuel benefits.

The threshold spacing errors, schedule deviation, and time in LoS are metrics that were used to describe AMSTAR's operational performance, i.e., these metrics described how well AMSTAR precisely spaced aircraft pairs at the runway threshold in the presence of initial spacing errors. The number of additional speed changes, transit time, and fuel consumption metrics described AMSTAR's effect on aircraft when a precision-spacing system was used to control aircraft speeds, i.e., these metrics described how the speed commands increased (or decreased) transit times and fuel consumption.

D. Research Airspace

The simulated airspace used for the fast-time studies was the Dallas Fort-Worth (DFW) TRACON area. The DFW-TRACON is a symmetric four-corner airspace that is ideal for research of environmental and operational effects on arrival flow. Three standardized arrival routes were designed from the northwest, southwest and southeast corners of the TRACON, and the routes were named for their metering fixes.[2] Bambe is the northwest fix, Fever is the southwest, and Howdy is the southeast. All aircraft landed on runway 18R, which is a north-south runway at the DFW airport.

Figure 12 depicts the experiment airspace and the lateral arrival routes used for

[2]A metering fix is a point along an established approach route through which aircraft will enter the terminal airspace. Metering refers to a method of time-regulating arrival traffic to control the runway arrival rate.

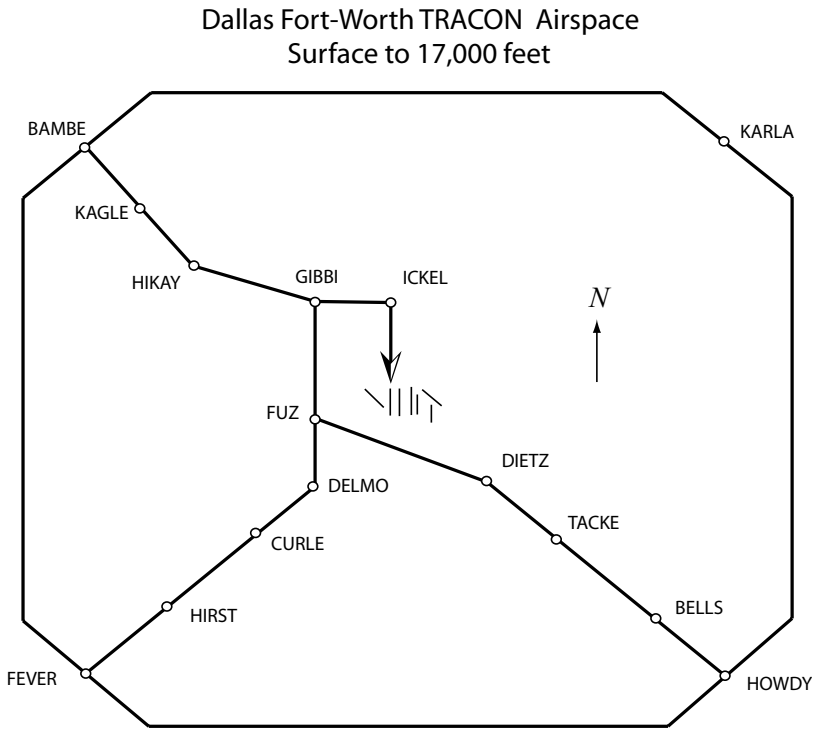

Fig. 12. DFW TRACON.

both this study and the NASA LaRC fast-time simulations. The step-descent and CDA routes were designed along these lateral approaches to the runway.

E. Experiment Design Criteria and Assumptions

The 3°-CDA trajectories that were used in the research were generated using the LNG system along the Bambe, Fever, and Howdy lateral routes. The LNG trajectories were generated offline with deceleration to the final approach speed occurring as late as possible in the approach. Real-time updates to the vertical trajectory, including those caused by speed changes prior to the extension of flaps, were not possible during this simulation. Therefore, the same CDA altitude and speed profiles were used for each aircraft arriving at the same metering fix. Because the LNG system generates ideal

CDA trajectories using individual aircraft drag characteristics and weight, trajectories generated for a Boeing 757 will be different from those generated for a 767. However, AMSTAR was designed with the constraint that all in-trail aircraft fly the same altitude and speed profiles. Therefore, only Boeing 757-200 aircraft were used in this study. As was previously described, LNG trajectories are wind-field specific; therefore, to match the zero-wind conditions of the LNG trajectory generation, no winds were assumed for the fast-time simulations.

The time-based, minimum-separation standard between two Boeing 757s is 100 seconds, which was converted from a 3-NM wake-vortex minimum-separation distance.[3] Using this minimum-separation standard, the maximum runway capacity is 36 aircraft per hour. This was the meter-fix spacing that was used for the baseline simulations and the simulations of the three approaches to combining CDAs and AMSTAR. The minimum-separation standard would not be used in actual operation, however the primary purpose of this research was to compare several methods of combining APS and CDAs, and 100-second spacing served as an appropriate means to test the limitations of the research approaches.

All of the fast-time simulations were run for 100-aircraft sequences. The simulations started aircraft at a specific metering fix: Bambe, Fever, or Howdy. The RTA errors were used to perturb the initial spacing between aircraft pairs. Each simulation scenario was repeated 40 times to remove any imposed bias due to the RTA-error randomization.

The metering-fix arrival sequence was designed to test each possible permutation of lead-aircraft/trailing-aircraft metering-fix pairing. This sequence was not randomized to avoid running a larger number of simulations to gain statistical significance.

[3]This 100-second spacing was also used in the AMSTAR fast-time study at LaRC.

The nine aircraft sequence is shown below:

B - B - F - H - F - F - B - H - H

where B indicates a Bambe arrival, F indicates a Fever arrival, and H indicates a Howdy arrival. This sequence was repeated eleven times during each 100-aircraft simulation.

AMSTAR fast-time simulation studies at LaRC did not show degraded system performance or instabilities for a 20-NM ADS-B range in comparison to a 90-NM range; therefore all simulations were run using a 90-NM range. This range permits communication between aircraft located at the Bambe and Howdy metering fixes.

The research assumptions are summarized below for clarity:

- *Same aircraft type:* All simulation aircraft were Boeing 757-200s. The minimum-separation spacing between aircraft pairs at the threshold was defined as 100 seconds.

- *Same weight:* All aircraft were initialized at 180,000 lbs, which was the weight of the aircraft in the LNG simulation that was run to generate the CDA trajectories.

- *One route:* One single step descent/3°-CDA/2°-CDA route was generated for each metering fix (one Bambe, one Fever, and one Howdy route).

- *No winds*

- *RTA errors:* RTA errors were randomly assigned using a 3σ-Gaussian distribution limited by ± 15 or ± 60 seconds.

- *Metering sequence:* The nine aircraft sequence was constant and evaluated each metering-fix arrival combination.

- *ADS-B range:* A 90-NM ADS-B range was used.

F. Research-Scenario Summary

The baseline scenarios and the scenarios for the approaches to combining AMSTAR and CDAs are summarized below. Each scenario had 40 simulation runs (for a total of 4,000 simulated aircraft per scenario), where the only differences from run to run were the RTA errors assigned to each aircraft. The scenarios were repeated twice for the ±15- and ±60-second-RTA-error cases.

- **Baseline Simulations**
  - Step descents with AMSTAR
  - 3°-CDAs without AMSTAR at maximum capacity (100-second spacing at the metering fix)
  - 3°-CDAs without AMSTAR at reduced capacity
- **Research-Approach Simulations**
  - 3°-CDAs with AMSTAR at maximum capacity
  - 3°-CDAs with AMSTAR and spoilers at maximum capacity
  - 2°-CDAs with AMSTAR at maximum capacity

CHAPTER VI

SIMULATION ENVIRONMENT

A. Flight Research Simulation System

A desktop, aviation research simulation tool called the Traffic Manager (TMX) was used for this study. TMX was developed by the National Research Laboratory of the Netherlands (NLR) with support from NASA LaRC. This software has been a key element in aviation research at both research facilities because of its ability to simulate up to 1000 aircraft simultaneously while operating in either real-time or fast-time. These capabilities make TMX a very useful tool for high-density traffic operations research. TMX is a medium-fidelity simulation system with over 200 different aircraft performance models, autoflight models, and an ADS-B model. For APS research, the AMSTAR system has been integrated with TMX. TMX features are further described by Bussink *et al.* in [17].

1. TMX Aircraft Performance Models

The six degree-of-freedom TMX performance models were developed using Eurocontrol's Base of Aircraft Data (BADA)[1] [18]. TMX uses the BADA models to calculate aircraft performance envelopes for different flight phases. Typical aircraft dynamic models integrate twelve Equations of Motion (EOM) to determine the six states of the aircraft (three position states and three orientation states), where the inputs to the EOM are thrust and control surface deflections. However, the TMX aircraft states are determined using update equations, where the aircraft speed, vertical speed, altitude

[1]BADA performance models cover 99% of the aircraft currently operating in Europe. The BADA models are used by 27 research institutions, 25 universities, 15 air navigation service providers, and ATM companies to build new operational systems.

and heading are intended to track commands that are generated from a desired route. State updates are limited by the specific aircraft performance envelope.

This type of system control is known as kinematic control. The system tracks a reference command and the necessary "input" values are post computed from EOM. This concept is often used for positional control of robots. The process for updating the aircraft states at each time step starts by comparing the commanded values (speed, vertical speed, altitude, and heading) to the current values. The thrust required to meet the commanded values is calculated. If the required thrust exceeds the maximum thrust achievable by the aircraft, the commanded values are reset to the maximum value that will allow the aircraft to be updated without exceeding its performance limits. Aircraft speed updates are also evaluated to ensure that the new speed will fall between the minimum speed (i.e., stall speed) and the maximum operating speed.

2. Integration of AMSTAR in TMX

AMSTAR has been integrated into TMX[2] and coupled to the autothrottle system, where it is engaged by activating a new speed mode called Pair Dependent Speed (PDS). In TMX, PDS can only be used when the aircraft is fully coupled to its FMS, i.e., the aircraft is guided both laterally and vertically. To activate PDS, a lead aircraft call sign and a desired spacing are commanded. From an operational standpoint, PDS is activated when a flight crew receives their lead aircraft call sign and a desired spacing from ATC. The TMX inputs to AMSTAR are as follows [17]:

- *Command Data:* lead aircraft and spacing interval

[2]The TMX/AMSTAR software used in this research was revised in August 2004. The simulation results presented here may not match results run with a later revision.

- *Leading Aircraft Data:* state, route name, final approach speed, and weight class
- *Trailing Aircraft Data:* state, route name, final approach speed, and weight class
- *Environment Data:* airport elevation, approach winds
- *Time Data:* current time and increment

AMSTAR uses the aircraft data from ADS-B to generate 4D trajectories for both the lead and trailing aircraft. AMSTAR returns a speed command to the TMX-aircraft autothrottle based upon the difference in the aircraft-pair ETAs at the runway threshold, where speed updates are limited to ±10% of the nominal speed profile. In this study, aircraft states in TMX were updated in 0.25-second increments and AMSTAR was run at the same 4-Hz rate.

3. CDA Trajectories in TMX and AMSTAR

The Fever lateral route, as shown in Figure 8, was flown using the LNG system in *FMS-Autoflight Simulation Tools for Windows* (FastWin). FastWin is a low-fidelity simulation system with detailed aerodynamic and engine performance models. It was developed at NASA LaRC as a research pilot station for real-time flight simulation and was used in the development of the LNG algorithms [19]. The FastWin simulation output data included altitude and speed profiles for the 3°-LNG trajectory. The TCPs from the altitude and speed data were used to generate the 3°-CDA routes in TMX by creating waypoints where TCPs occurred.

The 3°-CDA TCPs were defined by their distance from the runway threshold (along the lateral route), an altitude, and a speed. For new waypoints that repre-

sented TCPs, the appropriate latitude and longitude coordinates were calculated at the desired distance from the threshold along the lateral route. Each waypoint is defined by its latitude, longitude, altitude, flight-path angle from the previous waypoint altitude, speed, and deceleration from the previous waypoint speed. The waypoint decelerations were adjusted to provide a smooth speed profile. The waypoint information was stored in a file, which was read by both TMX and AMSTAR to regenerate the route within the simulation environment.

4. Model Improvements

To verify the Boeing 757-200 performance model fidelity in TMX, the TMX results for the 3°-CDA trajectory were compared to the FastWin-simulation results. This was done to calibrate the TMX performance model specifically for CDA operations. Figure 13 compares the indicated air speed (IAS), altitude, acceleration, flap configuration, thrust, and fuel-flow plots for the TMX and FastWin simulations.

Figure 13 shows some noticeable differences in the TMX and FastWin performance models. Differing performance characteristics included:

1. Final approach speed
2. Deceleration rate
3. Flap configuration
4. Thrust
5. Fuel flow

Changes were made to the performance model for these characteristics to improve the fidelity of the Boeing 757-200 model in TMX. These changes are described in more detail below.

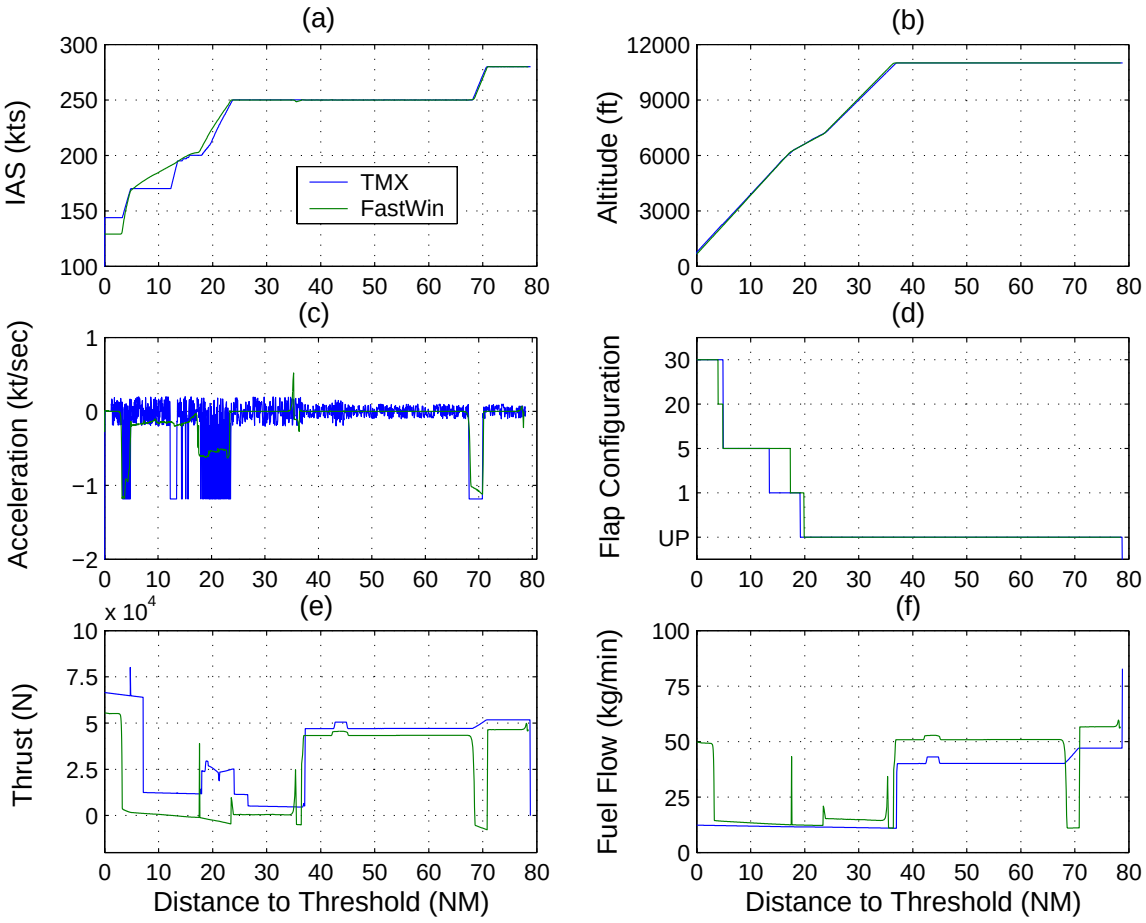

Fig. 13. TMX and FastWin comparison prior to model improvements (3°-CDA).

1. **Final approach speed**

   In Figure 13 (a), the FastWin aircraft had a landing speed of 130 knots (kts), whereas the TMX aircraft landed at 143 kts. TMX calculates the minimum landing speed, V_{min}, from the following:

$$V_{min} = 1.3V_{stall}\sqrt{\frac{m}{m_{ref}}} + 10$$

   where 1.3 is a factor recommended by the BADA manual for all aircraft operations, V_{stall} is the stall speed at the reference mass, m_{ref}, and m is the simulated aircraft mass. A commercial-airline Boeing 757 Operations Manual states that the landing speed is 130 kts for a 180,000-lb aircraft. Adjusting the BADA factor to 1.17 provides the correct landing speed of 130 kts. Although this change improves the Boeing 757 fidelity, it may adversely affect the landing speeds of other TMX aircraft models.

2. **Deceleration rate**

   Figure 13 (a) shows differences in the speed profiles between the two simulation systems. These discrepancies are due to differences in the deceleration rates of the two models. Plot (c) shows that the TMX aircraft decelerated at the same rate regardless of whether the aircraft was in level flight or descending, whereas the FastWin aircraft decelerated at a lesser rate during descent. The BADA manual recommends a maximum longitudinal acceleration/deceleration of 2.0 ft/s^2 (1.18 kt/sec) and this value was implemented in TMX as the maximum deceleration regardless of flight-path angle. To compensate for a descending aircraft, $g\gamma$ was subtracted from the maximum longitudinal acceleration, where g is the acceleration due to gravity in kts per second (kt/sec) and γ is the flight-path angle in radians; for a 3°-flight-path angle, the $g\gamma$ term is approximately

equal to 1 kt/sec. This change was necessary to properly simulate the diminished deceleration capabilities that are characteristic of CDA operations. The deceleration rates are also affected by the flap configuration, i.e., the landing flap configuration obviously creates more drag than the cruise configuration, thus higher deceleration rates are expected. While FastWin has deceleration rates for each flap configuration, TMX multiplies the maximum longitudinal rate by a factor of 2.10 when the aircraft descends below a certain altitude, thus simulating higher drag for the landing configuration.

3. **Flap configuration**

   The flap configuration was hardcoded into TMX to match the flap changes in FastWin (plot (d)), and the landing-gear threshold was increased to 1,550 feet from 500 feet above the ground level (agl) to match the FastWin data. These changes correspond to TCPs in the LNG generated CDA route.

4. **Thrust**

   The thrust plot, plot (e), shows that the TMX aircraft increased power about 4 NM before the FastWin aircraft. TMX increased the throttle when the aircraft passed the maximum threshold for landing, which is defined by the BADA Manual as 3,000 feet. This value was changed to 2,000 feet to command a later power increase.

5. **Fuel flow**

   Fuel-flow models can vary significantly depending on the fidelity of the engine models and thrust calculations. The difference in fuel-flow rates from zero to 10 NM from the runway is the major difference in plot (f). The TMX plot does not reflect all of the trends in the thrust plot, specifically the trend at 20 NM from

the threshold. The BADA Manual defines three regions of fuel consumption: nominal, cruise, and minimum. Nominal and cruise fuel flow are a function of thrust and airspeed, whereas minimum fuel flow is a function of altitude alone. Previously, the minimum fuel flow was used for idle descents, approach, and landing phases. To more accurately match the thrust plot trends, the minimum fuel flow is now only used for idle descent conditions, and the approach and landing phases are modeled using the nominal fuel-flow calculations.

Figure 14 compares the TMX and FastWin results after making the aforementioned changes to the performance model. The acceleration plot, (c), shows that the deceleration rates were limited when the aircraft was not in level flight. These improvements are reflected in the speed profile, plot (a). The flap configurations were identical and the fuel flow plot, (f), more accurately reflected the changes in the thrust plot, (e).

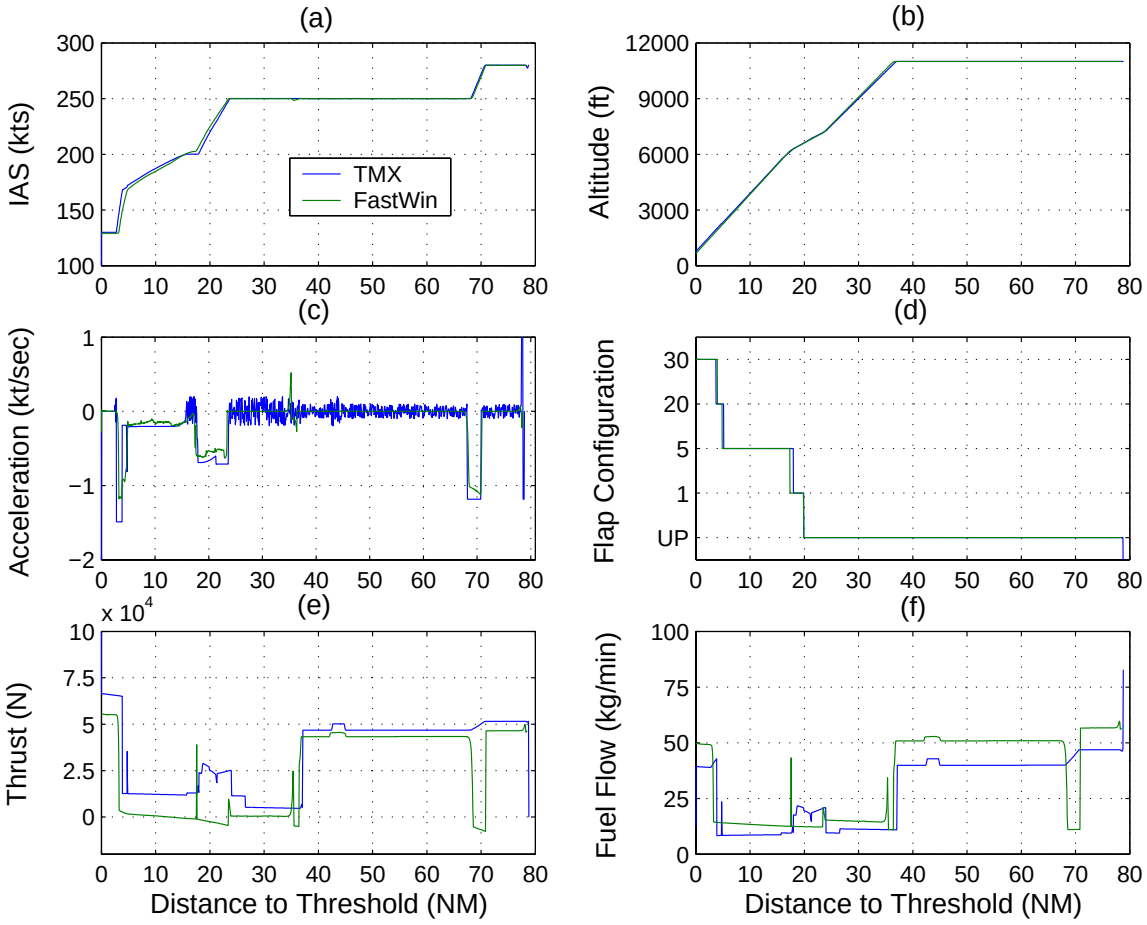

Fig. 14. TMX and FastWin comparison after model improvements (3°-CDA).

FastWin was also used to generate a step-descent profile to compare with the TMX output. In addition to the previous changes listed, the FMS type was changed to match the FastWin simulation results. The FMS type dictates when the aircraft starts descending and decelerating to meet a waypoint constraint. Figure 15 compares two FMS types, where the FMS was changed from the type in plot (a) to the type in plot (b). Changes to the FMS type did not affect the CDA routes because the altitude and speed profiles should be "continuous" without any TODs or bottoms of descent (BODs).

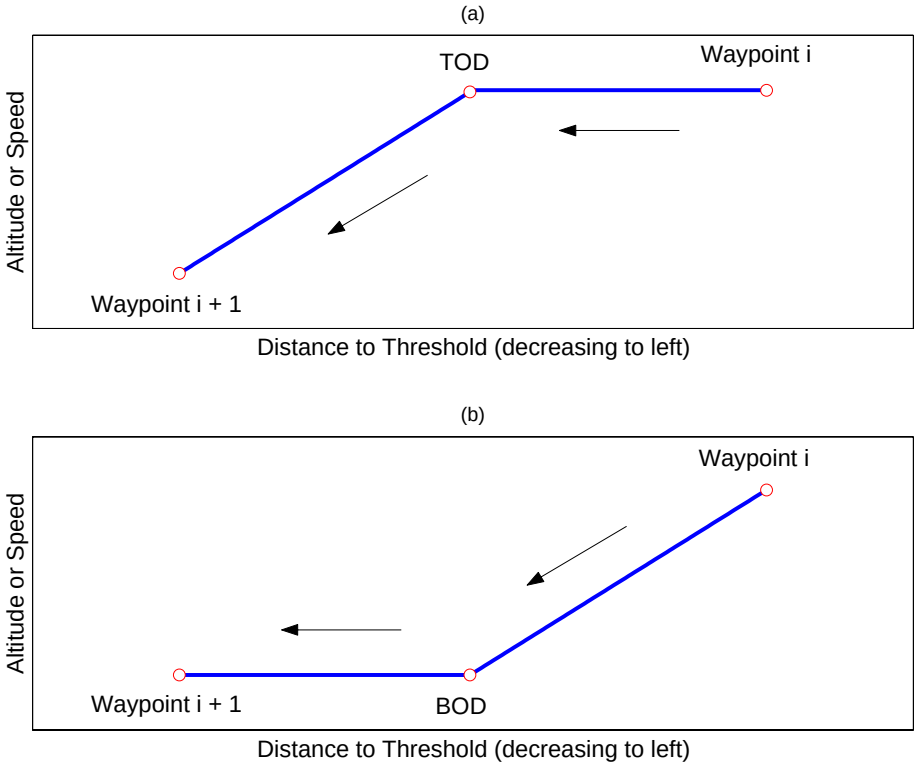

Fig. 15. FMS-type comparison. One FMS type, (a), calculates a TOD where the aircraft can start descending or decelerating and still meet the constraint altitude and speed at the next waypoint, whereas the other FMS type, (b), descends and decelerates immediately after passing the last waypoint.

Figures 16 and 17 compare the TMX and FastWin results for step-descent routes before and after the performance model improvements. The described model improvements clearly resulted in better model agreement between the two simulations.

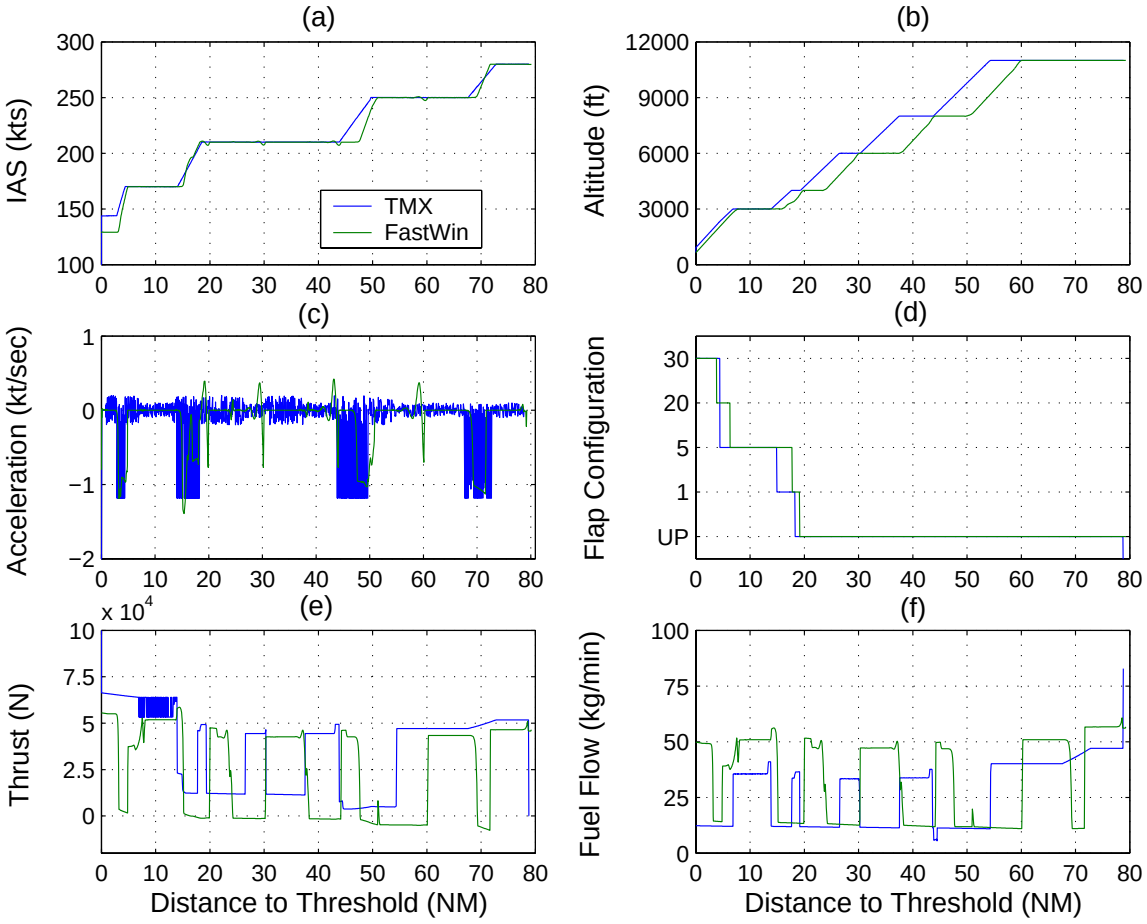

Fig. 16. TMX and FastWin comparison prior to model improvements (step descents).

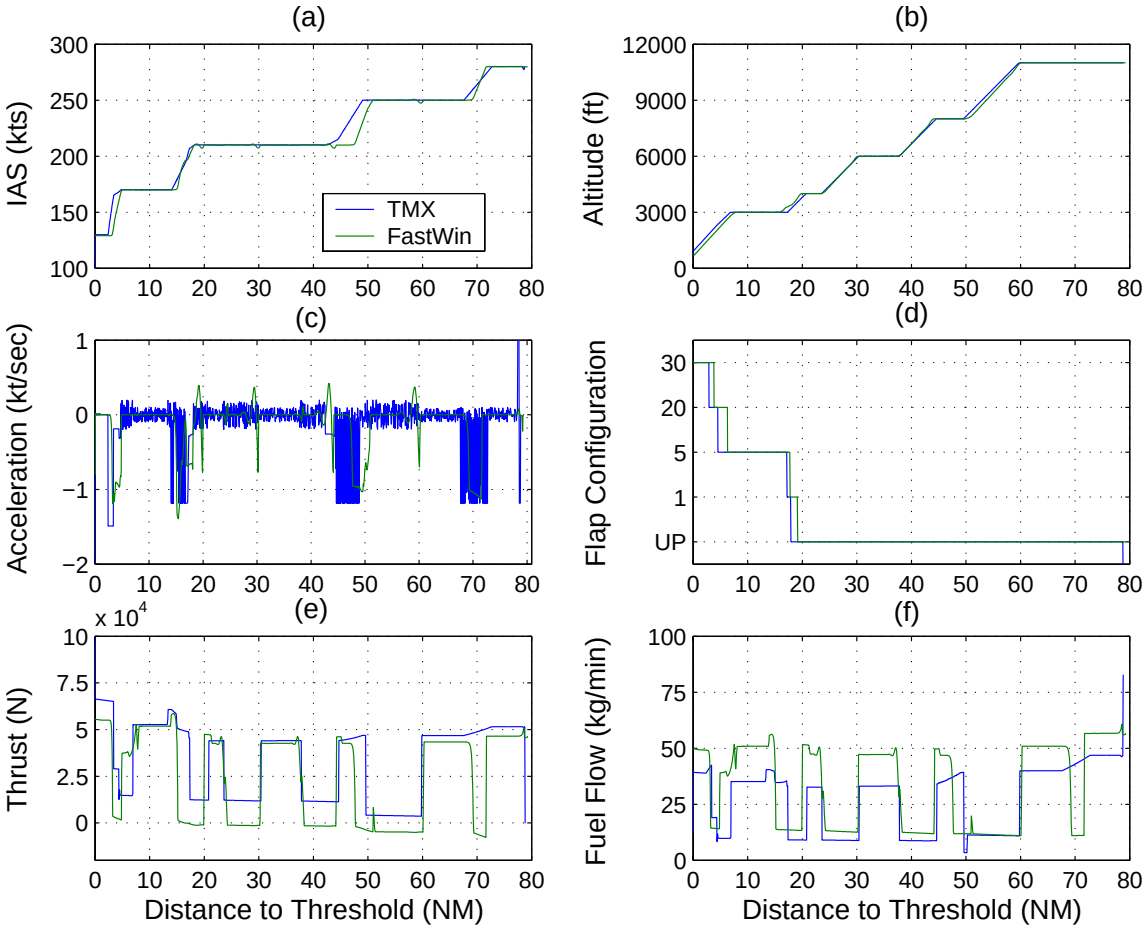

Fig. 17. TMX and FastWin comparison after model improvements (step descents).

FastWin was also used to generate 2°-CDAs, though the LNG system was not used. The TCPs were used to generate routes, and to determine appropriate flap-configuration speed schedules in TMX. Simulation comparisons between TMX and FastWin yielded good results.

The flap-configuration speed schedules and landing-gear altitudes differed for all three route types. Table I compares the flap and landing-gear constraints for the step-descent, 3°-CDA, and 2°-CDA routes that were used in the experiment. These values were taken from the FastWin results.

Table I. Flap and Gear Constraints for Experimental Routes.

	Step Descents	**3°-CDA**	**2°-CDA**
Flaps 1	209 kts	219 kts	238 kts
Flaps 5	205 kts	201 kts	204 kts
Flaps 20	171 kts	173 kts	161 kts
Flaps 30	149 kts	163 kts	148 kts
Gear	2300 ft (agl)	1550 ft (agl)	1550 ft (agl)

5. Spoiler Model

The second approach to combining APS and CDAs included the use of spoilers to increase drag, or deceleration capability, during descent. To simulate the spoilers, a simple, low-fidelity model was implemented in TMX, where spoilers were activated if the difference between the actual speed and the AMSTAR-commanded speed was greater than 15 kts. The aircraft continued to use spoilers until the difference in the actual and commanded speeds was approximately zero. The BADA manual suggests

a drag factor of 1.6 to simulate spoiler drag, and the acceleration rates were set to the full-flap configuration rates. The spoilers were designed so that they could not be used when the aircraft was in ILS mode.

B. Scenario Generator

A Scenario Generator (SG) was developed in Matlab to create the TMX input files for the different scenarios described in the previous chapter. TMX input files contained the following information about each aircraft in a simulation run:

- *Aircraft Start Time:* The aircraft start time in an hours, minutes, seconds format (HH:MM:SS.SS) determined when the aircraft should be initialized. All simulation runs started at 00:00:00.00 and the input file was read chronologically.

- *Initial Conditions:* Aircraft initial conditions in the form of latitude, longitude, heading, altitude, and speed determined where and how the aircraft was initialized. All of the aircraft were initialized at an altitude of 11,000 feet and positioned at one of the metering fixes (Bambe, Fever, or Howdy). If the aircraft started at the Bambe fix, the initial speed was 250 kts, whereas the Fever and Howdy aircraft started at 280 kts. The initialization speeds are based upon the STARs that are currently in use at the DFW TRACON.

- *Route Name:* The route name told TMX what route that particular aircraft should fly. Route information was stored in .RTE files that contained waypoint information, which included altitude and speed constraints.

- *Aircraft Mass:* All of the TMX aircraft were initialized at 180,000 lbs to facilitate a better comparison to the FastWin results shown previously.

- *AMSTAR Mode:* The AMSTAR mode was chosen based upon the desired scenario. Aircraft flew the nominal speed and altitude profiles when AMSTAR was not used to precisely space the aircraft pairs. If precision spacing was desired, the PDS command named the lead aircraft and the desired time-based spacing with the lead.

Determining the aircraft start times for each simulation run was the primary purpose for developing the SG. Due to the differences in the route lengths, each route had a different transit time. This difference resulted in the more difficult task of determining the aircraft initialization times based upon a desired landing sequence. For example, because the Bambe route had the shortest transit time, a Bambe aircraft landing first was not necessarily the first aircraft to initialize in the simulation.

SG inputs were the metering fix sequence (B-B-F-H-F-F-B-H-H), desired spacing at the metering fix (in seconds), the RTA error limits ($\pm$15 or $\pm$60 seconds), the descent type (step descent or CDA), and the AMSTAR mode (nominal profiles or precision spacing). The runway schedule was calculated based upon the metering sequence and the desired spacing at the metering fix. Subtracting the appropriate route transit time from the landing schedule provided the initialization time that would achieve almost perfect spacing at the threshold. RTA errors were randomly assigned to each aircraft and these errors were added to the initialization time to perturb initial spacing between aircraft pairs. Positive RTA errors caused the aircraft to start "later" than desired and negative RTA errors started the aircraft "early". The aircraft start times were sorted chronologically and the information for each individual aircraft was written to the TMX input file. This process was automated to write 40 input files for each scenario. A input-file example is shown in Appendix B.

CHAPTER VII

NOMINAL TRAJECTORIES

This chapter will describe the nominal altitude and speed profiles and the respective transit times, and fuel consumption for the step descent, 3°-CDA, and the 2°-CDA routes. The nominal trajectories would be the expected trajectories if there was no interaction between aircraft pairs, i.e., no precision spacing tool was used. The nominal speed profiles are also an input to the speed control law in Figure 5. When AMSTAR was used to precisely space aircraft pairs, the commanded speed changes affected the transit times and fuel consumptions. The nominal routes were used as a measure of how AMSTAR affected overall system efficiency.

A. Nominal Altitude and Speed Profiles

Figures 18, 19, and 20 compare the altitude and speed profiles of the CDA and step-descent routes for the three lateral DFW routes (Bambe, Fever, and Howdy) that were flown in the experiment.

The noise benefits of both the 3°- and 2°-CDA routes are intuitive based upon the observable differences in altitude as the distance from the runway threshold increases when compared to the step descents. Figure 21 shows the altitude differences for the nominal 2°- and 3°-CDA trajectories (compared to the step descents) along the Bambe, Fever, and Howdy routes, respectively. The greatest differences in altitude occurred between 35 and 40 NM to the runway threshold for all three routes. The 3°-CDA trajectory along the Fever route had the maximum altitude difference of 5,000 feet at a distance of 37 NM from the runway, whereas the 2°-CDA trajectory had a 3,400-foot difference at the same distance.

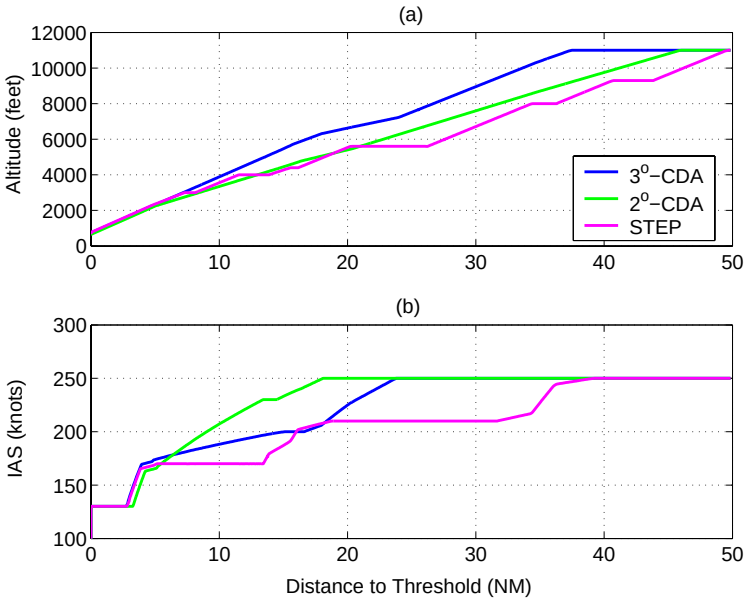

Fig. 18. Nominal Bambe altitude and speed profiles.

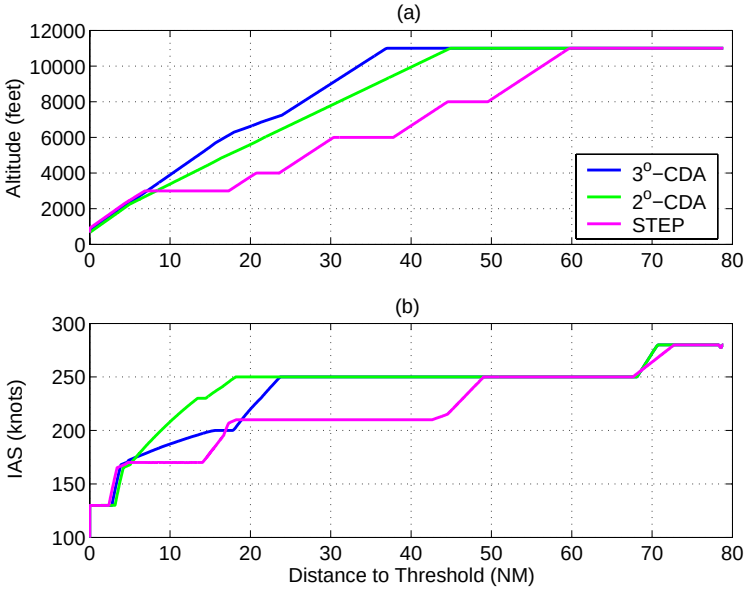

Fig. 19. Nominal Fever altitude and speed profiles.

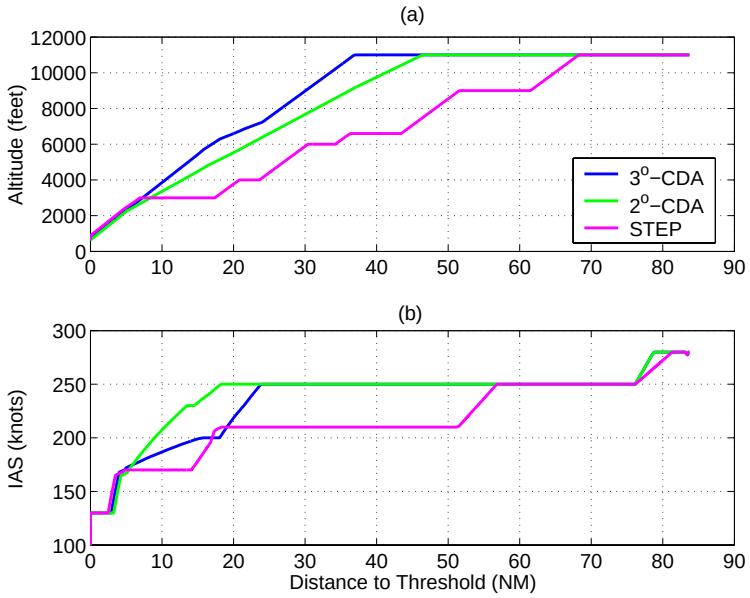

Fig. 20. Nominal Howdy altitude and speed profiles.

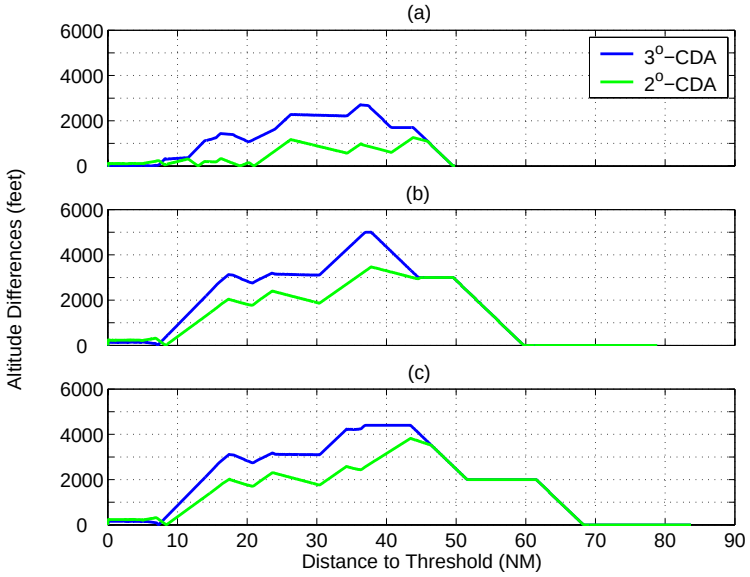

Fig. 21. Differences in CDA altitudes compared to step descent altitudes. Plots (a), (b), and (c) are for the Bambe, Fever, and Howdy routes, respectively.

B. Nominal Transit Times

The route transit times for the step and continuous descents were programmed in the Scenario Generator to determine the aircraft start times at the metering fixes for each scenario. Five aircraft were simulated from each metering fix to find the mean transit time for each route. These results are in Table II below, where the transit-time decreases when compared to the traditional step descents are shown in parentheses.

Table II. Nominal Transit Times.

Metering Fix	**Step (sec)**	**3°-CDA (sec) (% Decrease)**	**2°-CDA (sec) (% Decrease)**
Bambe	837	770 (8.00)	745 (11.00)
Fever	1239	1119 (9.69)	1087 (12.27)
Howdy	1324	1180 (10.88)	1152 (12.99)

C. Nominal Fuel Consumption

Using 100 aircraft from each metering fix, the fuel-consumption means and standard deviations were calculated. Differences in the fuel consumption were a result of noise on the aircraft dynamics simulated in TMX. The mean fuel consumption for each route and descent type is listed in Table III. The standard deviation of the fuel consumption was less than or equal to 0.52 kg for all of the routes. The CDA fuel consumption is compared to the step-descent fuel consumption, and the fuel savings are shown in parentheses. The 2°-CDA routes are more fuel efficient than the 3° routes due to their shorter level altitude segments and transit times.

Table III. Mean Fuel Consumption for Nominal Trajectories.

Metering Fix	**Step-Descent** (kg)	**3°-CDA** (kg) (% Decrease)	**2°-CDA** (kg) (% Decrease)
Bambe	296.22	266.61 (10.00)	226.34 (23.59)
Fever	566.08	513.69 (9.25)	470.09 (16.96)
Howdy	606.00	550.97 (9.08)	502.71 (17.04)

CHAPTER VIII

BASELINE RESULTS FOR STEP DESCENTS WITH AMSTAR

This chapter will examine the simulation results of step descents with AMSTAR that were subjected to ±15- and ±60-second-RTA errors. The aircraft were spaced 100 seconds apart at the metering fixes and were then subjected to the assigned RTA errors. This metering-fix spacing is the maximum runway capacity for Boeing 757s. Results across 40 simulation runs, which total 4,000 simulated aircraft, will be evaluated for the performance metrics described in Chapter V.

A. ±15-second RTA Error Case

The RTA errors that were assigned in a single 100-aircraft simulation run are shown in Figure 22, where plot (a) shows the RTA error that was assigned to each aircraft in the 100-aircraft sequence and the distribution of the errors is shown in plot (b). The mean RTA error was 0.24 seconds with a standard deviation of 4.34 seconds.

The RTA errors averaged over 40 simulations are shown in Figure 23. Plot (a) shows the mean RTA errors that were applied to each aircraft in the sequence. The mean RTA error for the 40 runs was 0.06 seconds with a standard deviation of 4.93 seconds, which is close to the expected standard deviation of five seconds.

1. Spacing Errors and Schedule Deviation

The schedule deviation and spacing errors are illustrated in Figure 24 for a single, 100-aircraft simulation. The lead aircraft is assigned a zero-second spacing error and all of the trailing aircraft are scheduled to arrive at the runway threshold in 100-second intervals. The actual time of arrival (ATA) with respect to the scheduled

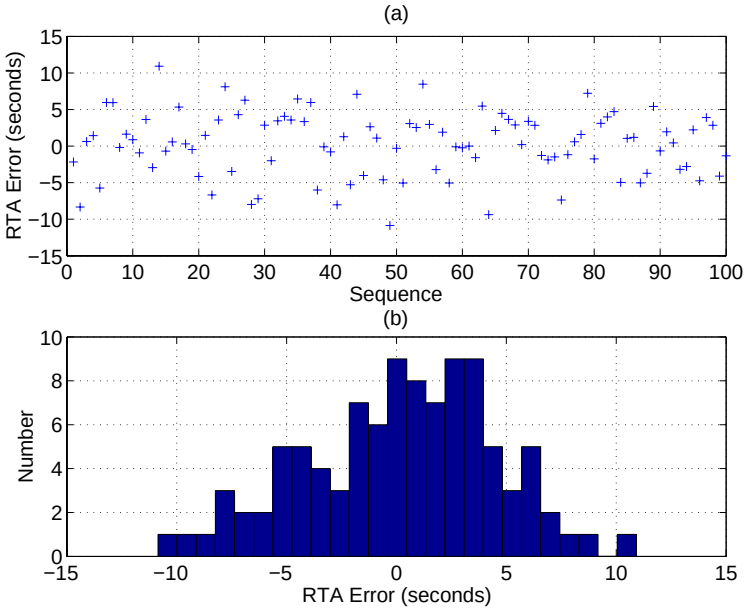

Fig. 22. ±15-second-RTA-error distribution.

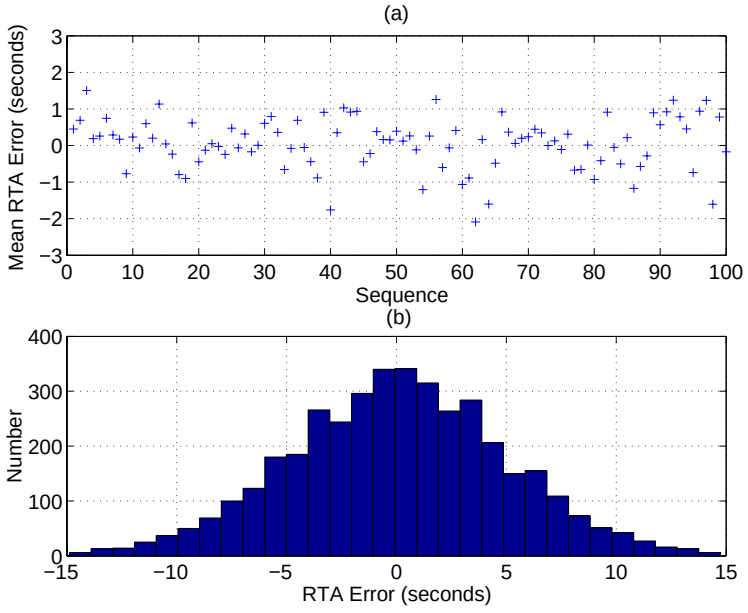

Fig. 23. ±15-second-RTA-error distribution over 40 simulations.

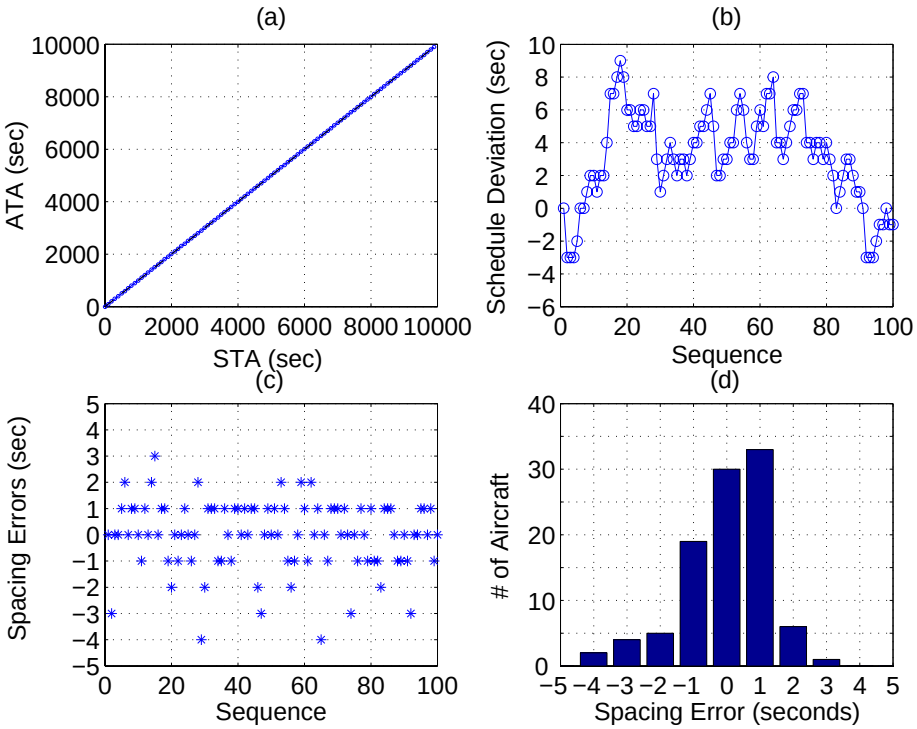

Fig. 24. Spacing errors and schedule deviation for the step descents with AMSTAR (±15-second case).

time of arrival (STA) is shown in plot (a). Ideally, this plot should be linear with a slope of one. In this case, the ATA of the 100th aircraft was one second less than the STA, which can be seen more clearly in the schedule deviation plot, (b). Plot (b) shows some oscillation with a maximum schedule deviation of nine seconds. This plot does not grow without bound, thus indicating system stability. Plots (c) and (d) show the pair-wise threshold spacing errors by sequence number[1] and the spacing error distribution, respectively. The results over a 100-aircraft simulation show small variability in the spacing errors with no outliers; 82% of the spacing errors are within

[1]For example, the threshold spacing error of the 3rd aircraft represents the difference in actual spacing and the desired spacing between itself and its lead aircraft (aircraft #2).

±1 second.

The spacing errors for each aircraft were averaged over 40 simulations, where the assigned RTA errors were the only variables between the different simulations. Figure 25, plots (a) and (b), show the mean spacing errors and the mean spacing-error distribution by metering fix, respectively. The color of the data point represents the

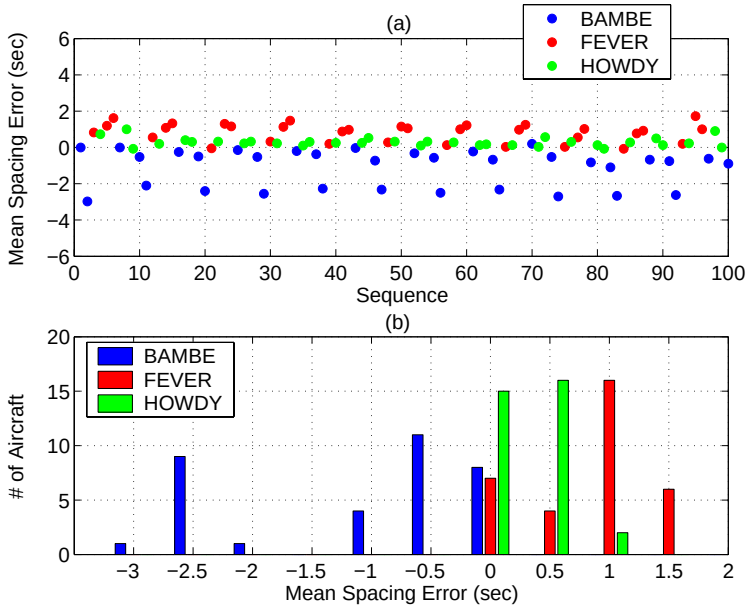

Fig. 25. Mean spacing errors for the step descents with AMSTAR (±15-second case).

metering fix of the trailing aircraft in the pair. The mean of the average spacing errors shown in Figure 25 is −0.01 seconds with a standard deviation of 1.06 seconds. Plot (b) shows two distinct distributions and these different distributions are reflected in plot (a), where every ninth aircraft has a mean spacing error less than −2 seconds. The more negative spacing errors were from Bambe aircraft that trailed Bambe aircraft. Similar behavior was also demonstrated between the consecutive Fever aircraft, though these aircraft demonstrated smaller spacing-error variability. These behaviors were also present in the individual simulation run, though they were less recognizable

when only one 100-aircraft simulation was evaluated.

Table IV confirms what is shown in Figure 25: the aircraft leaving from the Bambe metering-fix had a mean spacing error less than zero and a larger standard deviation than aircraft leaving from Fever and Howdy. Aircraft leaving from Howdy had the smallest variability in spacing errors and a mean close to zero. A Bambe aircraft had the most negative spacing error of -5 seconds, which is equivalent to a 95-second spacing with its lead aircraft.

Table IV. Spacing Errors for Step Descents with AMSTAR ($\pm$15-second Case).

Spacing Error	**Bambe**	**Fever**	**Howdy**
max (seconds)	2	4	4
mean (seconds)	-1.11	0.82	0.29
STD (seconds)	1.26	1.04	0.94
min (seconds)	-5	-3	-2

The average schedule deviation (see Figure 26) exhibited periodic behavior due to the spacing-error patterns present when the results from several simulations were averaged. The period of oscillation is nine aircraft, which is the length of the metering-fix sequence that was described in Chapter V.

2. Losses of Separation

The use of a precision-spacing system helped to prevent and minimize losses of separation between aircraft pairs. Figure 27 shows the amount of time that separation was lost between each aircraft pair in the single 100-aircraft simulation. Eleven aircraft lost separation with their leads for an average of two seconds. Those aircraft that lost separation also had negative spacing errors with their leads, which is an intuitive

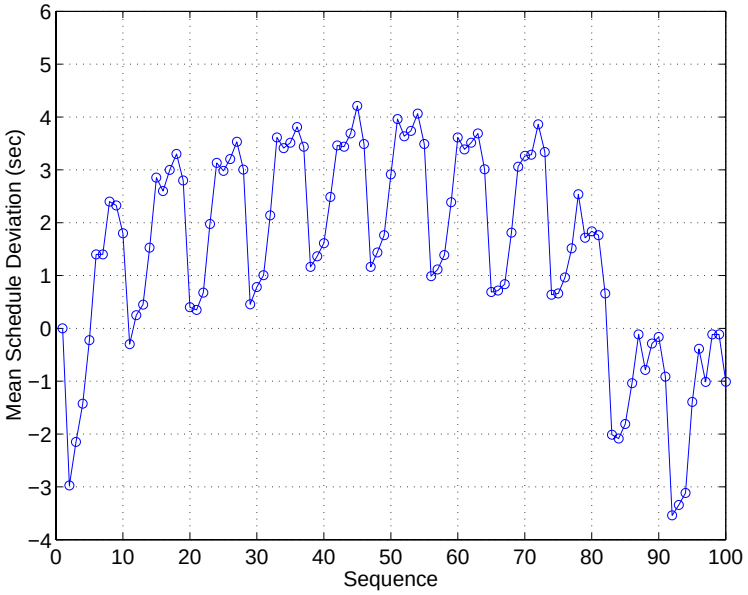

Fig. 26. Mean schedule deviation for the step descents with AMSTAR (±15-second case).

result. Four aircraft lost separation near the threshold for three seconds, which was the maximum time spent in a LoS situation. The minimum lateral separations that were experienced by these aircraft are listed in Table V.

Figure 28 shows the maximum amount of time in a LoS situation in each of the 40 simulations. Only one simulation had an aircraft that lost separation for 5 seconds. Out of 4,000 aircraft, 392 lost separation, which is 9.80% of the arrival stream, but only five aircraft lost separation for more than three seconds (0.13%). A three second LoS was approximately equal to a minimum lateral separation of 2.90 NM (from Table V).

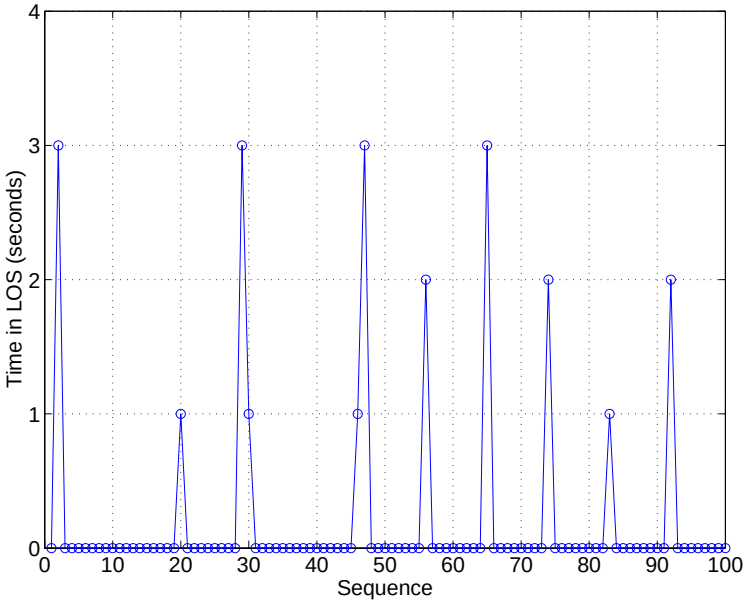

Fig. 27. Losses of separation for the step descents with AMSTAR (±15-second case).

Table V. Minimum Lateral Separation for Aircraft with 3-second LoS.

Aircraft #	**Lateral Separation (NM)**	**Spacing Error (seconds)**
2	2.90	-3
29	2.91	-4
47	2.90	-3
65	2.89	-4

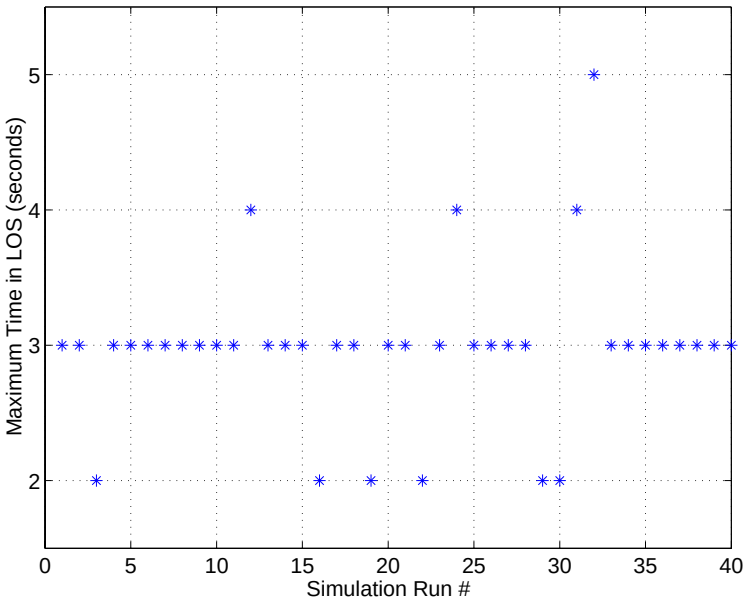

Fig. 28. Maximum time in LoS for the step descents with AMSTAR (±15-second case).

3. Speed Changes

The number of AMSTAR-induced speed changes in a single simulation run is shown in Figure 29, where the mean number of additional speed changes was 3.66. The 57th and 80th aircraft had seven additional speed changes; the actual and commanded IAS time histories and the magnitudes of the speed changes for these aircraft are shown in Figure 30. Larger magnitude changes were intrinsic to the nominal speed profile, whereas smaller magnitude changes (around ±10 knots) were a result of AMSTAR maintaining precise spacing between aircraft pairs.

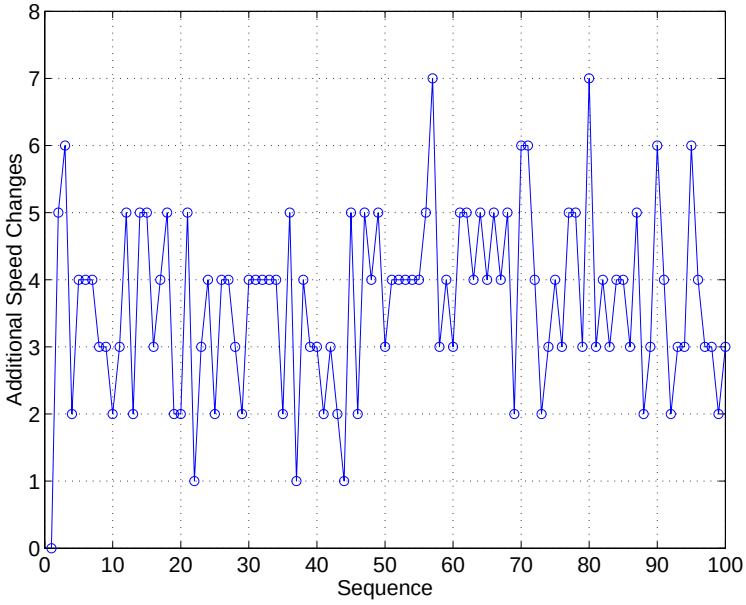

Fig. 29. Additional speed changes for the step descents with AMSTAR (±15-second case).

The additional speed changes averaged over the 40 simulations are shown in Figure 31, where the different metering fixes are indicated. The Bambe aircraft on average experienced fewer speed changes with a mean of 3.46 additional speed changes; however, the Bambe route is the shortest of the three routes. Aircraft

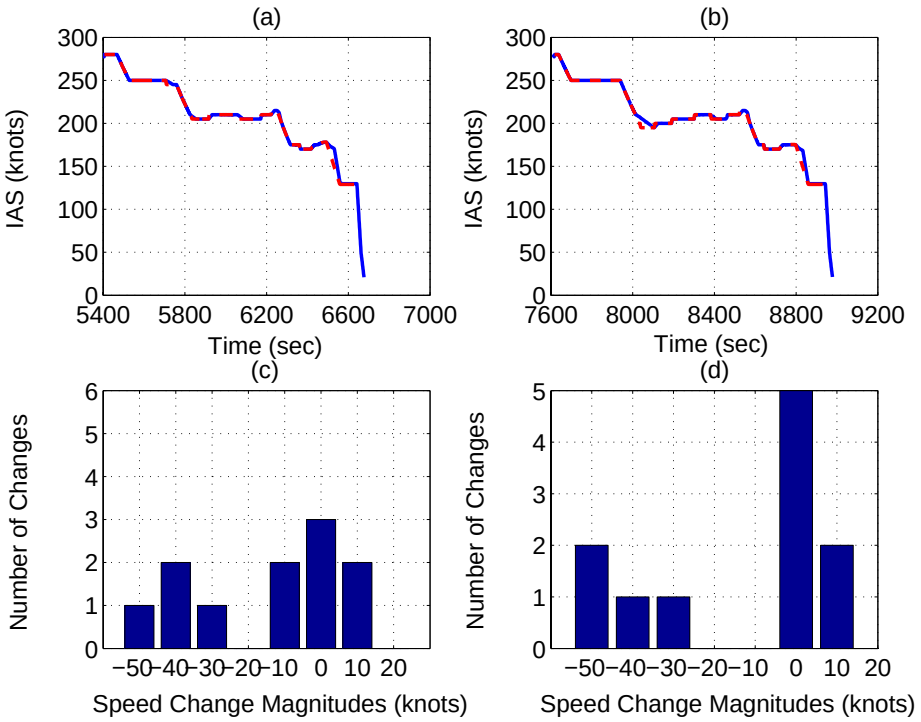

Fig. 30. Speed changes for the 57th and 80th aircraft flying step descents with AMSTAR (±15-second case). Plots (a) and (b) are the IAS time histories for aircraft numbers 57 and 80, respectively (the AMSTAR commanded speed is shown in red). The speed change magnitudes are shown in plots (c) and (d).

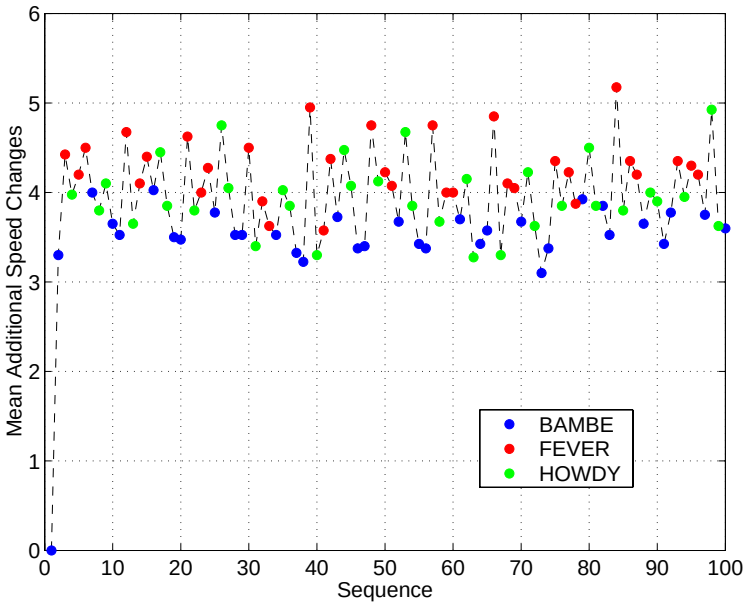

Fig. 31. Mean additional speed changes for the step descents with AMSTAR (±15-second case).

leaving from the Fever metering fix experienced an average of 4.30 additional speed changes, and Howdy aircraft experienced an average of 3.97 changes.

4. Transit Times

The transit-time differences were averaged over 40 simulations (see Figure 32). The mean percent difference in transit times was 0.16% with a standard deviation of 0.54%. Overall, the transit times increased by as much as 23 seconds and decreased by as much as 21 seconds. After approximately the 80th aircraft, the mean transit-time differences decreased. This difference may be a result of the precision of the time data that was recorded. Because more significant changes in transit time were evaluated, the precision problem was not an issue in this study.

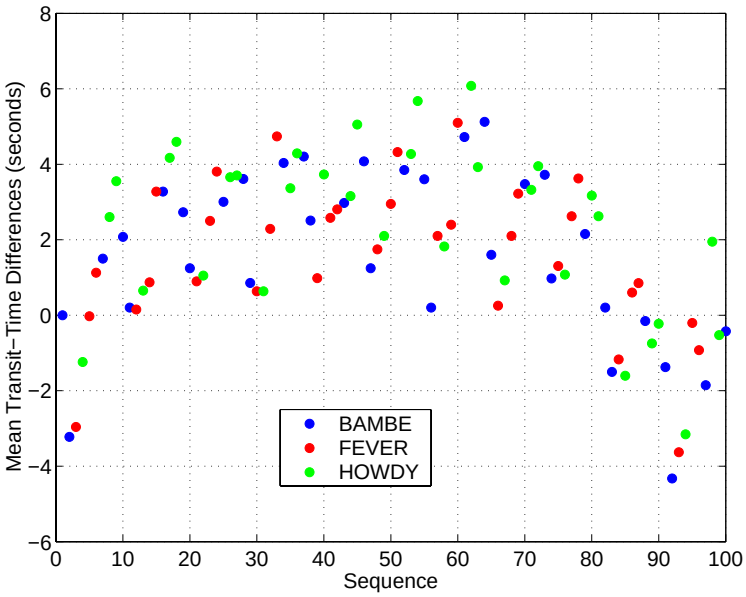

Fig. 32. Mean transit-time differences for the step descents with AMSTAR (±15-second case).

5. Fuel Consumption

The fuel consumption was averaged over the 40 simulations, and these values are shown in Figure 33, where the dashed black lines are the mean fuel consumption for each metering fix, and the solid black lines are the nominal step-descent fuel consumption values provided in Chapter VII. Plots (a) and (b) show patterns in the Bambe and Fever fuel usage that are related to the AMSTAR-induced speed changes. Table VI details the fuel consumption for the 40 simulation runs, where the values in parentheses are the percent differences from the nominal fuel-consumption values in Table III. Overall, the fuel-consumption standard deviations were small, and AMSTAR did pose a significant cost to fuel use.

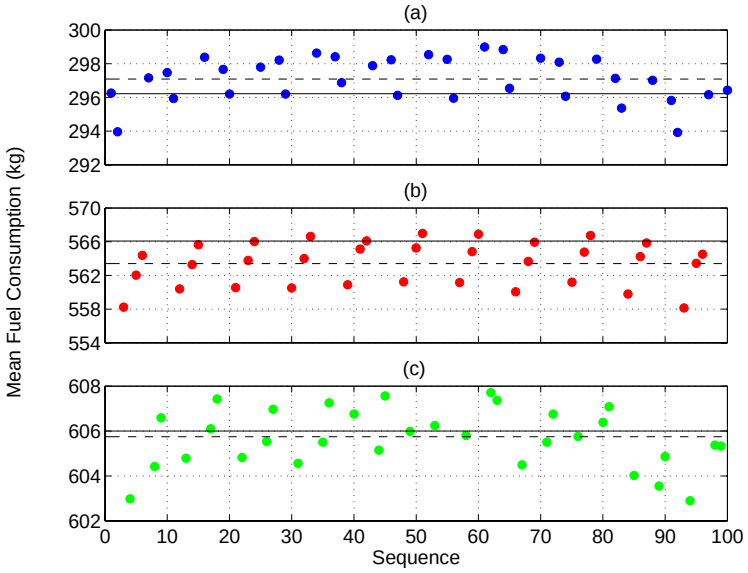

Fig. 33. Mean fuel consumption for the step descents with AMSTAR (±15-second case). Plots (a), (b), and (c) are for aircraft flying the Bambe, Fever, and Howdy routes, respectively.

Table VI. Fuel Consumption for Step Descents with AMSTAR (±15-second Case).

Fuel Consumption	**Bambe**	**Fever**	**Howdy**
max (kg)	304.93 (2.94)	574.69 (1.52)	618.64 (2.09)
mean (kg)	297.09 (0.29)	563.40 (-0.47)	605.75 (-0.04)
STD (kg)	1.31	2.62	1.35
min (kg)	289.22 (-2.36)	551.63 (-2.55)	592.13 (-2.29)

B. ±60-second RTA Error Case

The aircraft flying step descents in this scenario were subjected to ±60-second RTA errors at the metering fixes. The RTA errors assigned in the first simulation run and the mean RTA errors over 40 simulations are shown in Figures 34 and 35, respectively. The mean RTA error in Figure 34 is 0.96 seconds with a standard deviation of 17.37 seconds. For the 40 simulations, the mean RTA error was 0.23 seconds with a standard deviation equal to 19.72 seconds.

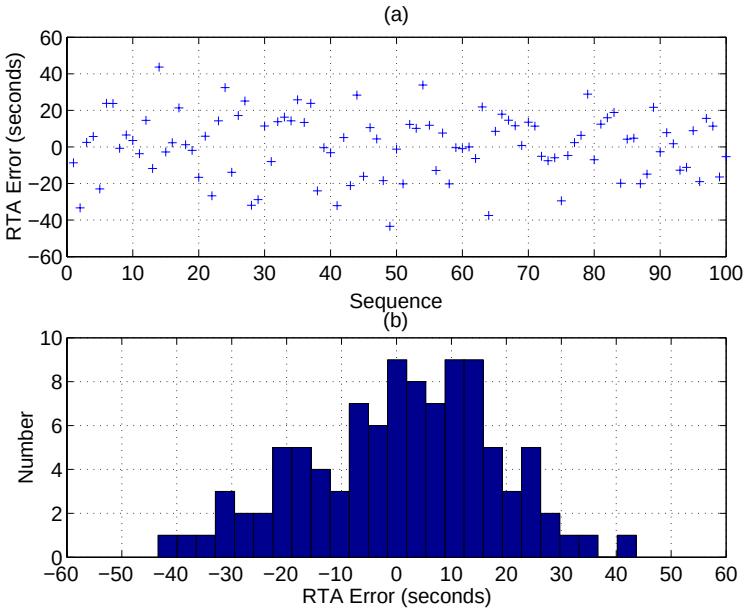

Fig. 34. ±60-second-RTA-error distribution.

1. Spacing Errors and Schedule Deviation

The spacing errors and schedule deviation are shown in Figure 36 for a single 100-aircraft simulation. A maximum schedule deviation of twenty seconds occurred twice during the 100 aircraft sequence (shown in plot (b)). From plots (c) and (d), the mean

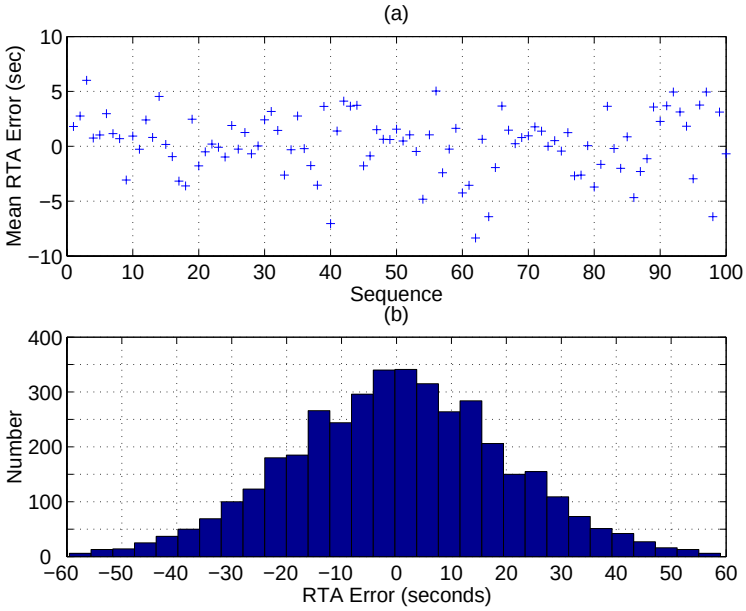

Fig. 35. ±60-second-RTA-error distribution over 40 simulations.

pair-wise spacing error was 0.10 seconds with a standard deviation of 1.80 seconds. For this RTA-error case, the minimum spacing between aircraft was 96 seconds, which is the same as for the ±15-second case.

The mean spacing error over 40 simulations was 0.01 seconds with a standard deviation of 2.22 seconds. Figure 37 shows the same behavior that was observed in Figure 25, where Bambe aircraft that trailed other Bambe aircraft on average had more negative spacing errors than the other eight aircraft in the sequence. Table VII lists the spacing-error statistics by metering fix for the 40 simulation runs. The standard deviations of the spacing errors were approximately twice the standard deviations for the ±15-second-RTA-error case, and the maximum and minimum spacing errors were larger in magnitude.

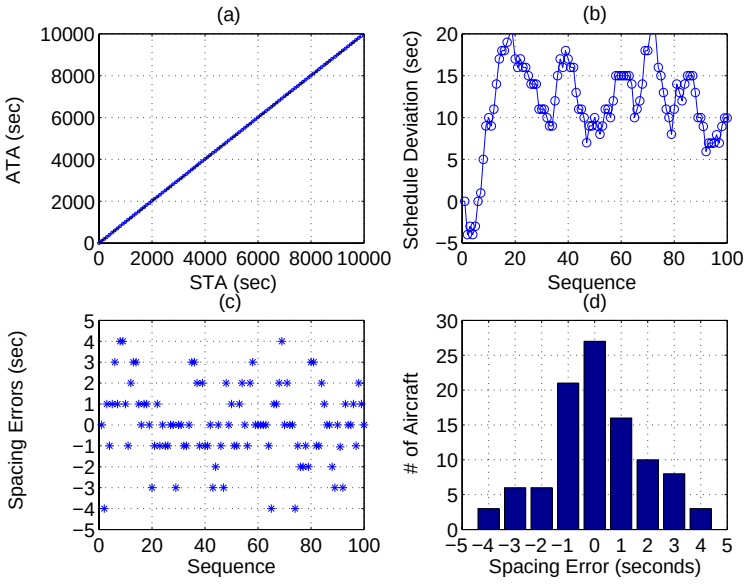

Fig. 36. Spacing errors and schedule deviation for the step descents with AMSTAR (±60-second case).

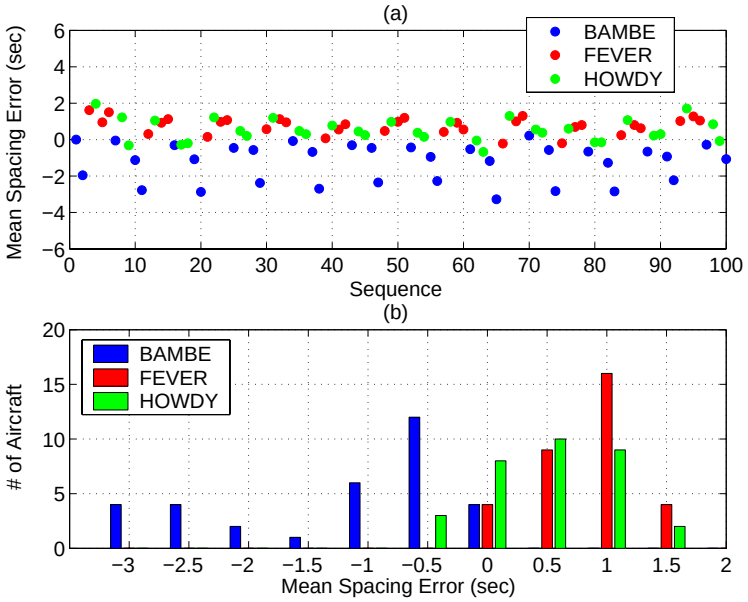

Fig. 37. Mean spacing errors for the step descents with AMSTAR (±60-second case).

Table VII. Spacing Errors for Step Descents with AMSTAR (±60-second Case).

Spacing Error	**Bambe**	**Fever**	**Howdy**
max (seconds)	18	11	9
mean (seconds)	-1.23	0.78	0.52
STD (seconds)	2.01	1.97	2.10
min (seconds)	-7	-4	-7

2. Losses of Separation

Based upon the spacing errors shown in Figure 36, the amount of time in LoS situations was expected to be similar to the results for the ±15-second-RTA-error case. Figure 38 shows that twelve aircraft lost separation with their leads within the single 100-aircraft simulation; however, only one aircraft lost separation for three seconds, whereas four aircraft lost separation for three seconds in the ±15-second case. In this case, the three-second LoS was equal to approximately 2.90 NM of separation.

The maximum time in a LoS in each of the 40 simulations is shown in Figure 39, where nine scenarios had aircraft that lost separation for more than seven seconds. Eight of these aircraft were initialized in a LoS situation due to the assigned RTA errors of the lead and trailing aircraft, where the lead aircraft started late, the trailing aircraft started early, and both aircraft were leaving from the same metering fix. In the cases where the aircraft started in a LoS situation, AMSTAR was able to increase the pair-wise spacing to greater than 3 NM and decrease the spacing errors to a range of ±3 seconds. These situations would not occur in actual ATC operations, because ATC would have directed those aircraft that were too close to their leads to leave the arrival stream.

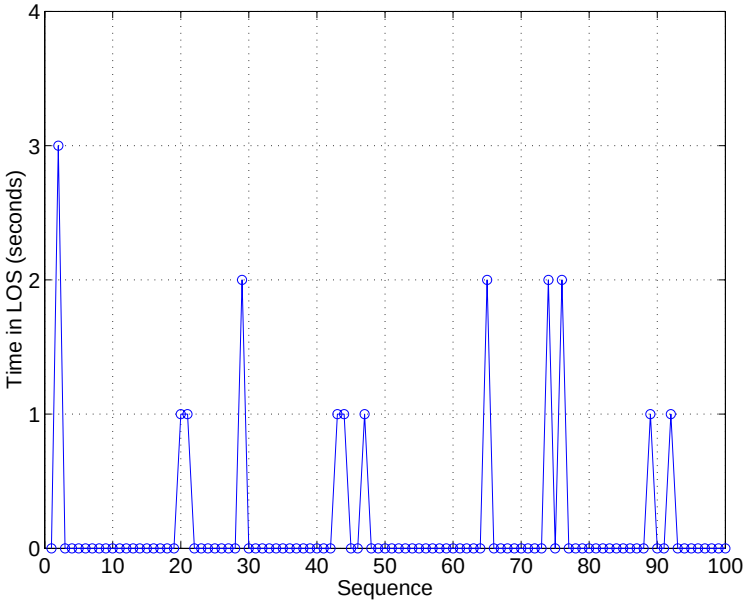

Fig. 38. Losses of separation for the step descents with AMSTAR (±60-second case).

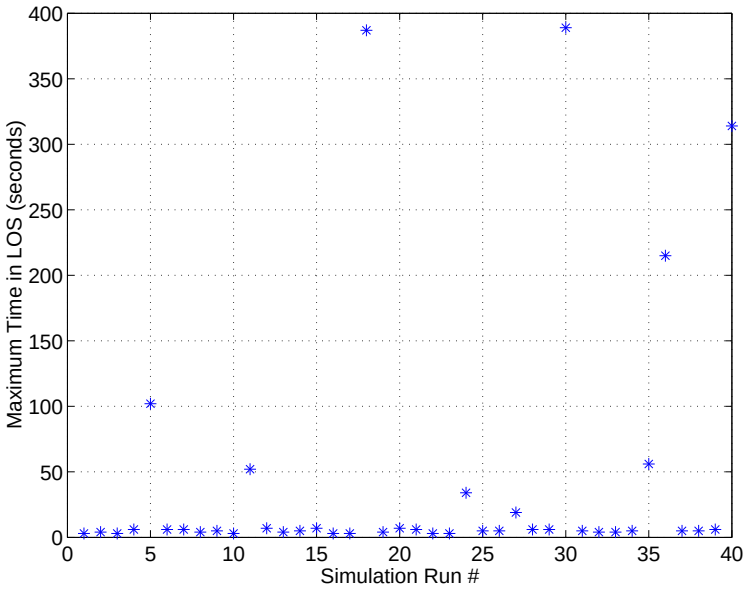

Fig. 39. Maximum time in LoS for the step descents with AMSTAR (±60-second case).

Figure 40 compares the actual and commanded speed time histories of the 6th aircraft in scenario 24, the 45th aircraft in scenario 27, and their lead speed time histories. The 6th aircraft in scenario 24 entered the TRACON approximately 30 seconds (desired spacing was 100 seconds) after its lead and was in a LoS situation for 34 seconds where it flew within 2.72 NM of its lead. Scenario 27 had a maximum LoS for 19 seconds when the 45th aircraft lost separation with its lead. In this case, the aircraft did not initialize in a LoS, but the initial spacing was small enough that when the lead aircraft began to decelerate, the trailing aircraft was commanded to decelerate quickly. The aircraft lost separation when it was unable to decelerate quickly enough, though the aircraft pair only came as close as 2.98 NM. The 6th and 24th aircraft had 3-second and −1-second spacing errors at the threshold, respectively. These examples show that with the use of AMSTAR, more significant times in LoS do not necessarily indicate considerable lateral separation losses.

Out of the 4,000 aircraft simulated, 762 breached separation limits (19.05%). Only 95 of those aircraft (2.38%) lost separation for more than 3 seconds, though some of those separation losses were due to aircraft initializing in a LoS situation, which was not a realistic situation.

3. Speed Changes

Due to greater initial spacing errors, the mean number of AMSTAR-induced speed changes in the first simulation run increased from 3.66 for the ±15-second-RTA-error case to 4.67. The mean number of additional speed changes over 40 simulation runs, shown in Figure 41, demonstrated the nine-aircraft cyclic behavior that was seen in the mean-spacing-error plot. For the 40 simulations, the mean number of additional speed changes was 4.97. Those aircraft that started in LoS situations had an average of 9.36 additional speed changes. The mean number of AMSTAR-induced

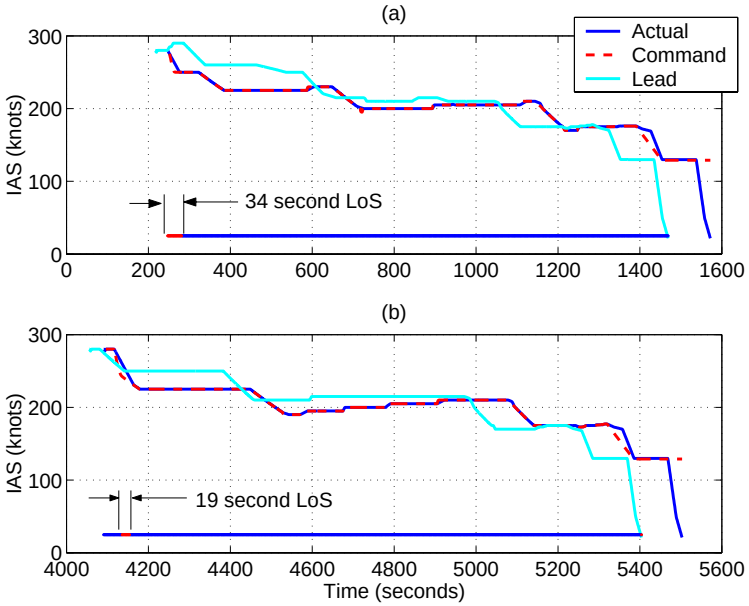

Fig. 40. Speed time histories for aircraft that lost separation flying step descents with AMSTAR. The time in a LoS for the (a) 6th aircraft in scenario 24 and the (b) 45th aircraft in scenario 27 is shown by the blue and red strip, where red indicates when the separation losses occurred.

speed changes was 3.84, 5.57, and 5.55 for aircraft leaving from the Bambe, Fever, and Howdy metering fixes, respectively. Bambe aircraft consistently experienced fewer speed changes, which may have led to the larger variability in the spacing-error results.

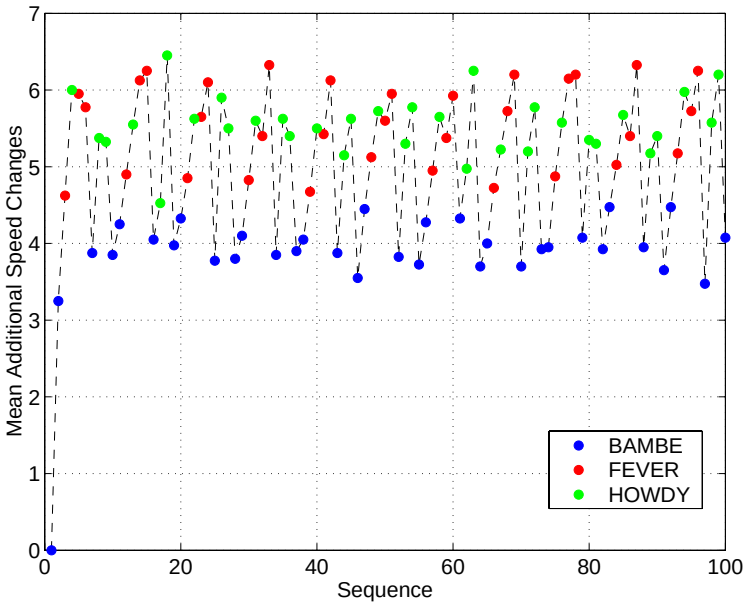

Fig. 41. Mean additional speed changes for the step descents with AMSTAR (±60-second case).

4. Transit Times

With the additional speed changes, some transit times were increased or decreased by as much as 40 seconds. Figure 42 shows the mean transit-time differences averaged over the 40 simulation runs, which shows that the mean differences tended to be positive, thus indicating that AMSTAR-induced speed changes resulted in longer transit times. The mean percent difference in transit times was 0.33% with a standard deviation of 1.96%.

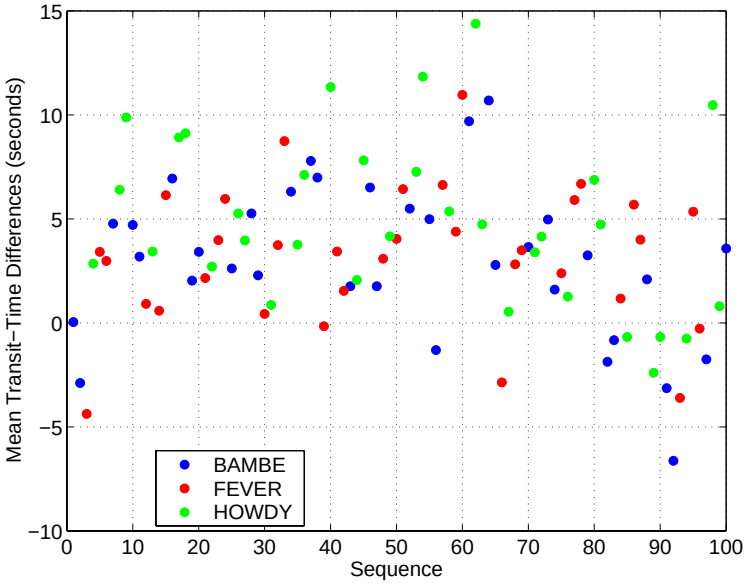

Fig. 42. Mean transit-time differences for the step descents with AMSTAR (±60-second case).

5. Fuel Consumption

Fuel consumption was impacted by some significant transit-time differences. Table VIII lists the maximum, minimum, mean and standard deviations of the fuel consumption, where some Bambe aircraft consumed almost 9% more than the nominal fuel use. However, some aircraft were more efficient than their nominal routes, thus resulting in mean fuel consumption values that did not differ significantly from the nominal values.

C. Summary of Results for Step Descents with AMSTAR

The results show that AMSTAR is able to reduce the initial spacing errors between aircraft pairs to acceptable threshold spacing errors. The ±15-second-RTA-error case showed no threshold spacing errors larger than 4 seconds or smaller than −5 seconds.

Table VIII. Fuel Consumption for Step Descents with AMSTAR (±60-second Case).

Fuel Consumption	**Bambe**	**Fever**	**Howdy**
max (kg)	322.58 (8.90)	594.01 (4.93)	645.40 (6.50)
mean (kg)	297.41 (0.40)	564.63 (-0.26)	608.24 (0.37)
STD (kg)	8.11	9.17	11.44
min (kg)	274.30 (-7.40)	542.00 (-4.25)	581.86 (-3.98)

In the ±60-second-RTA-error case, the spacing errors at the threshold were between 18 and −7 seconds. Whereas AMSTAR was unable to prevent all LoS from occurring, only 0.13% and 2.38% of the simulated aircraft lost separation for more than 3 seconds in the ±15- and ±60-second-RTA-error cases, respectively. The 3-second LoS time, which corresponded to approximately 2.90 NM of lateral separation at the threshold, will be used as a metric for the remaining results presented. The number of AMSTAR-induced speed changes increased with the larger initial spacing errors.

Both RTA-error cases demonstrated periodic behavior related to the nine-aircraft sequence that was repeated throughout each simulation run. Bambe aircraft consistently showed more negative spacing errors and fewer speed changes, which indicates that the routes themselves affected AMSTAR behavior.

AMSTAR-induced speed changes resulted in approximately 3% increases and 3% decreases in the fuel consumption when the RTA errors were limited to ±15 seconds. Increasing the RTA-error limit to ±60-seconds, resulted in larger fuel-consumption standard deviations, where some aircraft flying the Bambe route used almost 9% more fuel than the nominal consumption.

CHAPTER IX

BASELINE RESULTS FOR 3°-CDAS WITHOUT AMSTAR

This chapter will evaluate the capacity of 3°-CDAs without AMSTAR, again for the ±15- and ±60-second-RTA-error cases. The CDAs were first simulated 100 seconds apart at the metering fix, which is the maximum runway capacity. Based upon the results of these simulations, the capacity was decreased, and the threshold spacing errors and the separation losses were evaluated. The other performance metrics, speed changes, transit times, and fuel consumption, were not evaluated because AMSTAR was not used. Without the precision spacing system, no speed changes were commanded, thus the transit times and fuel consumption remained nominal.

A. ±15-second-RTA Error Case

The 3°-CDAs without AMSTAR were simulated using the same RTA errors that were used for the step-descent simulations, as shown in Figures 22 and 23.

1. Spacing Errors and Schedule Deviation

Simulating the 3°-CDAs without the precision spacing system resulted in unacceptable spacing errors across the runway threshold. Figure 43 shows that the spacing errors at the threshold have a similar distribution to the RTA errors for a single, 100-aircraft simulation. When no precision spacing system was used, there was no means to reduce the initial pair spacing. Plots (c) and (d) show threshold spacing errors between −14 and +14 seconds, which is equivalent to an 86- and a 114-second spacing between aircraft pairs, respectively. These spacing errors resulted in a maximum schedule deviation of 13 seconds (plot (b)). The mean spacing error is −0.01 seconds with a standard deviation of 6.19 seconds.

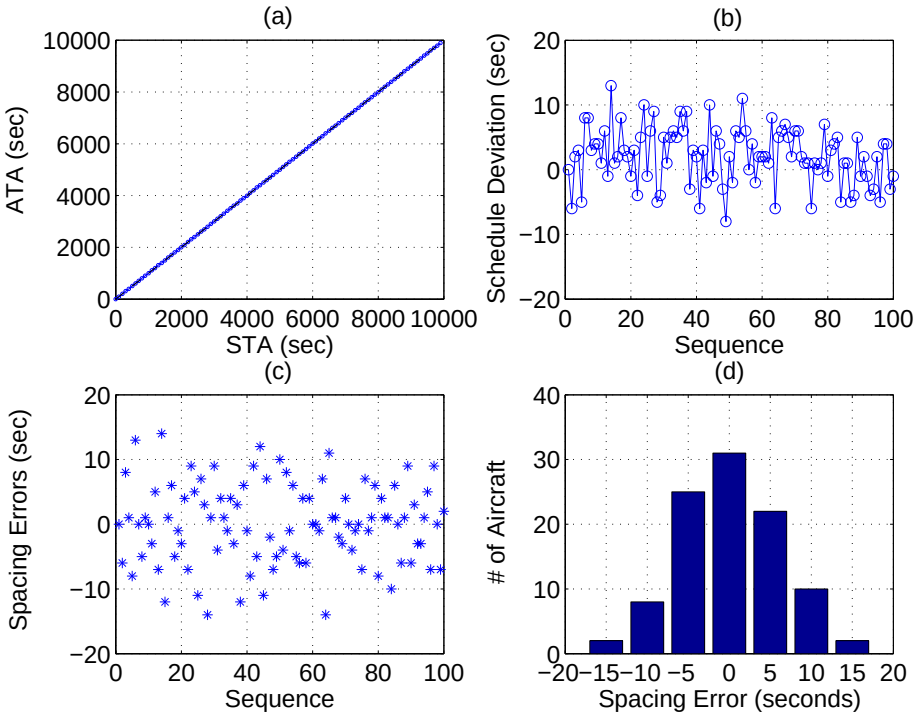

Fig. 43. Spacing errors and schedule deviation for the 3°-CDAs without AMSTAR (±15-second case).

When AMSTAR was not used, no noticeable patterns were apparent in the spacing errors averaged over 40 simulations (as in Figures 25 and 37). The mean spacing error over the 40 simulation runs was −0.03 seconds with a standard deviation of 6.83 seconds, where the maximum and minimum spacing errors were 26 seconds and −22 seconds, respectively.

2. Losses of Separation

With no precision spacing system to minimize the initial spacing errors, 36 losses of separation occurred between aircraft pairs in a single 100-aircraft simulation; Figure 44 shows the amount of time that each aircraft lost separation. In this case, losses of

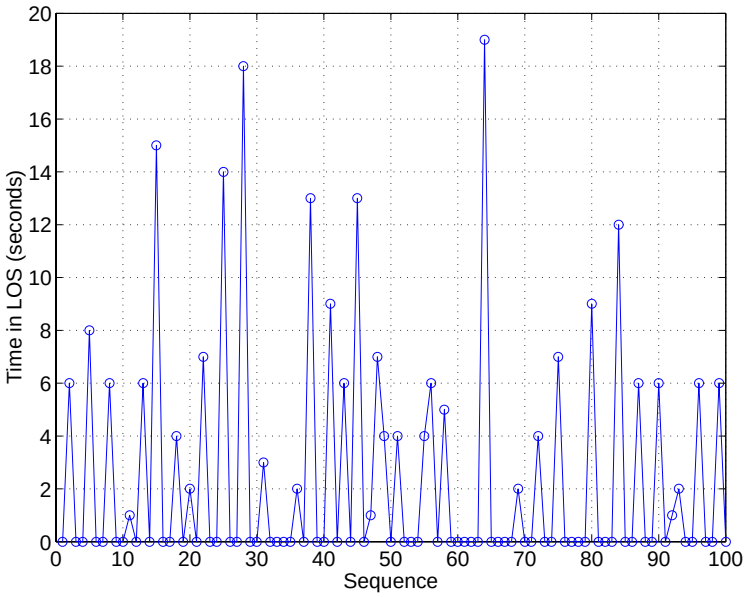

Fig. 44. Losses of separation for the 3°-CDAs without AMSTAR (±15-second case).

separation occurred at the runway threshold when the leading aircraft had a positive RTA error (arrived at the metering fix late) and the trailing aircraft had a negative RTA error (arrived at the metering fix early). The initial spacing was inadequate for the pair-compression effects near the runway.

In the first simulation run, the 63rd aircraft arrived at the metering fix 5.48 seconds late, and the 64th aircraft arrived 9.37 seconds early, thus the resultant spacing at the metering fix was 85.15 seconds (a 14.85-second initial spacing error), which ultimately resulted in a 19-second LoS. The resultant fix spacing is found by subtracting the difference in the lead-aircraft RTA error and the trailing-aircraft RTA error from the desired spacing at the metering fix (in this scenario, the desired spacing was 100 seconds). Table IX shows the resultant pair-wise spacing at the metering fix, the threshold spacing errors, the time in a LoS, and the minimum lateral separation reached for the seven aircraft that lost separation for more than 10 seconds (as shown

Table IX. Aircraft That Lost Separation for More than 10 seconds.

Aircraft #	Pair-Spacing at Fix (seconds)	Threshold Spacing Error (seconds)	Time in LoS (seconds)	Minimum Lateral Distance (NM)
15	88.40	-12	15	2.59
25	88.42	-11	14	2.62
28	85.76	-14	18	2.52
38	88.03	-12	13	2.62
45	88.90	-11	13	2.64
64	85.15	-14	19	2.50
84	90.34	-10	12	2.65

in Figure 44).

Figure 45 illustrates the relationship between the resultant metering-fix spacing and the time in LoS. The black lines depict the "boundaries" where a LoS between aircraft pairs should be expected when no precision spacing tool was used. Any initial spacing error less than -1 second resulted in a LoS.

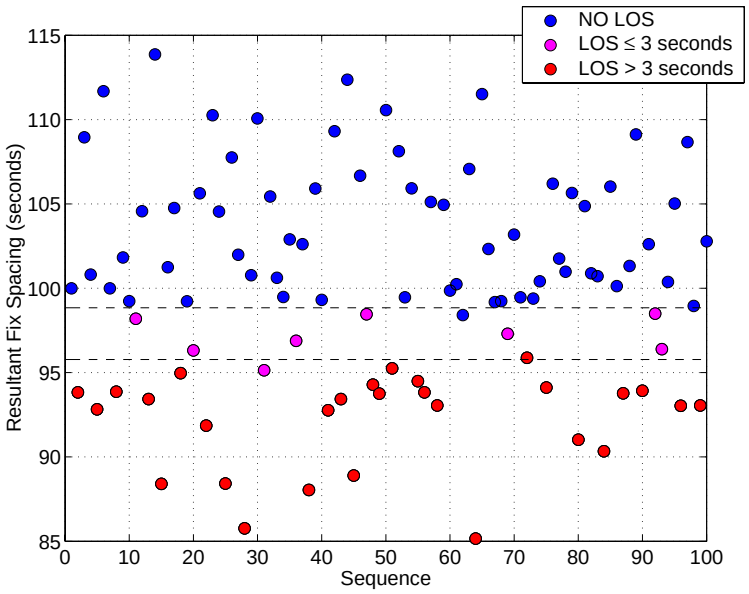

Fig. 45. Relationship between losses of separation and fix spacing.

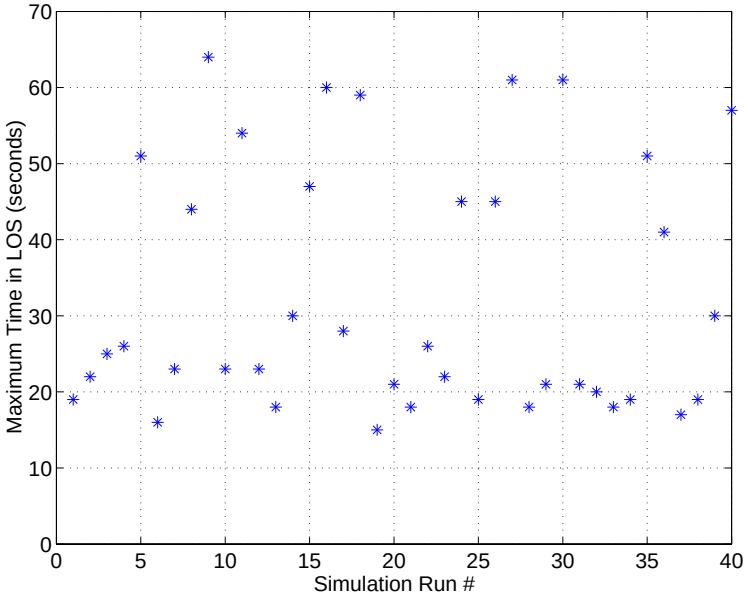

Fig. 46. Maximum time in LoS for the 3°-CDAs without AMSTAR (±15-second case).

Figure 46 shows the maximum amount of time in a LoS situation in each of the 40 simulation runs. The ninth scenario had an aircraft that lost separation for 64 seconds and came within 2.23 NM of its lead. This aircraft had a resultant fix spacing of 78.21 seconds, which is an initial spacing error of 21.79 seconds.

The data from the 40 simulation runs was used to evaluate the minimum-lateral-distance relationship to LoS times and to runway threshold spacing errors; these relationships are illustrated in Figure 47. Plot (a) shows a nonlinear relationship between minimum distance and LoS time, which was fit with a 4th-order polynomial, whereas plot (b) shows a linear relationship between minimum distance and threshold spacing errors. From these relationships, the minimum lateral distance between aircraft pairs can be found from either the threshold spacing error or the time that separation was lost. These relationships are only valid for separation losses near the runway threshold.

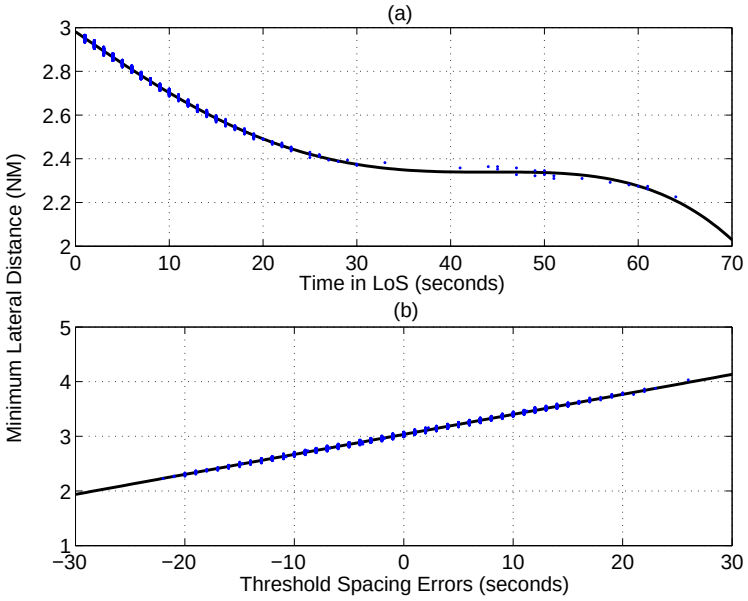

Fig. 47. Minimum distance relationship to LoS time and threshold spacing.

Out of the 4,000 aircraft simulated over the 40 runs, 1,576 lost separation with their lead (39.40%). Of those aircraft that lost separation, 1,046, or 26.15%, lost separation for more than 3 seconds, which is a lateral separation less than 2.90 NM (from Figure 47). More than 360 aircraft (9%) lost separation for more than 10 seconds or at least came as close as 2.7 NM to their lead. This capacity is obviously not acceptable for current-day operations.

To reduce the number of separation losses, the desired pair-spacing at the metering fix was increased. When no precision spacing tool was used, the aircraft pairs had no interaction; therefore, increasing the initial spacing biased the spacing errors at the threshold by the same amount. For example, a −15-second spacing error will be a −5-second error when the fix spacing is increased from 100 to 110 seconds.

Table X shows the breakdown in spacing errors, in 10-second increments by percentage, of the 4,000 aircraft simulated with a 100-second spacing at the metering

Table X. Spacing Errors and LoS for 100-second Metering-Fix Spacing (±15-second Case).

Spacing Errors (seconds)	Percentage of 4,000 Aircraft
$<$ -20	0.08%
-20 $\leq$ and $<$ -10	6.40%
-10 $\leq$ and $<$ 0	40.55%
Total LOS	39.40%
LOS for $<$ 3 seconds	13.25%

fix. These results assisted in predicting what metering-fix spacing would result in a more acceptable number of separation losses. Negative spacing errors typically indicated a LoS based upon the results shown in Figures 45 and 47. From Table X, it can be seen that increasing the fix-spacing to 110 seconds, will still result in negative spacing errors for approximately 6.50% of the simulated aircraft. Increasing the fix-spacing to 120 seconds will eliminate all spacing errors, with the exception of roughly one-tenth of a percent of the 4,000 aircraft (4 aircraft).

An increase in metering-fix spacing to 110 seconds did not reduce the variability in threshold crossing errors, but it did increase all of the spacing errors in Figure 43 by approximately 10 seconds, as was previously discussed. Figure 48, plots (a) and (b), show the shift in the mean spacing error for one 100-aircraft simulation. Fewer aircraft arrived with an inadequate spacing with their leads when the metering-fix spacing was increased to 110 seconds. Over the 4,000 aircraft in 40 simulation runs, the mean spacing error was 9.87 seconds with a 6.90-second standard deviation.

The metering-fix spacing was also increased to 120 seconds and the results from these simulations are compared to the 100- and 110-second results in Table XI.

Table XI. Comparison of Fix Spacing for ±15-second-RTA-Error Case.

	100-second Fix-Spacing	**110-second Fix-Spacing**	**120-second Fix-Spacing**
Mean Spacing Error (seconds)	−0.03	9.87	19.78
Standard Deviation (seconds)	6.83	6.90	7.11
Spacing Errors < 0 (seconds)	1881 (47.03%)	262 (6.55%)	5 (0.13%)
Total # of LoS	1576 (39.40%)	161 (4.03%)	1 (0.03%)
# of LoS > 3 seconds (2.90 NM)	1046 (26.15%)	75 (1.88%)	0 (0.00%)
Runway Capacity (aircraft per hour)	36	32	30

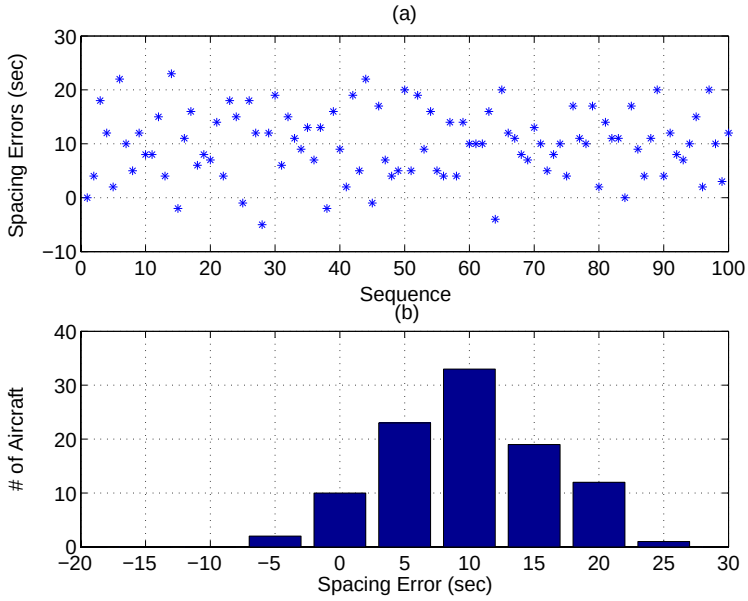

Fig. 48. Spacing errors for the CDAs without AMSTAR (110-second spacing at fix).

B. ±60-second-RTA Error Case

The 3°-CDAs were subjected to RTA errors limited by ±60 seconds, as shown in Figures 34 and 35. In this case, the simulation again started with an initial metering-fix spacing of 100-seconds to evaluate the spacing errors. The procedure outlined in the previous section was followed to determine the appropriate metering-fix spacing for CDAs subjected to ±60-second RTA errors.

1. Spacing Errors and Schedule Deviation

The spacing errors and schedule deviation for a single 100-aircraft simulation are shown in Figure 49, where plots (c) and (d) show the spacing-error variability for CDAs flying without a precision spacing system and subjected to ±60-second RTA errors at the metering fix. Over 40 simulations, the mean spacing error was −0.05

seconds with a standard deviation of 27.17 seconds.

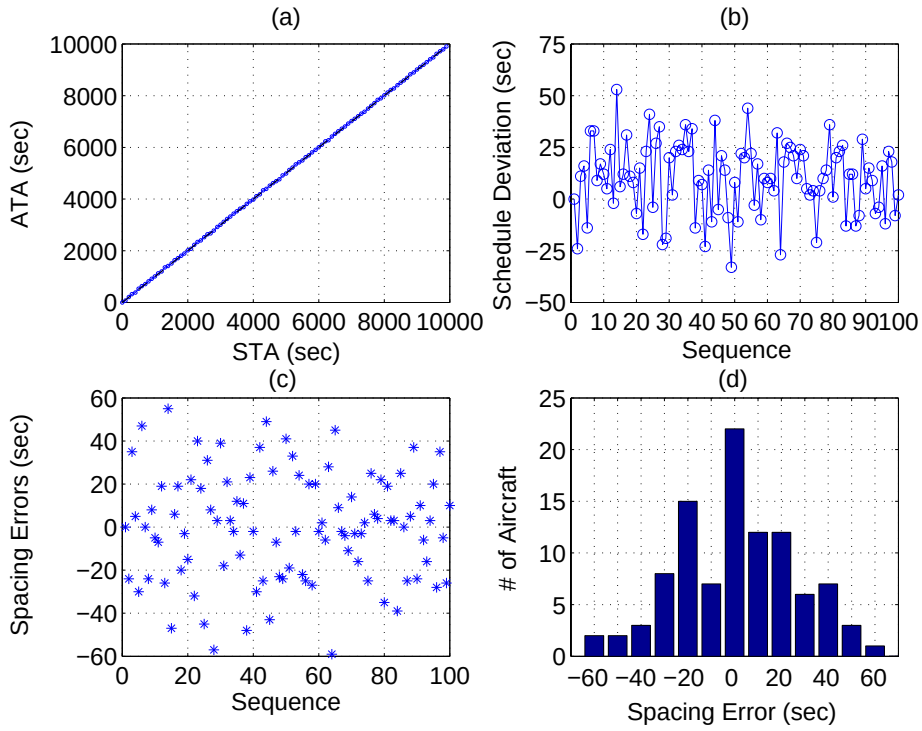

Fig. 49. Spacing errors and schedule deviation for the 3°-CDAs without AMSTAR (±60-second case).

2. Losses of Separation

Out of 4,000 aircraft, 1,875 aircraft or 46.88% lost separation; however, in this case, only a small percentage of those were minor losses of 3 seconds or less. Certain combinations of RTA errors actually resulted in losses of separation for the entire routes, e.g., the 72nd aircraft in the 30th scenario lost separation for 1,204 seconds where it came within 0.1860 NM of its lead. This aircraft started in a LoS situation and had unacceptable spacing for the entire route. Obviously, this is an unrealistic situation and would never occur in actual operation.

Table XII. Spacing Errors and LoS for 100-second Metering-Fix Spacing (±60-second Case).

Spacing Errors (seconds)	Percentage of 4,000 Aircraft
$<$ -70	0.50%
-70 $\leq$ and $<$ -60	0.83%
-60 $\leq$ and $<$ -50	1.78%
-50 $\leq$ and $<$ 0	45.85%
Total LOS	46.88%
LOS for $<$ 3 seconds	43.63%

Table XII shows percentages of aircraft that had negative spacing errors within certain ranges for a 100-second spacing at the metering fix. These values were used to provide guidance in choosing a metering-fix spacing that resulted in more appropriate numbers of separation losses. Table XII shows that increasing the metering-fix spacing to 150 seconds would still result in negative spacing errors for approximately 3% of the 4,000 aircraft, whereas increasing the spacing to 160 seconds would result in negative spacing errors for only slightly more than 1% of the total aircraft. Table XIII compares the spacing errors and number of separation losses for 150-, 160-, and 170-second fix spacing. The 170-second-spacing case shows only a small percentage of the aircraft losing separation for more than 3 seconds, which may be deemed an acceptable number in actual operation.

C. Summary of Results for 3°-CDAs without AMSTAR

When no precision spacing system was used, decreased runway capacities resulted in more acceptable numbers of separation losses. For the maximum runway capacity

Table XIII. Fix-Spacing Comparison for ±60-second-RTA-Error Case.

	150-second Fix-Spacing	**160-second Fix-Spacing**	**170-second Fix-Spacing**
Mean Spacing Error (seconds)	49.46	59.36	69.26
Standard Deviation (seconds)	27.61	27.82	28.07
Spacing Errors < 0 (seconds)	122 (3.05%)	52 (1.30%)	20 (0.50%)
Total # of LoS	109 (2.73%)	44 (1.1%)	17 (0.43%)
# of LoS > 3 seconds (2.90 NM)	89 (2.23%)	36 (0.90%)	11 (0.28%)
Runway Capacity (aircraft per hour)	24	22	21

(36 aircraft per hour) and ±15-second RTA errors, 39.40% of the simulated aircraft lost separation and 26.15% came closer than 2.90 NM to their lead (a 3-second LoS). Increasing the metering-fix spacing to 110 seconds, eliminated many of these separation losses, and a 120-second spacing virtually eliminated all losses, which is a capacity reduction of 4 and 6 aircraft per hour, respectively. In the ±60-second-RTA-error case, almost 47% of the aircraft lost separation at the maximum capacity, and the metering-fix spacing had to be increased to as much as 170 seconds. This is a 21-aircraft-per-hour runway capacity, which is a capacity loss of 15 aircraft per hour.

CHAPTER X

APPROACHES TO COMBINING APS AND CDAS

This chapter will evaluate the performance metrics for the three approaches to combining APS and CDA operations. These metrics are evaluated for both ±15- and ±60-second RTA errors. All of the approaches were tested at the maximum runway capacity, which equated to a 100-second spacing at the metering fixes.

A. 3°-CDAs with AMSTAR

Using AMSTAR to precisely space 3°-CDA routes was the first approach to combining the APS and CDA concepts. This approach was evaluated for the two RTA-error cases.

1. ±15-second RTA Error Case

Spacing Errors and Schedule Deviation

Over a single 100-aircraft simulation, the maximum schedule deviation was 12 seconds, as shown in Figure 50, plot (b). The schedule deviation plot did not grow without bound, thus indicating that the 3°-CDA routes and RTA-error conditions did not cause instabilities when used with AMSTAR. The spacing errors shown in plots (c) and (d), are a sharp contrast to those observed when no precision spacing system was used (see Figure 43). The spacing-error variability was reduced, with a 3.24-second standard deviation around a 0.03-second mean. Although AMSTAR reduced the standard deviation by approximately half when compared to the previous scenario, the distribution around the mean does not appear Gaussian-like. Eighty-two percent of the aircraft in the single simulation run had spacing errors greater than or

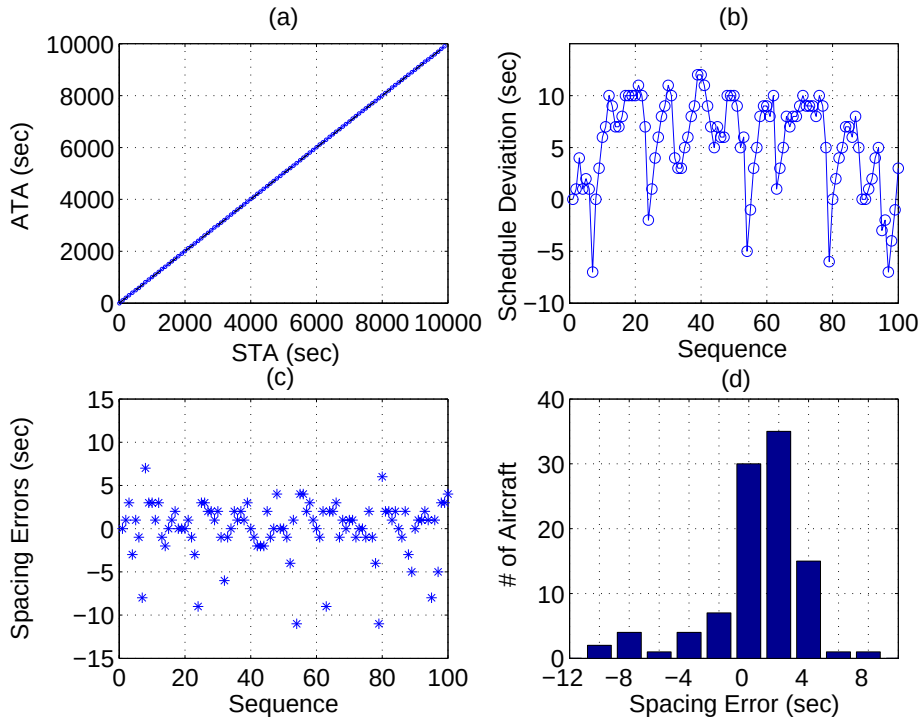

Fig. 50. Spacing errors and schedule deviation for the 3°-CDAs with AMSTAR (±15-second case).

equal to −1 second, however there were eighteen aircraft with spacing errors less than −1 second. Two aircraft had a −11-second spacing error, which was equivalent to an 89-second spacing with their leads. These outliers are indicative of the diminished deceleration capabilities of CDA operations, where aircraft were unable to decrease their speeds to prevent crossing the threshold too closely to their leads.

The spacing errors for each aircraft were averaged over 40 simulations and are shown in Figure 51, where plot (b) shows two separate mean-spacing-error distributions for aircraft leaving from the Fever and Howdy metering fixes. Plot (a) shows a periodic, nine-aircraft pattern, but it differs from the pattern seen when the spacing errors were averaged for the step descents with AMSTAR (Figure 25). Table XIV lists

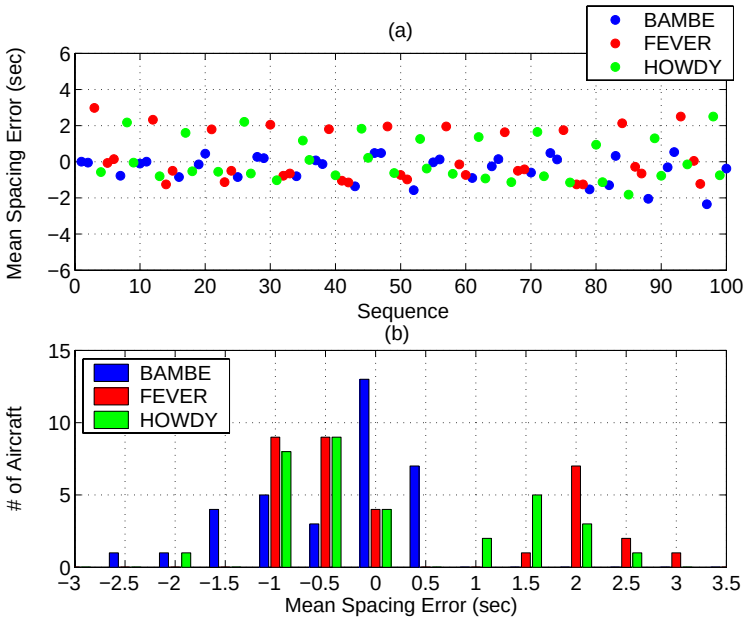

Fig. 51. Mean spacing errors for the 3°-CDAs with AMSTAR (±15-second case).

the spacing-error statistics by metering fix, and in this simulation run, the spacing-error standard deviations are approximately the same for all three metering fixes. The nine-aircraft pattern is also reflected in the mean schedule deviation averaged over 40 simulation runs (see Figure 52).

Table XIV. Spacing Errors for 3°-CDAs with AMSTAR (±15-second Case).

Spacing Error	**Bambe**	**Fever**	**Howdy**
max (seconds)	9	7	10
mean (seconds)	-0.37	0.24	0.09
STD (seconds)	2.60	2.58	2.83
min (seconds)	-12	-11	-13

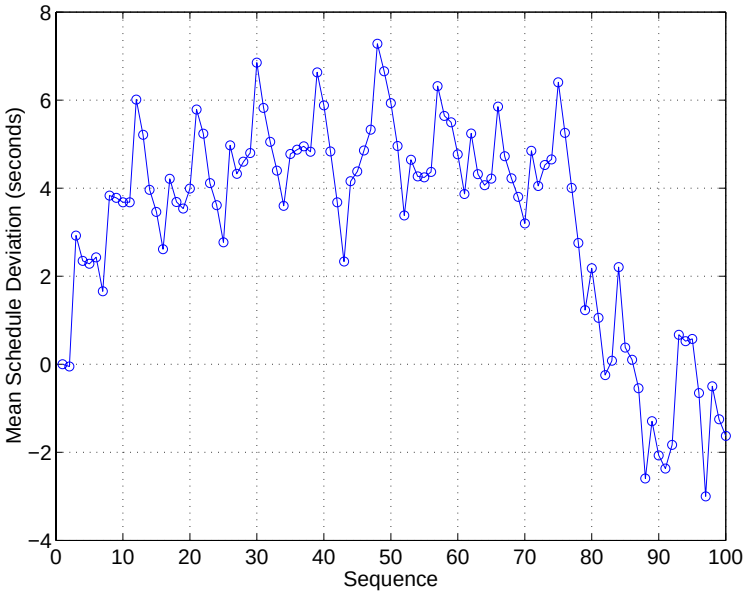

Fig. 52. Mean schedule deviation for the 3°-CDAs with AMSTAR (±15-second case).

Losses of Separation

Within one simulation run, eighteen aircraft lost separation with their leads for an average of 4.94 seconds (see Figure 53). Seven of these aircraft lost separation for less than 3 seconds, which was already determined to be approximately a 2.90-NM separation between aircraft pairs.

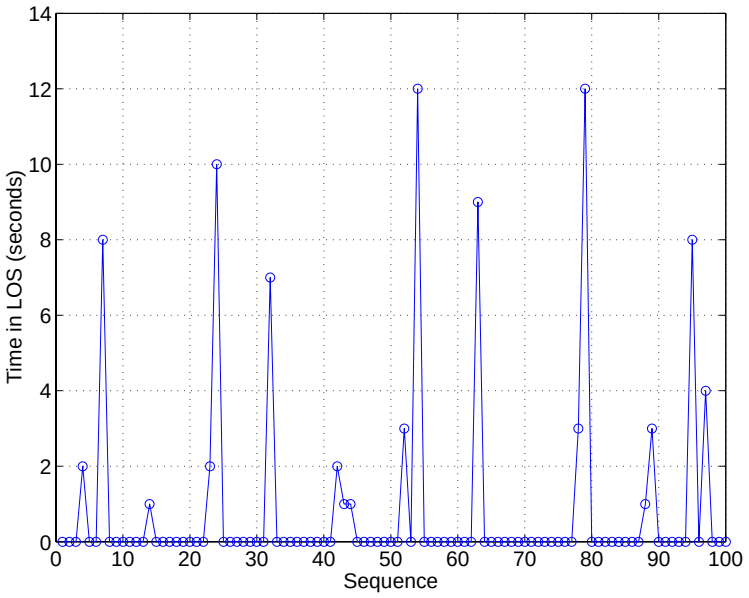

Fig. 53. Losses of separation for the 3°-CDAs with AMSTAR (±15-second case).

The results in the previous chapter showed the distinct relationship between the resultant fix spacing and the time in LoS. When AMSTAR was used to precisely space the aircraft pairs, no clear relationship existed between the "expected" initial spacing and how long the aircraft would lose separation at the threshold. The initial spacing can only be considered "expected" because AMSTAR commanded speed changes to the aircraft in the sequence, and when trailing aircraft were initialized at the metering fix, the leads may have already changed speed. The actual initial spacing was then no longer equal to the "expected" initial spacing. Figure 54 shows that no relationship

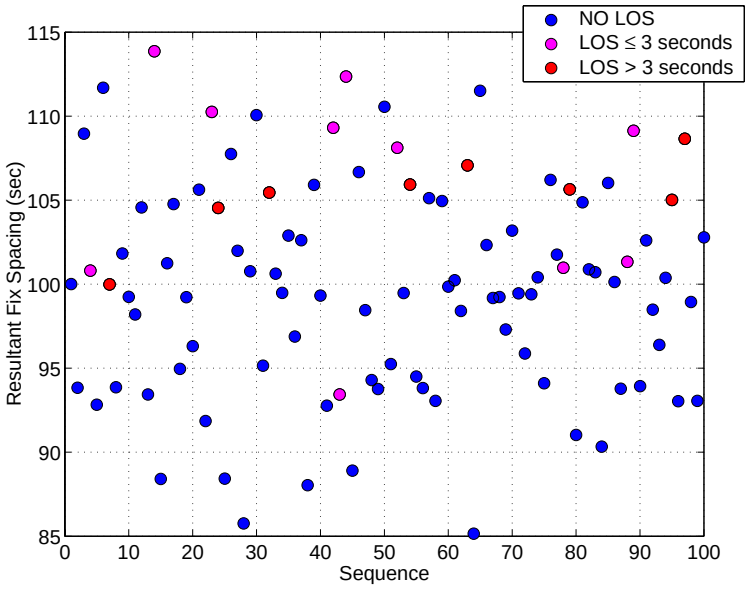

Fig. 54. Relationship between LoS time and the "expected" initial spacing when AMSTAR was used.

exists between the "expected" initial spacing and the time in LoS.

The maximum time that separation was lost in each scenario is shown in Figure 55, where 16 seconds was the maximum LoS time between two aircraft. Figure 45 indicates that this LoS time is roughly equivalent to a 2.57-NM separation. Over the 40 simulation runs, 679 aircraft or 16.98% lost separation with their leads. Only 259 or 6.48% lost separation for more than 3 seconds. While these results are a significant improvement over the results for the 3°-CDAs without AMSTAR, the number of separation losses would likely be unacceptable in current-day operation.

Speed Changes

Figure 56 shows the number of AMSTAR-induced or additional speed changes in an individual simulation run. Over the 100-aircraft sequence, the mean number of additional speed changes was 1.59, which is less than the mean number of speed

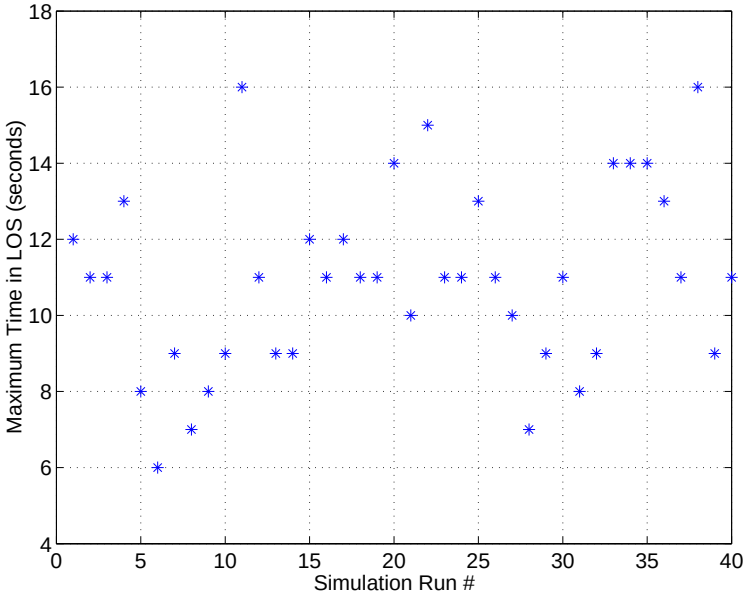

Fig. 55. Maximum time in a LoS for the 3°-CDAs with AMSTAR (±15-second case).

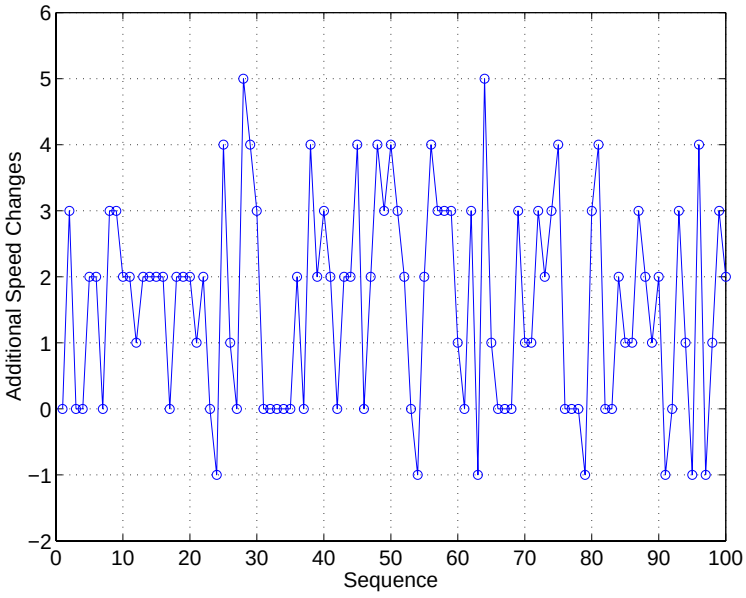

Fig. 56. Additional speed changes for the 3°-CDAs with AMSTAR (±15-second case).

changes that were experienced by aircraft that flew the step descents. Seven aircraft had a negative number of additional speed changes, which was a result of AMSTAR-commanded decelerations that occurred in such a manner as to smooth the speed profile into one continuous deceleration.

Figure 57 compares the speed time histories of the 24th and the 28th aircraft. The 24th aircraft was one of the aircraft with a negative number of additional speed changes, and the 28th aircraft had five additional speed changes, which was the maximum number in this simulation run. The 24th aircraft was commanded to

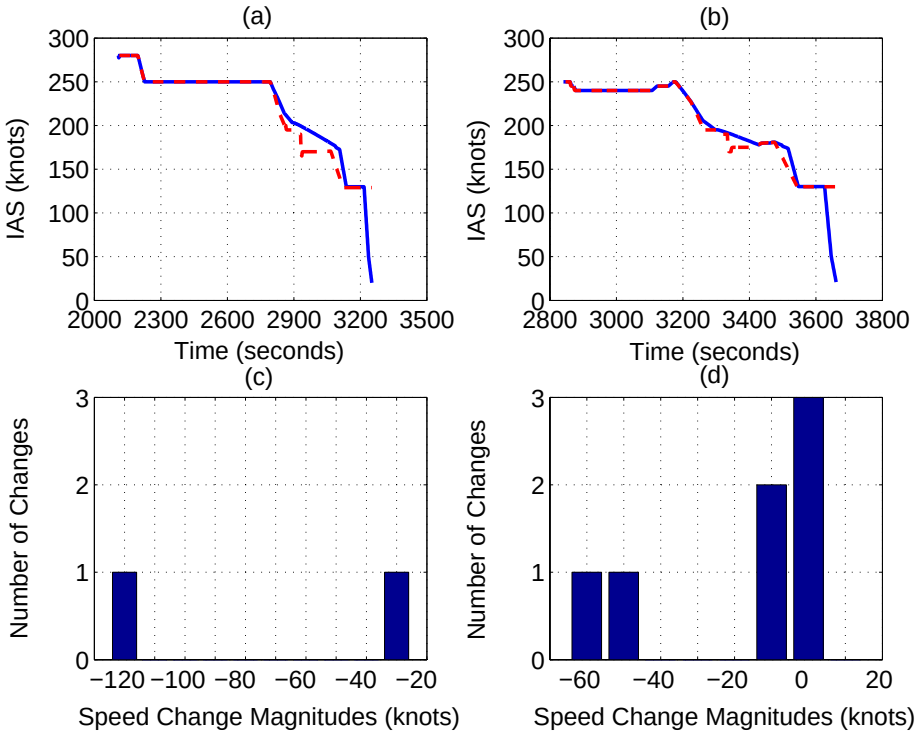

Fig. 57. Speed time-histories and speed change magnitudes for the 24th and 28th aircraft (3°-CDAs with AMSTAR). Plots (a) and (b) are the IAS time histories for aircraft numbers 24 and 28, respectively. The AMSTAR-commanded speeds are shown in red. The speed-change magnitudes are shown in plots (c) and (d).

decelerate once it started to slow from 250 kts. Ultimately, this aircraft was unable to decelerate enough to reduce its spacing error with its lead, which was equal to −9 seconds at the threshold. AMSTAR commanded the 28th aircraft to change speed five times to maintain precise spacing with its lead, which resulted in a 2-second spacing error at the runway threshold. As was shown in Figure 54, the expected initial spacing errors of these aircraft alone could not predict the threshold spacing results. The 24th aircraft and its lead had an expected initial spacing at the metering fix that was greater than 100 seconds; however, AMSTAR ultimately commanded the 24th aircraft to decelerate.

The number of additional speed changes averaged over 40 simulations runs is shown in Figure 58, where the mean number of AMSTAR-induced speed changes was 1.70. Aircraft leaving from the Bambe fix had an average of 1.37 additional speed changes, aircraft leaving from Fever had 1.91 changes, and aircraft leaving from Howdy had 1.84 changes. On average, Bambe aircraft again had fewer speed changes, which is evident in Figure 58.

Transit Times

Over the 4,000 simulated aircraft, AMSTAR increased the 3°-CDA route transit times by as much as 27 seconds and decreased the transit times by as much as 30 seconds. The transit times averaged over 40 simulation runs had a mean difference of 0.36% and a standard deviation equal to 0.76%; the mean transit-time difference of each aircraft over the 40 runs is shown in Figure 59.

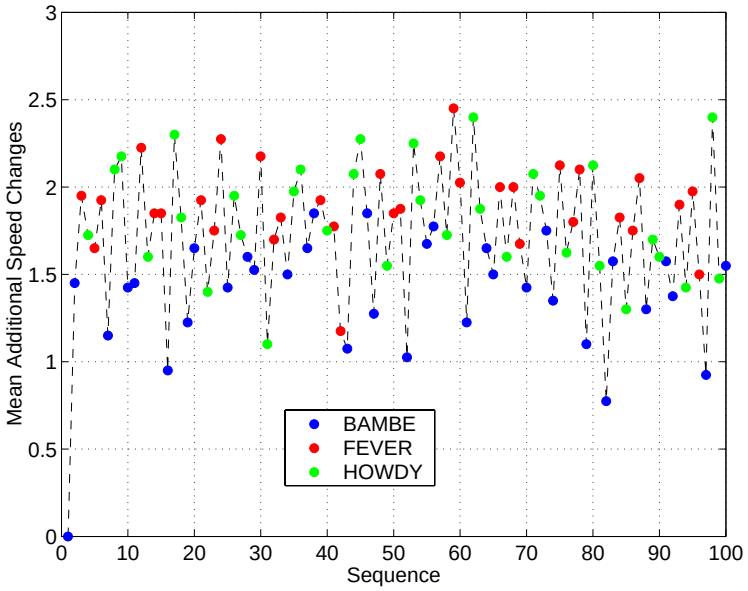

Fig. 58. Mean additional speed changes for the 3°-CDAs with AMSTAR (±15-second case).

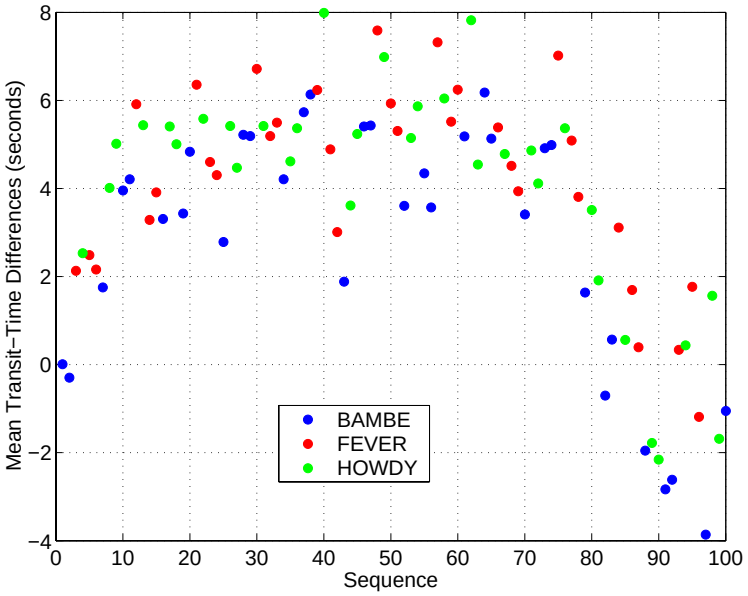

Fig. 59. Mean transit-time differences for the 3°-CDAs with AMSTAR (±15-second case).

Fuel Consumption

The fuel consumptions averaged over the 40 simulation runs are shown in Figure 60, where the dashed lines indicate the mean fuel consumption for that route, and the solid lines represent the nominal values for 3°-CDAs as given in Chapter VII. The effects of the simulation time precision are obvious in this case.

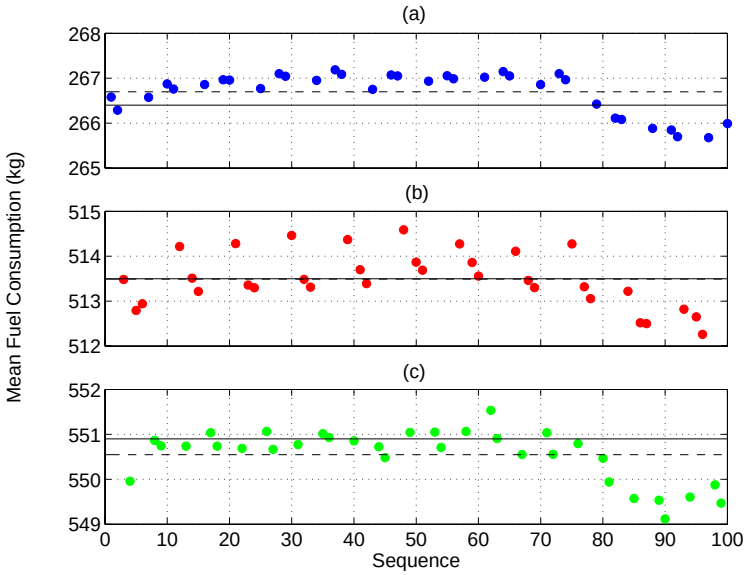

Fig. 60. Mean fuel consumption for the 3°-CDAs with AMSTAR (±15-second case). Plots (a), (b), and (c) are for aircraft flying the Bambe, Fever, and Howdy routes, respectively.

Table XV lists the mean, maximum, and minimum fuel consumption values by metering fix. The percent differences from nominal are included in parentheses. These results show that AMSTAR did not pose a significant cost to the CDA fuel consumption. At most, AMSTAR-induced speed changes only resulted in 1% more fuel usage, and the mean fuel consumption was very close to the nominal 3°-CDA values given in Chapter VII.

Table XV. Fuel Consumption for 3°-CDAs with AMSTAR (±15-second Case).

Fuel Consumption	**Bambe**	**Fever**	**Howdy**
max (kg)	269.06 (1.00)	517.57 (0.79)	554.83 (0.71)
mean (kg)	266.70 (0.11)	513.49 (-0.00)	550.55 (-0.06)
STD (kg)	0.84	1.27	1.35
min (kg)	263.01 (-1.27)	509.58 (-0.76)	544.95 (-1.08)

2. ±60-second RTA Error Case

Spacing Errors and Schedule Deviation

When the 3°-CDAs were subjected to ±60-second RTA errors at the metering fix, a maximum schedule deviation of 26 seconds occurred in a single 100-aircraft simulation. Again, AMSTAR was able to reduce the spacing-error variability at the threshold (in comparison to the baseline when AMSTAR was not used), but there were still spacing errors as small as −24 seconds (a 76-second spacing between the lead and trailing aircraft). Figure 61 shows the spacing error distribution in plot (d), which has a mean spacing error of 0.10 seconds and a 7.87-second standard deviation.

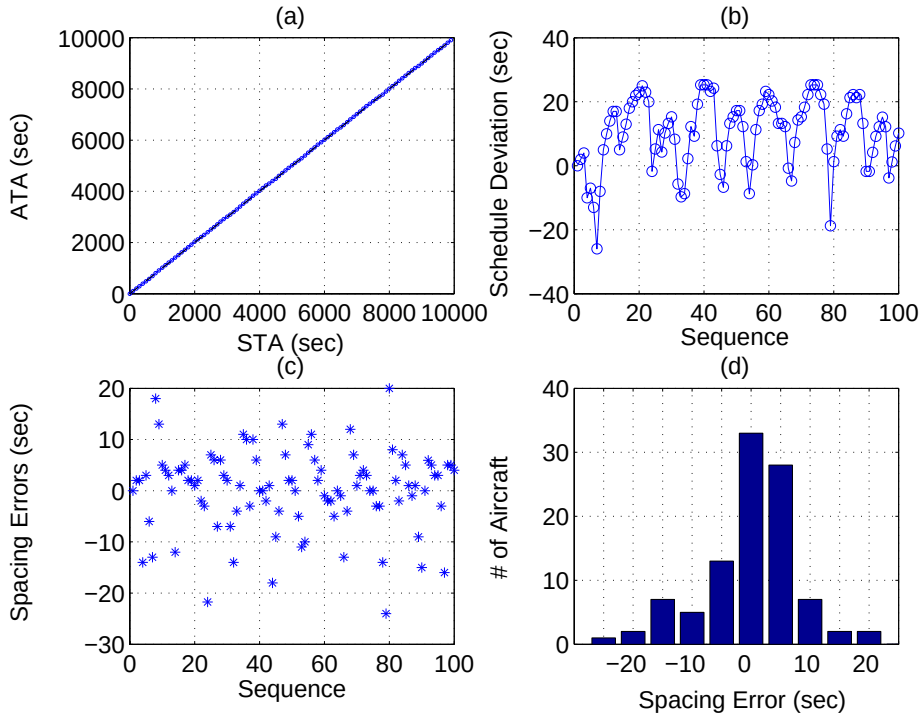

Fig. 61. Spacing errors and schedule deviation for the 3°-CDAs with AMSTAR (±60-second case).

Figure 62 shows the spacing errors averaged over 40 simulation runs. These plots still exhibit the nine-aircraft periodic behavior that was present in previous results; however, the larger RTA errors make the pattern less distinct. Table XVI details the spacing errors for this scenario. This table confirms that on average, the aircraft flying the Bambe route differed in behavior than those flying the Fever and Howdy routes. Aircraft flying from the Bambe metering fix had greater variability in spacing errors, and the mean spacing error was negative.

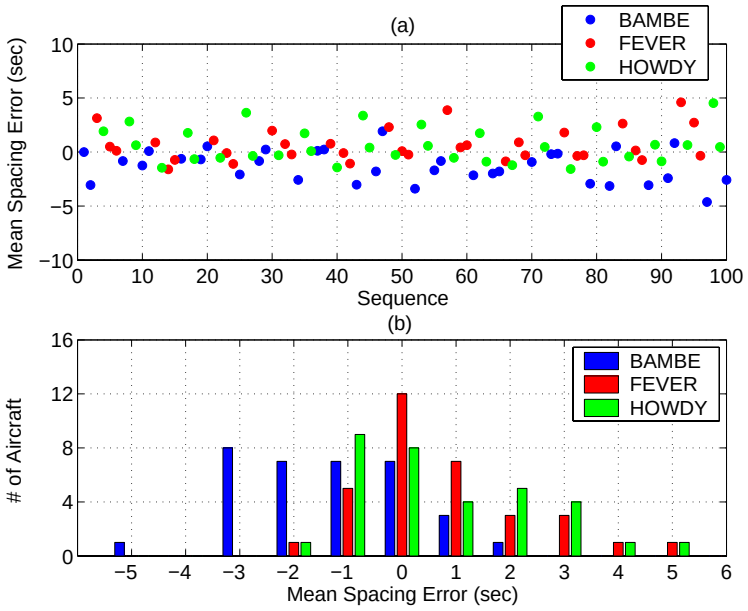

Fig. 62. Mean spacing errors for the 3°-CDAs with AMSTAR (±60-second case).

Losses of Separation

Out of the 40 simulation runs, thirty-six of those simulations had an aircraft that lost separation for more than 50 seconds (see Figure 63). Some of these separation losses were due to initializing aircraft in a LoS situation, however many of these losses were a result of decreased deceleration capabilities that prevented aircraft from reducing their

Table XVI. Spacing Errors for 3°-CDAs with AMSTAR (±60-second Case).

Spacing Error	Bambe	Fever	Howdy
max (seconds)	27	27	27
mean (seconds)	-1.30	0.64	0.67
STD (seconds)	8.59	7.27	7.27
min (seconds)	-39	-27	-28

initial pair-wise spacing errors. Out of 4,000 aircraft, 1,183 (29.58%) lost separation, which is a 17.30% improvement over the scenario where no precision-spacing tool was used. Of those aircraft that lost separation, 780 (19.50%) lost separation for more than 3 seconds, which was a 24.13% improvement.

Speed Changes

The Bambe aircraft experienced an average of 3.00 additional speed changes, Fever experienced 4.01 additional changes, and Howdy experienced 4.22 additional changes. These averages were approximately twice the number of speed changes when the 3°-CDAs were subjected ±15-second RTA errors. Again, aircraft flying the Bambe route had fewer AMSTAR-induced speed changes than aircraft flying the other routes.

Transit Times

For the 40 simulations, the transit times increased by as much as 49 seconds and decreased by as much as 59 seconds. The mean transit-time difference was 0.27% with a standard deviation of 2.69%. The standard deviation for the ±60-second RTA error case was more than three times that for the ±15-second RTA error case, which is the same trend that was observed when the RTA-error cases were compared for the step-descent routes.

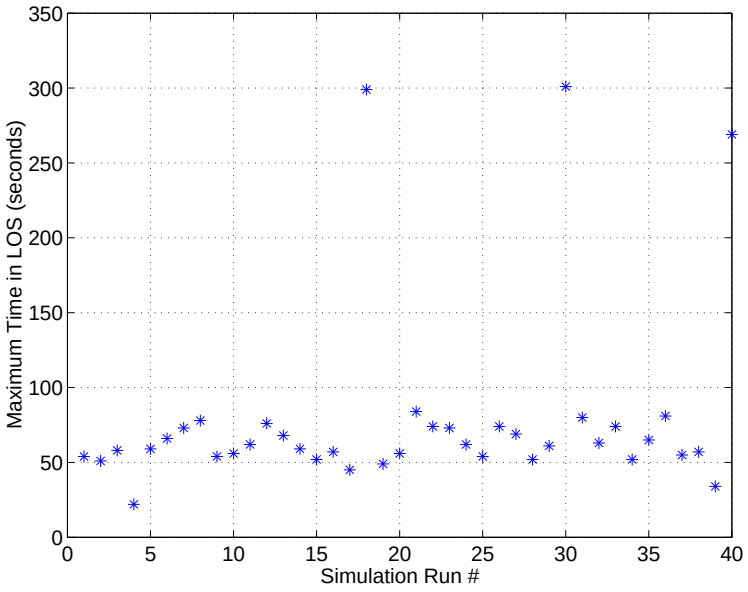

Fig. 63. Maximum time in a LoS for the 3°-CDAs with AMSTAR (±60-second case).

Fuel Consumption

Table XVII presents the fuel consumption results for this scenario. There was a greater cost to the fuel benefits when the initial spacing errors were larger; however, some aircraft were more fuel efficient than the nominal case. The standard deviations were less than those experienced by the aircraft flying step descents for the same RTA-error case.

3. Summary of Results for the 3°-CDAs with AMSTAR

Whereas AMSTAR reduced the variability of the spacing errors at the threshold and the number of separation losses in comparison to the baseline scenario of 3°-CDAs without AMSTAR, the maximum capacity could not be achieved using AMSTAR; 6.48% and 19.50% of the 4,000 aircraft lost separation for more than 3 seconds for the ±15- and ±60-second-RTA-error cases, respectively.

Table XVII. Fuel Consumption for 3°-CDAs with AMSTAR (±60-second Case).

Fuel Consumption	**Bambe**	**Fever**	**Howdy**
max (kg)	277.15 (4.03)	532.18 (3.64)	571.51 (3.74)
mean (kg)	267.01 (0.23)	514.44 (0.18)	551.92 (0.19)
STD (kg)	2.83	4.26	4.99
min (kg)	259.41 (-2.62)	505.13 (-1.63)	540.59 (-1.87)

Similar trends that were observed with the step-descent simulations persisted with the 3°-CDA simulations when AMSTAR was used. The mean spacing-error plots exhibited a nine-aircraft periodic behavior associated with the sequence of metering-fix arrivals, though this pattern was less pronounced for the ±60-second-RTA-error case. Aircraft leaving from the Bambe metering fix typically had larger spacing-error variability and fewer speed changes, which was also a result in the step-descent scenarios.

The standard deviations of the fuel consumption increased with the larger initial spacing errors, however these values were less than those seen in the step-descent simulations. In the ±15-second-RTA-error case, the fuel use only increased or decreased by approximately 1% of the nominal values. The ±60-second RTA errors resulted in fuel consumption increases of at most 4.0% and decreases of at most 2.6%

B. 3°-CDAs with AMSTAR and Spoilers

The second approach to combining APS and CDAs was to fly the 3°-CDAs with AMSTAR and to use spoilers to increase drag when necessary. The results for the ±15- and ±60-second-RTA-error cases are discussed below.

1. ±15-second RTA Error Case

Spacing Errors and Schedule Deviation

The benefit of the spoiler model is evident in Figure 64, where there is reduced variability in the spacing errors in comparison to the previous scenario, which did not include spoilers. The mean spacing error for this single 100-aircraft simulation is 0.05 seconds with a standard deviation of 1.99 seconds. Plot (b) shows a maximum schedule deviation of 15 seconds, which is slightly more than the previous scenario.

The spacing errors averaged over 40 simulation runs and separated by metering fix are shown in Figure 65, where these plots again show the nine-aircraft pattern that was evident in the other scenarios where AMSTAR was used. Plot (b) shows two separate distributions for the Fever and Howdy aircraft, as was shown in Figure 51.

The spacing-error statistics by metering fix are listed in Table XVIII. The reduction in the spacing-error standard deviation is the most notable difference when the spoilers were modeled in contrast to the previous scenario. The minimum spacing errors were smaller in magnitude, thus further indicating improved deceleration.

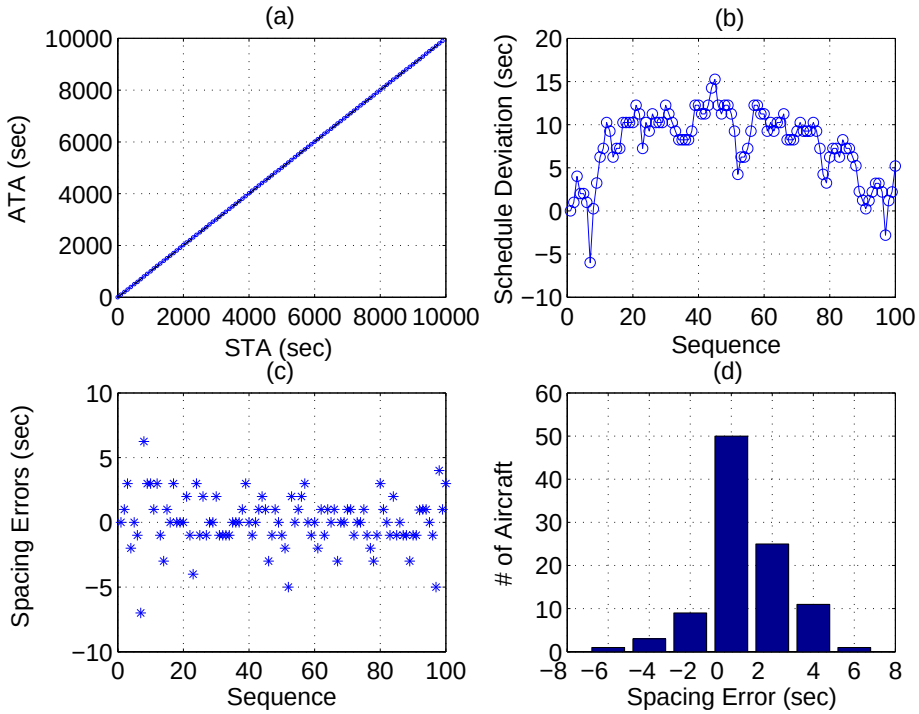

Fig. 64. Spacing errors and schedule deviation for the 3°-CDAs with AMSTAR and spoilers (±15-second case).

Table XVIII. Spacing Errors for 3°-CDAs with AMSTAR and Spoilers (±15-second Case).

Spacing Error	**Bambe**	**Fever**	**Howdy**
max (seconds)	5	7	10
mean (seconds)	-0.50	0.42	0.14
STD (seconds)	1.94	1.74	1.74
min (seconds)	-11	-5	-9

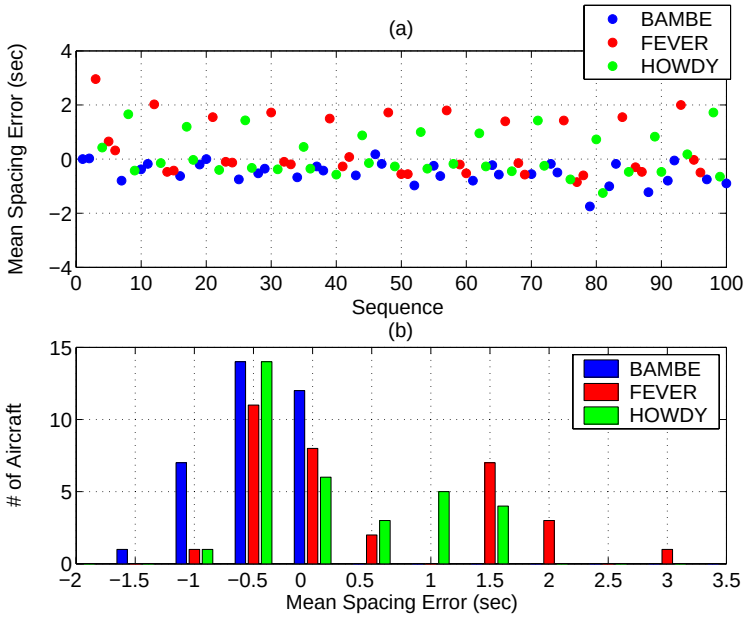

Fig. 65. Mean spacing errors for the 3°-CDAs with AMSTAR and spoilers (±15-second case).

Losses of Separation

In the previous scenario, eighteen aircraft lost separation for an average of almost five seconds in one single simulation. With improved deceleration capability in this scenario, only eleven aircraft lost separation for an average of 2.64 seconds (see Figure 66). Furthermore, of these eleven aircraft, only three lost separation for more than three seconds.

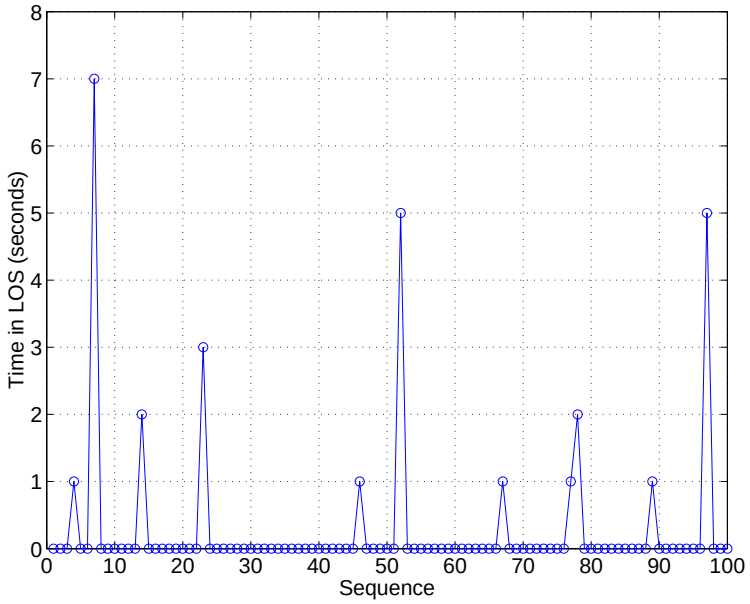

Fig. 66. Losses of separation for the 3°-CDAs with AMSTAR and spoilers (±15-seconds).

Figure 67 shows the total time that each aircraft in the sequence deployed spoilers. Twelve aircraft used spoilers for an average of 10.58 seconds. Aircraft that used spoilers did not lose separation with their leads and had an average threshold spacing error of 0.33 seconds. Recall that in the previous scenario, eighteen aircraft lost separation in the individual simulation run that was evaluated. In this scenario, nine of those aircraft deployed spoilers and prevented a LoS.

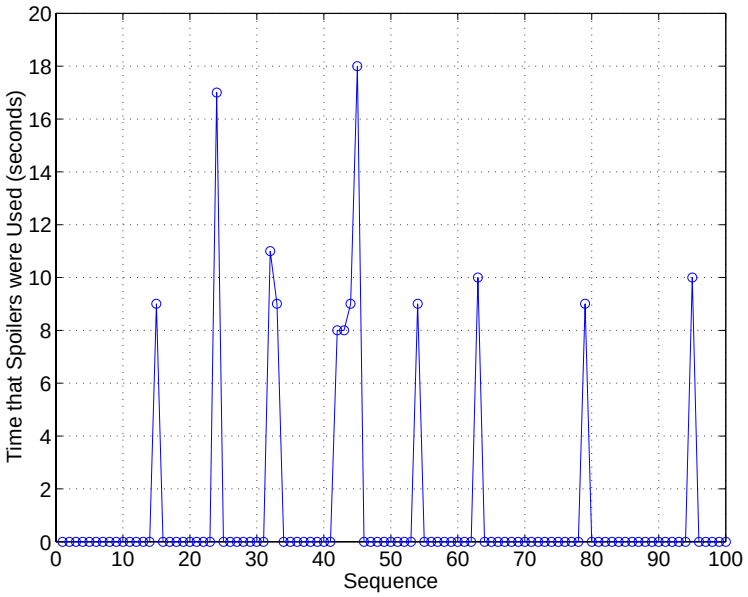

Fig. 67. Total time that spoilers were used by each aircraft (±15-second case).

The 45th aircraft used spoilers for a total of eighteen seconds. Figure 68 shows the actual- and commanded-speed time histories, and where the spoilers provided increased drag to meet the AMSTAR-commanded speed is indicated. The arrow indicates the change in the slope of the speed plot when spoilers were used.

Of the 4,000 aircraft simulated, 412 lost separation (10.30%), but only 87 of those (2.18%) lost separation for more than 3 seconds. Approximately 15% of the aircraft used spoilers for an average of 8.53 seconds. Only 10 aircraft that used spoilers also lost separation, and those losses were limited to 3 seconds, or 2.90 NM.

Speed Changes

In this scenario, the mean number of speed changes was 1.77, which is just slightly more than the previous scenario. In this case, only two aircraft had a negative number of additional speed changes in comparison to seven when spoilers were not used.

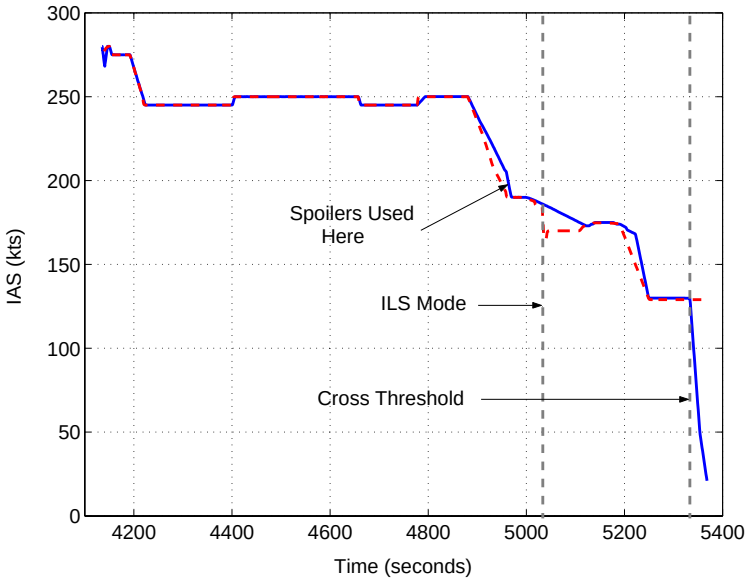

Fig. 68. Speed time history of 45th aircraft. The actual IAS is shown by the blue line, and the AMSTAR-commanded speed is shown by the red line.

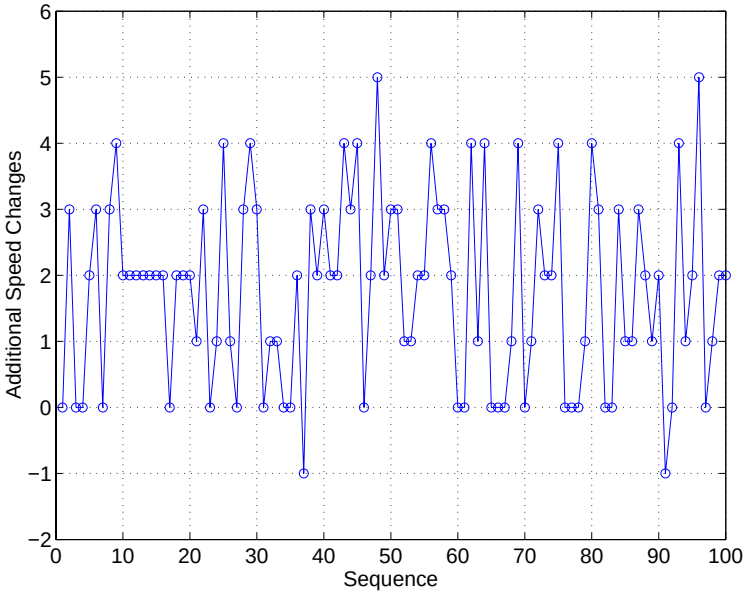

Fig. 69. Additional speed changes for the 3°-CDAs with AMSTAR and spoilers (±15-second case).

The number of additional speed changes averaged over 40 simulation runs was 1.90, which was again an increase over the previous scenario. Aircraft flying through the Bambe metering fix still had fewer speed changes with a mean of 1.42. Fever and Howdy aircraft had average additional speed changes of 2.22 and 2.06, respectively.

Transit Times

Over 40 simulations, the mean percent difference in transit times was 0.55% with a standard deviation of 0.67%. This mean is slightly higher than the previous scenario, which indicates that the use of spoilers tended to increase the average transit times; however, the standard deviation was less than the case where spoilers were not used. The transit times were increased and decreased by as much as 28 seconds.

Fuel Consumption

The fuel consumption is summarized in Table XIX; the fuel-consumption means and standard deviations increased over all of the routes in comparison to the scenario when no spoilers were used. Improved spacing-error variability resulted in decreased fuel efficiency; however, the fuel cost was not significant.

Table XIX. Fuel Consumption for 3°-CDAs with AMSTAR and Spoilers (±15-second Case).

Fuel Consumption	**Bambe**	**Fever**	**Howdy**
max (kg)	271.89 (2.06)	523.92 (2.03)	560.85 (1.81)
mean (kg)	267.27 (0.33)	516.00 (0.49)	552.93 (0.37)
STD (kg)	0.99	1.80	1.64
min (kg)	263.40 (-1.12)	511.90 (-0.31)	548.24 (-0.48)

2. ±60-second RTA Error Case

Spacing Errors and Schedule Deviation

The schedule deviation and spacing errors for the ±60-second-RTA-error case are shown in Figure 70, where the variability in the spacing errors is a surprising result. Although it was expected that the spoilers would improve the system performance by reducing the spacing errors between aircraft pairs, the improvement was more significant than anticipated. The mean spacing error in Figure 70, plots (c) and (d), is 0.16 seconds with a standard deviation of 2.43 seconds.

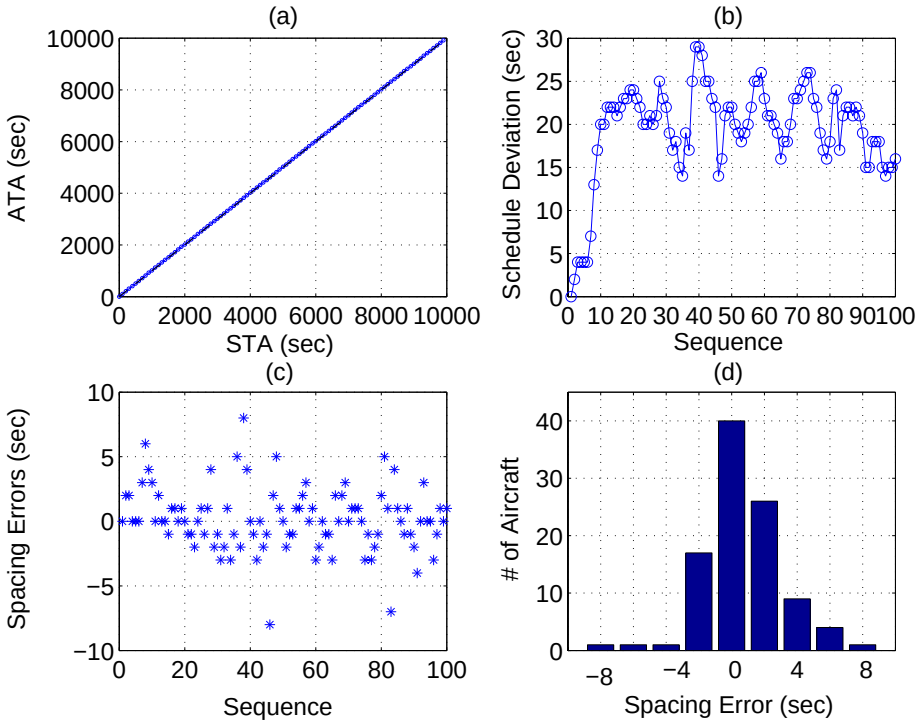

Fig. 70. Spacing errors and schedule deviation for the 3°-CDAs with AMSTAR and spoilers (±60-second case).

The mean spacing errors by metering fix still exhibited periodic behavior, but the variability was less than that seen when spoilers were not used (see Figure 71). The

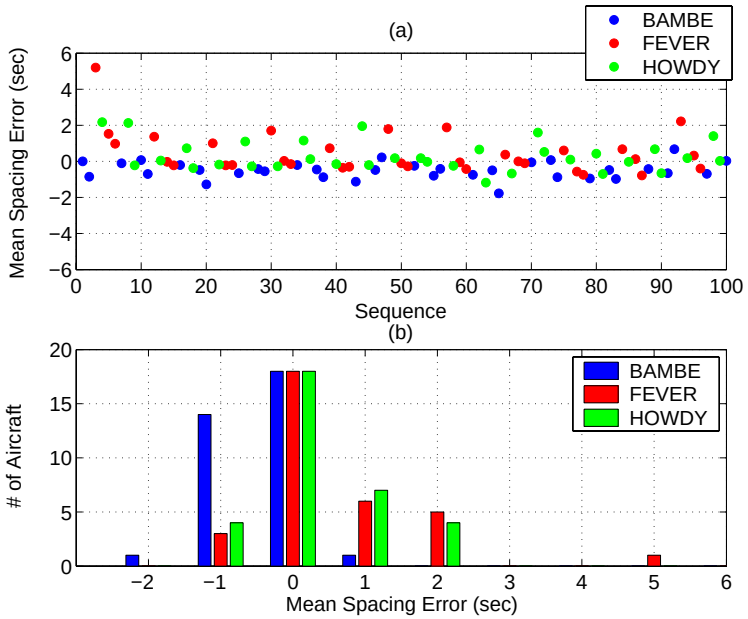

Fig. 71. Mean spacing errors for the 3°-CDAs with AMSTAR and spoilers (±60-second case).

spacing-error statistics for each metering fix are listed in Table XX. The standard deviations are significantly reduced from the AMSTAR scenario where no spoilers were modeled. The minimum spacing errors of aircraft leaving from Fever and Howdy increased from −27 and −28 seconds in the scenario without spoilers to −7 and −11 seconds in this scenario, respectively.

Losses of Separation

In a single 100-aircraft simulation, seventeen aircraft lost separation, and only two of those lost separation for more than 3 seconds. These results are comparable to the ±15-second-RTA-error case, likely due to the use of spoilers. Thirty-two aircraft used spoilers for an average of 11.28 seconds, and those aircraft had a mean spacing error of 0.50 seconds.

In this scenario, 869, or 21.73% of the 4,000 aircraft simulated, lost separation

Table XX. Spacing Errors for 3°-CDAs with AMSTAR and Spoilers (±60-second Case).

Spacing Error	**Bambe**	**Fever**	**Howdy**
max (seconds)	14	28	26
mean (seconds)	-0.50	0.47	0.31
STD (seconds)	3.12	3.09	3.03
min (seconds)	-17	-7	-11

with their leads. This is a 25.15% improvement over the results when no precision spacing tool was used and a 7.85% improvement when AMSTAR was used without spoilers. Of the 869 aircraft that lost separation, only 196 (4.90%) lost separation for more than 3 seconds, which is fewer than the number in the ±15-second-RTA-error case with AMSTAR and no spoilers. One-third of the 4,000 aircraft used spoilers for a mean of 11.89 seconds, where 47 seconds was the maximum amount of time that spoilers were used.

Speed Changes

Over the 40 simulation runs, aircraft leaving from the Bambe metering fix experienced an average of 3.21 additional speed changes. The aircraft leaving from Fever and Howdy experienced 4.48 and 4.70 additional speed changes on average. These mean values are slightly greater than the results for the scenario without spoilers.

Transit Times

The mean transit-time difference was 1.12% with a standard deviation of 2.24% over 4,000 aircraft. The standard deviation did not change significantly from the scenario without spoilers, however the mean transit-time difference increased by 0.85%. This

change indicates that more aircraft were able to decelerate to achieve smaller spacing errors, thus increasing the mean transit times. Overall, the maximum transit-time increase was 93 seconds, which is almost twice the increase without spoilers, and the maximum decrease was 69 seconds.

Fuel Consumption

Adding the use of spoilers significantly impacted the maximum fuel consumption, however the standard deviation of the fuel usage was not noticeably impacted. The fuel consumption statistics by metering fix are detailed in Table XXI.

Table XXI. Fuel Consumption for 3°-CDAs with AMSTAR and Spoilers (±60-second Case).

Fuel Consumption	**Bambe**	**Fever**	**Howdy**
max (kg)	286.52 (7.55)	542.36 (5.62)	582.79 (5.79)
mean (kg)	269.42 (1.13)	518.70 (1.01)	556.27 (0.98)
STD (kg)	2.81	4.56	4.71
min (kg)	261.66 (-1.78)	507.56 (-1.16)	542.44 (-1.54)

3. Summary of Results for the 3°-CDAs with AMSTAR and Spoilers

Adding the use of spoilers improved the spacing-error variability. The minimum spacing errors were less negative, and fewer losses of separation occurred between aircraft pairs. When the aircraft were subjected to ±15-second RTA errors, only 2.18% of the 4,000 aircraft lost separation for more than 3 seconds, which is a 4.30% improvement over the scenario without spoilers. The ±60-second-RTA-error case showed a 14.60% improvement in the same metric, where only 4.90% lost separation for more than 3 seconds. Spoiler use increased from 15% to 33% of the aircraft

simulated when the RTA-error limits increased from ±15 to ±60 seconds.

The mean number of speed changes increased when spoilers were used, and then the increase in RTA errors more than doubled the mean number of AMSTAR-induced speed changes. These increases in the number of speed changes resulted in longer transit times, which then resulted in a greater cost to the fuel benefit than when no spoilers were used, particularly in the ±60-second-RTA-error case.

C. 2°-CDAs with AMSTAR

Using AMSTAR to precisely space aircraft flying 2°-CDA routes was the third and final approach to combining APS and CDA concepts. These scenarios were evaluated for the two RTA-error cases.

1. ±15-second RTA Error Case

Spacing Errors and Schedule Deviation

It was expected that 2°-CDA operations would have reduced spacing-error variability because of improved deceleration capabilities during descent, however Figure 72 shows similar results to the scenario that simulated 3°-CDAs without spoilers. The mean spacing error in Figure 72 is 0.15 seconds with a standard deviation of 3.59 seconds.

Averaging the spacing errors of each aircraft in the sequence over 40 simulations shows that the 2°-CDAs present very different results from the 3°-CDA scenarios. The nine-aircraft pattern is still present, however the behavior is different from previous results. This is evident in the spacing-error means for each metering fix in Table XXII. Table XXII also shows an increase in the spacing-error variability of aircraft leaving from the Bambe and Fever metering fixes when compared to the results of the 3°-CDAs-with-AMSTAR scenario.

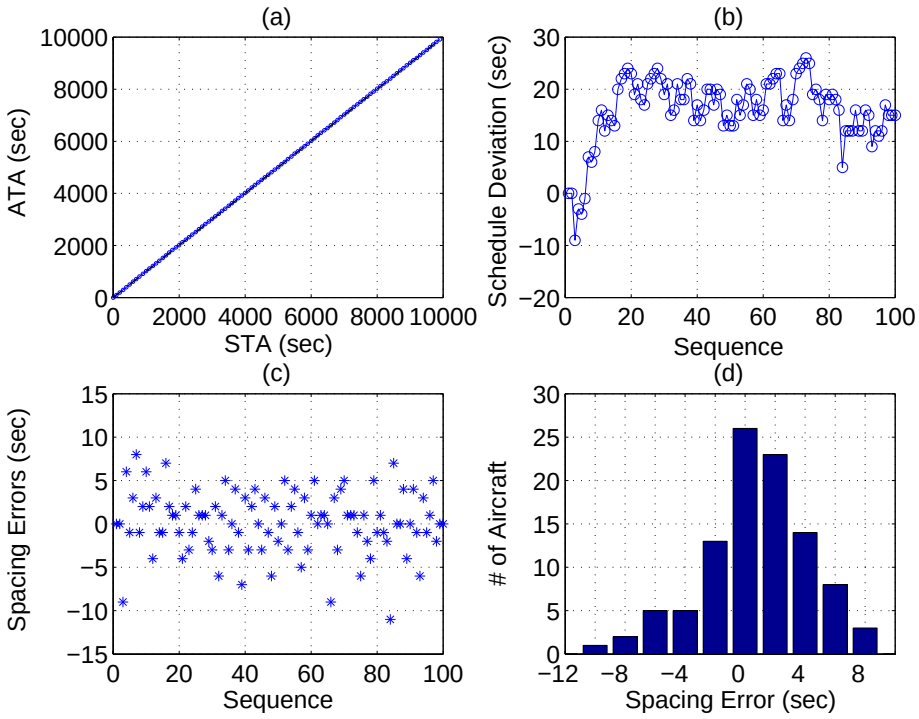

Fig. 72. Spacing errors and schedule deviation for the 2°-CDAs with AMSTAR (±15-second case).

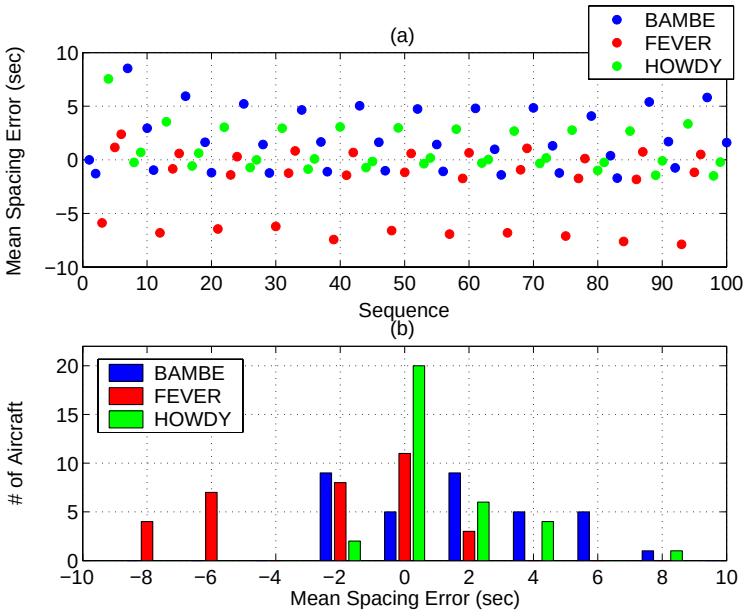

Fig. 73. Mean spacing errors for the 2°-CDAs with AMSTAR (±15-second case).

Table XXII. Spacing Errors for 2°-CDAs with AMSTAR (±15-second Case).

Spacing Error	**Bambe**	**Fever**	**Howdy**
max (seconds)	13	8	12
mean (seconds)	1.85	-2.42	0.92
STD (seconds)	3.14	3.88	2.50
min (seconds)	-8	-14	-5

Losses of Separation

In one simulation run, 24 aircraft lost separation for an average of 4.17 seconds. Fourteen of those aircraft lost separation for more than 3 seconds (see Figure 74). The maximum LoS time in each of the 40 simulation runs is shown in Figure 75, where the results are comparable to the 3°-CDAs-with-AMSTAR scenario results.

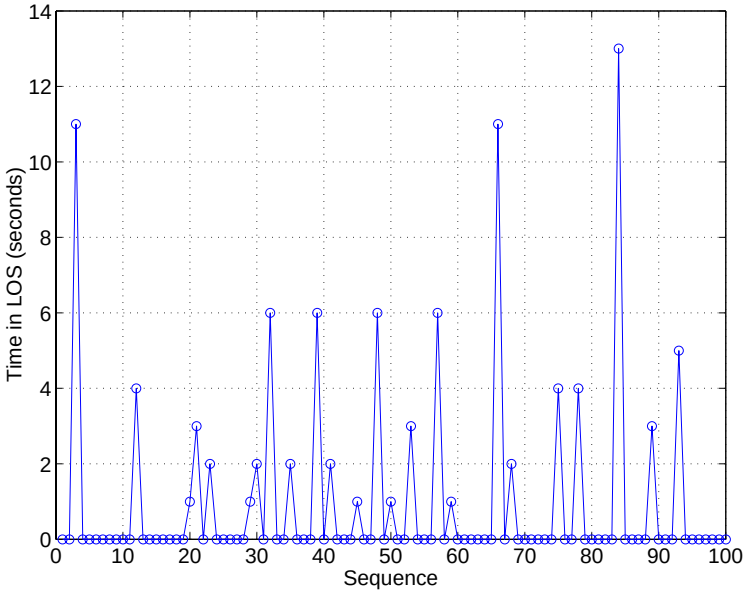

Fig. 74. Losses of separation for the 2°-CDAs with AMSTAR (±15-second case).

It was expected that the 2°-CDAs would show improved spacing performance over the 3°-CDAs with spoilers, however these results showed that out of 4,000 aircraft, 816 aircraft, or 20.40%, lost separation in comparison to the 679 aircraft, or 16.98%, that lost separation in the 3°-CDA case without spoilers. Of those that lost separation, 424 aircraft, or 10.60%, lost separation for more than 3 seconds, which is equivalent to losing more than 0.10-NM of separation. Only 259 aircraft, or 6.48%, lost separation for more than 3 seconds in the 3°-CDA scenario without spoilers.

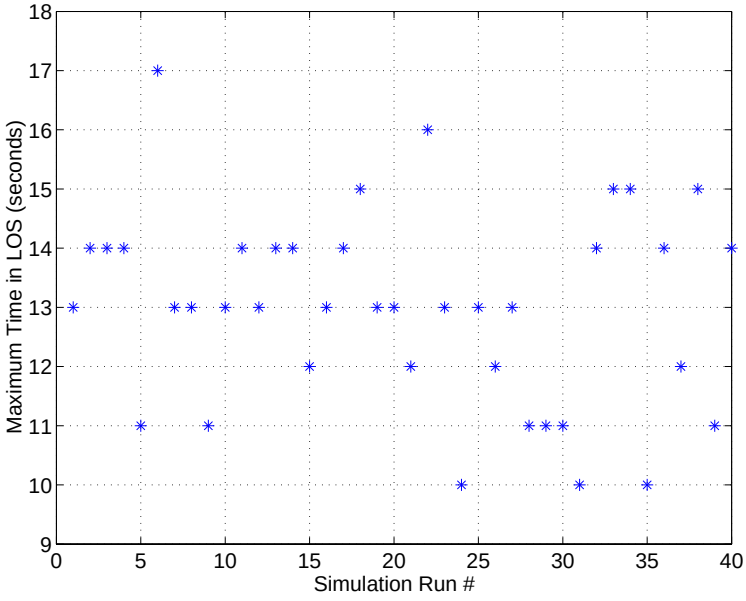

Fig. 75. Maximum time in a LoS for the 2°-CDAs with AMSTAR (±15-second case).

Speed Changes

The mean number of AMSTAR-induced speed changes in one simulation run was 3.69, which was more than twice the number of speed changes for the 3°-CDAs with and without spoilers. The additional speed changes are shown in Figure 76. The 52nd aircraft had seven AMSTAR-induced speed changes, which ultimately resulted in a 5-second spacing error with its lead aircraft. The 66th aircraft only had one additional speed change, and it had a −9-second spacing error with its lead at the threshold. Figure 77 shows the speed time histories and the magnitudes of the speed changes for these two aircraft. Plot (c) shows six speed changes, which were smaller in magnitude. These speed changes helped to maintain precise spacing, however several small changes would not be ideal in actual operation.

The number of additional speed changes by metering fix is shown in Figure 78, where the nine-aircraft periodic behavior is obvious. Aircraft leaving from the Bambe

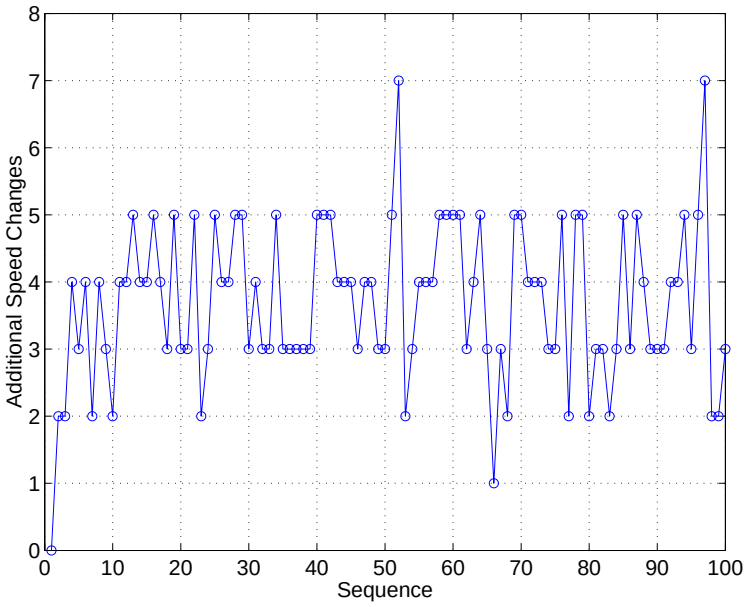

Fig. 76. Additional speed changes for the 2°-CDAs with AMSTAR (±15-second case).

metering fix had a mean of 3.79 additional speed changes, Fever aircraft had a mean of 3.54, and Howdy aircraft had a mean of 3.77. These values are greater than the number of speed changes in the scenario that included spoilers. In this scenario, the Bambe aircraft did not statistically have fewer speed changes as in previous results.

Transit Times

The maximum transit-time increase was 29 seconds, and the maximum decrease was 33 seconds over 40 simulations. Over these simulation runs, the mean percent difference was 0.78% with a standard deviation of 0.88%. These results indicate that AMSTAR tended to increase the 2°-CDA transit times. Figure 79 shows the transit-time increases averaged over 40 simulation runs, where it can be seen that aircraft leaving from the Bambe metering fix typically had greater transit-time increases than aircraft that flew the Fever and Howdy routes.

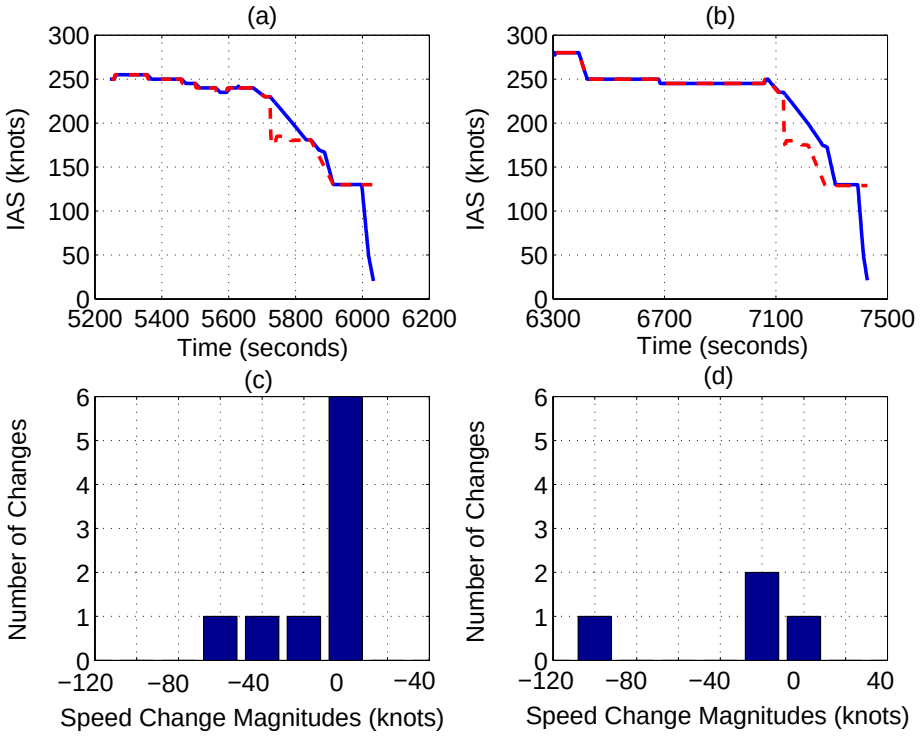

Fig. 77. Speed time histories and speed-change magnitudes for the 52nd and the 66th aircraft (2°-CDAs with AMSTAR). Plots (a) and (b) are the IAS time histories for aircraft numbers 52 and 66, respectively, and the speed-change magnitudes are shown in plot (c) and (d). The AMSTAR-commanded speeds are shown in red.

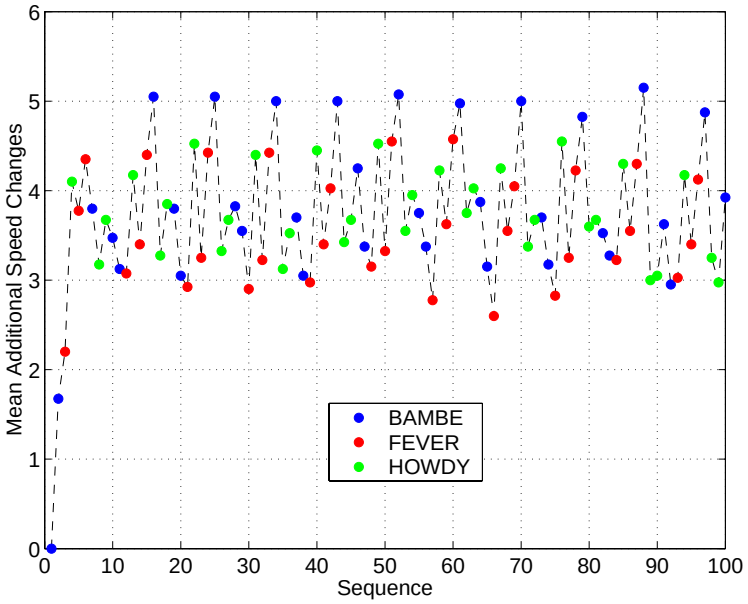

Fig. 78. Mean additional speed changes for the 2°-CDAs with AMSTAR (±15-second case).

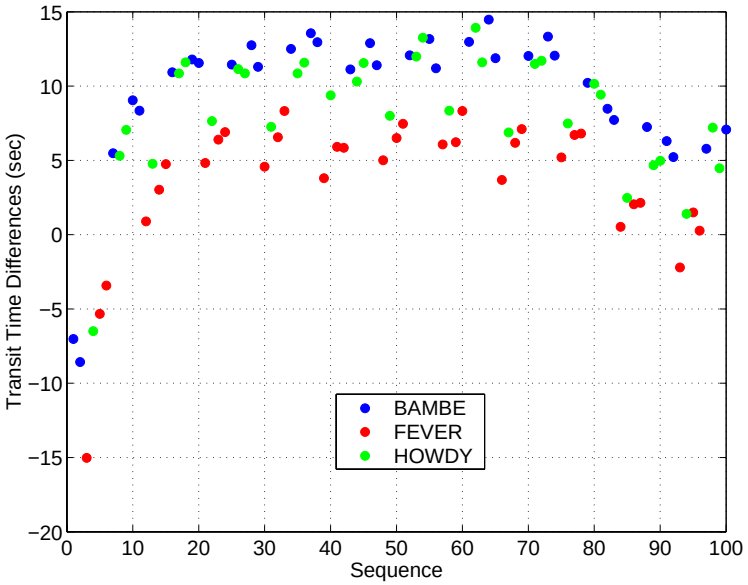

Fig. 79. Mean transit-time differences for the 2°-CDAs with AMSTAR (±15-second case).

Fuel Consumption

The fuel consumption for the 2°-CDAs with AMSTAR is detailed in Table XXIII. These results show that AMSTAR tended to decrease the fuel consumption from nominal, thus making the routes more efficient. The Bambe aircraft had the greatest transit-time increases, however the fuel use did not reflect a significant cost to the CDA fuel efficiency.

Table XXIII. Fuel Consumption for 2°-CDAs with AMSTAR (±15-second Case).

Fuel Consumption	**Bambe**	**Fever**	**Howdy**
max (kg)	228.77 (1.07)	471.20 (0.24)	505.15 (0.48)
mean (kg)	225.43 (-0.40)	466.65 (-0.73)	501.14 (-0.31)
STD (kg)	1.46	1.61	1.66
min (kg)	217.20 (-4.04)	460.91 (-1.95)	495.74 (-1.39)

2. ±60-second RTA Error Case

Spacing Errors and Schedule Deviation

The spacing-error results for a single 100-aircraft simulation run were surprising when the 2°-CDAs were subjected to ±60-second RTA errors. Figure 80 shows that the variability of the spacing errors around zero was less than in the ±15-second-RTA-error case. This result can also be seen in Figure 81, which does not show the distinct distributions between the metering fixes that were characteristic of previous results.

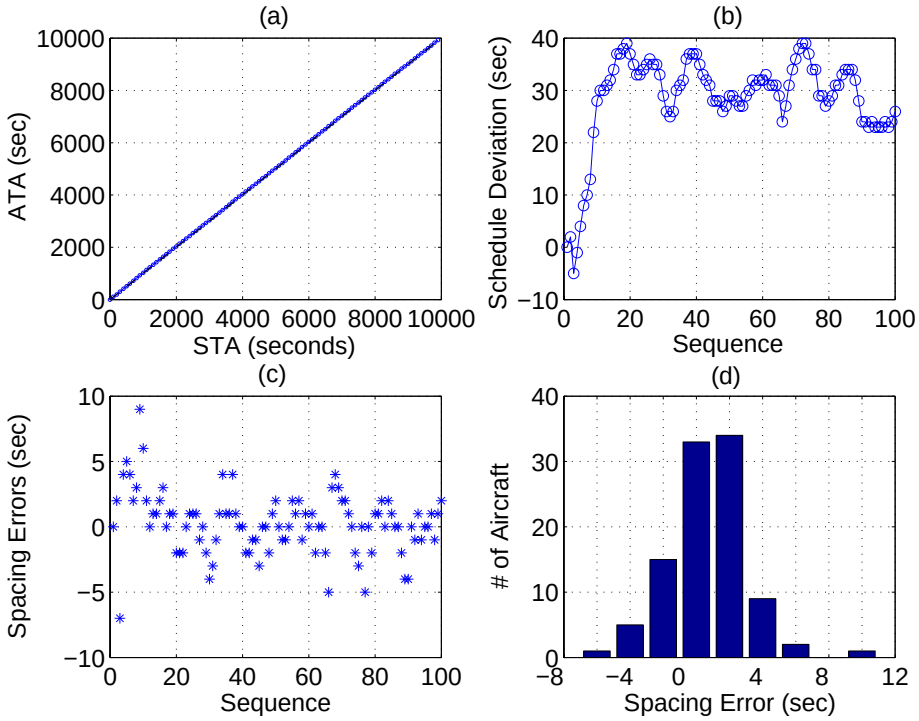

Fig. 80. Spacing errors and schedule deviation for the 2°-CDAs with AMSTAR (±60-second case).

Table XXIV lists the maximum, minimum, and mean spacing errors by metering fix. The spacing-error standard deviations were only slightly greater than the standard deviations calculated in the 3°-CDA scenario that used spoilers.

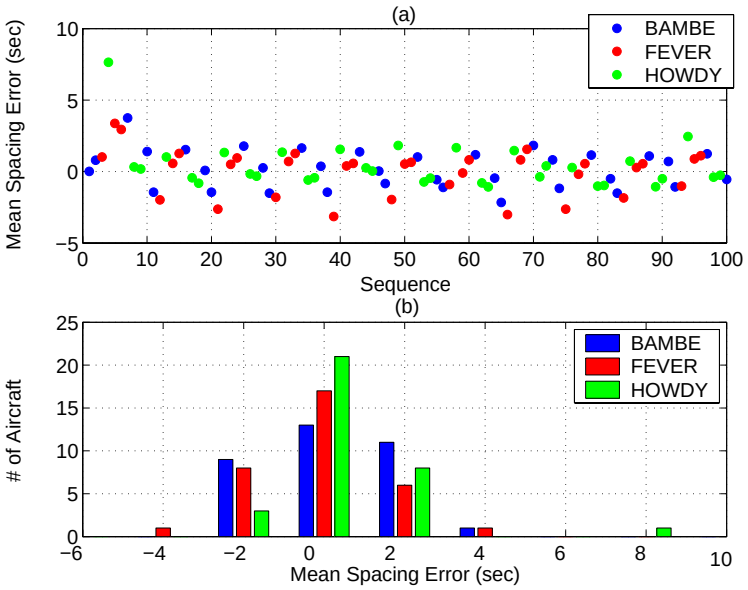

Fig. 81. Mean spacing errors for the 2°-CDAs with AMSTAR (±60-second case).

Table XXIV. Spacing Errors for 2°-CDAs with AMSTAR (±60-second Case).

Spacing Error	**Bambe**	**Fever**	**Howdy**
max (seconds)	32	17	19
mean (seconds)	0.18	0.00	0.37
STD (seconds)	3.44	3.46	3.64
min (seconds)	-11	-14	-11

Losses of Separation

In this scenario, 996 aircraft (out of the 4,000 simulated aircraft) lost separation with their leads, which is 24.90% of the stream. Of those aircraft that lost separation, only 267, or 6.68%, lost separation for more than 3 seconds, which is actually an improvement over the 2°-CDA results for ±15-second-RTA errors.

Speed Changes

For the 40 simulation runs, the Bambe, Fever, and Howdy aircraft experienced an average of 4.07, 5.06, and 5.57 additional speed changes, respectively. As was expected, the larger initial spacing errors resulted in a greater number of speed changes. In contrast to the 2°-CDA results for ±15-second-RTA errors, the aircraft leaving from Bambe did have the least number of speed changes on average, which was the result of the other scenarios that were evaluated.

Transit Times

The maximum transit-time increase was 94 seconds and the maximum decrease was 57 seconds, which is a similar result to that seen in previous scenarios with ±60-second RTAs.

Fuel Consumption

Table XXV details the fuel-consumption statistics for this RTA-error case. As shown in other results for the ±60-second RTA errors, increasing the initial spacing errors resulted in higher fuel consumption. In this case, the mean fuel-consumption values for all three metering fixes were greater than the nominal values, which implies that on average these routes were less efficient when subjected to more significant initial spacing errors.

Table XXV. Fuel Consumption for 2°-CDAs with AMSTAR (±60-second Case).

Fuel Consumption	**Bambe**	**Fever**	**Howdy**
max (kg)	243.41 (7.54)	486.98 (3.59)	522.87 (4.01)
mean (kg)	229.06 (1.20)	471.90 (0.39)	506.16 (0.69)
STD (kg)	4.02	4.07	4.63
min (kg)	214.38 (-5.29)	459.69 (-2.21)	492.78 (-1.98)

3. Summary of Results for the 2°-CDAs with AMSTAR

When the 2°-CDAs were subjected to ±15-second RTA errors, the results did not show an improvement over the 3°-CDAs with spoilers as expected and were actually worse than the 3°-CDAs without spoilers. However, in the ±60-second-RTA-error case, the spacing-error results were comparable to the 3°-CDAs-with-spoilers scenario for the same RTA-error limit. The periodic spacing-error behavior was also present in these results, although the pattern differed from that observed with the step-descent and 3°-CDA routes. Losses of separation for more than 3 seconds occurred for 10.60% and 6.68% of the aircraft when subjected to the ±15- and ±60-second-RTA-error conditions, respectively. Increasing the RTA errors actually improved the system performance when the 2°-CDA routes were flown.

The 2°-CDA routes experienced more additional speed changes on average than the 3°-CDAs with and without spoilers. The ±15-second case had a surprising result when the Bambe aircraft experienced higher numbers of additional speed changes in comparison to Fever and Howdy aircraft. This result did not persist in the ±60-second-RTA-error case. Higher RTA errors posed a greater cost to CDA fuel benefits than the smaller RTA errors did, which was a consistent result across all scenarios.

CHAPTER XI

DISCUSSION OF RESULTS

The results of Chapter VIII showed that when AMSTAR was used to precisely space aircraft flying step descents, spacing-error variability and the number of separation losses were small even when aircraft were metered at the maximum runway capacity. Chapter IX illustrated that a decreased capacity was necessary to achieve acceptable numbers of separation losses when CDA operations were subjected to metering errors and no precision spacing system was used. Results in Chapter X showed that the Gaussian initial spacing errors could be reduced to a small variability around zero when AMSTAR was used to space the aircraft flying CDAs.

The spacing-error means and standard deviations for the baseline and CDA scenarios are listed in Table XXVI, where the standard deviations are shown in parentheses. The CDA scenarios without AMSTAR are for the case where aircraft were spaced 100 seconds apart at the metering fix. The smallest spacing-error variations were seen with the step descents for both the ±15- and ±60-second-RTA-error cases. Adding the use of spoilers reduced the variation that was seen with the 3°-CDAs with AMSTAR and no spoilers.

The number of separation losses for each scenario is shown in Table XXVII, where the results of this table show the strong correlation between spacing errors and separation losses. Those scenarios with larger standard deviations also experienced a greater number of separation losses. Fewer separation losses occurred when AMSTAR was used to precisely space CDAs in comparison to when no precision spacing tool was used; however, the step descents remained the best scenario for runway capacity.

For both the ±15- and ±60-second-RTA-error cases, the 3°-CDAs with spoilers was the best approach to combining the CDA operations with the precision spacing

Table XXVI. Comparison of Spacing Errors and Standard Deviations.

Scenario	Bambe (sec)	Fever (sec)	Howdy (sec)
±15-second-RTA-Error Scenarios			
Step-Descents with AMSTAR	−1.11 (1.26)	0.82 (1.04)	0.29 (0.94)
3°-CDAs without AMSTAR	0.19 (6.60)	−0.49 (6.96)	0.22 (6.91)
3°-CDAs with AMSTAR	−0.37 (2.60)	0.24 (2.58)	0.09 (2.83)
3°-CDAs with AMSTAR and Spoilers	−0.50 (1.94)	0.42 (1.74)	0.14 (1.74)
2°-CDAs with AMSTAR	1.85 (3.14)	−2.42 (3.88)	0.92 (2.50)
±60-second-RTA-Error Scenarios			
Step-Descents with AMSTAR	−1.23 (2.01)	0.78 (1.97)	0.52 (2.10)
3°-CDAs without AMSTAR	0.64 (26.35)	−0.38 (27.60)	−0.42 (27.55)
3°-CDAs with AMSTAR	−1.30 (8.59)	0.64 (7.27)	0.67 (7.27)
3°-CDAs with AMSTAR and Spoilers	−0.50 (3.12)	0.47 (3.09)	0.31 (3.03)
2°-CDAs with AMSTAR	0.18 (3.44)	0.00 (3.46)	0.37 (3.64)

tool. Following that approach, the 3°-CDAs had the best capacity when the metering errors were limited to ±15 seconds, however for the ±60-second case, the 2°-CDAs were a significant improvement over the 3°-CDAs without spoilers. Regardless of the spacing-error variability, AMSTAR provided stable schedule deviations for all of the scenarios examined. Over the 100-aircraft scenarios that were simulated, none of the schedule deviations grew without bound.

As expected, the step descents had the best runway capacity due to the level altitude segments that permitted greater deceleration capabilities throughout most of the approach, whereas the CDA routes had decreased deceleration capability once

Table XXVII. Comparison of Separation Losses.

Scenario	**Total LoS** (%)	**LoS > 3 sec** (%)
±15-second-RTA-Error Scenarios		
Step-Descents with AMSTAR	9.80	0.13
3°-CDAs without AMSTAR	39.40	26.15
3°-CDAs with AMSTAR	16.98	6.48
3°-CDAs with AMSTAR and Spoilers	10.30	2.18
2°-CDAs with AMSTAR	20.40	10.60
±60-second-RTA-Error Scenarios		
Step-Descents with AMSTAR	19.05	2.38
3°-CDAs without AMSTAR	46.88	43.63
3°-CDAs with AMSTAR	29.58	19.50
3°-CDAs with AMSTAR and Spoilers	21.73	4.90
2°-CDAs with AMSTAR	24.90	6.68

the aircraft started to descend. The AMSTAR range-error filtering was designed for more aggressive spacing-error reduction as the trailing aircraft nears the runway threshold, and the most aggressive behavior occurs between 30 and 0 NM to the threshold. The 2°- and 3°-CDAs began their descents at 45 and 37 NM from the runway, respectively; therefore, AMSTAR was most aggressive after the aircraft had already started to descend. Further research into the AMSTAR gains and filtering, specifically for CDA routes, may show that more aggressive behavior earlier in the approach will provide reduced variability at the threshold.

The use of spoilers significantly impacted the spacing-error variability at the

runway threshold, thus reducing the number of separation losses. In the ±15-second case, only approximately 15% of the aircraft used spoilers for an average of 8.53 seconds, and in the ±60-second case, roughly 33% used spoilers for an average of 11.89 seconds. A small percentage of the 4,000 simulated aircraft actually used spoilers, yet the reduction in separation losses greater than 3 seconds was significant. These results indicate that small improvements in aircraft-pair spacing can lead to an overall improvement in system performance. A more accurate spoiler model may show further improvements.

The 2°-CDAs were expected to show smaller spacing-error variations at the runway threshold than the 3°-CDA results; however in the ±15-second-RTA-error case, the scenario with the 2°-CDAs showed the greatest number of separation losses. These results may be related to the AMSTAR range-error filtering. Aircraft flying the 2°-CDAs started their descent approximately 8 NM prior to those aircraft that were flying 3°-CDAs. Therefore, aircraft flying 3°-CDAs had additional distance to reduce spacing errors prior to the TOD, and the AMSTAR behavior was more aggressive in this distance. In the ±60-second-RTA-error case, the 2°-CDAs were a considerable improvement over the 3°-CDAs without spoilers. These results may be related to the notch filtering that is applied to the range errors; larger RTA errors led to larger errors in initial spacing, which AMSTAR handled more aggressively. In this RTA-error case, the improved deceleration capabilities of the 2°-CDA allowed for improved spacing at the threshold, and thus fewer separation losses.

When the spacing errors were averaged over 40 simulation runs, all of the scenarios exhibited cyclic behavior with a nine-aircraft period. These results indicate that both the design of the routes themselves and the metering-fix sequence have a greater affect on AMSTAR performance than the variation in RTA errors from simulation to simulation.

These nine-aircraft patterns were also observed in the plots of the additional speed changes averaged over the 40 simulations. The AMSTAR-induced speed changes are compared in Table XXVIII. In both RTA-error cases, the step descents and 2°-CDAs had larger numbers of additional speed changes than the 3°-CDAs. A large number of speed changes may be unacceptable to pilot and passenger comfort; therefore, the 3°-CDAs with AMSTAR may be more appealing to pilots. With the exception of one scenario, aircraft leaving from the Bambe metering fix consistently experienced fewer speed changes. This may be related to the length of the Bambe route, which is approximately 50 NM in comparison to the Fever and Howdy routes, which are roughly 80 and 84 NM, respectively.

Table XXVIII. Comparison of AMSTAR-Induced Speed Changes.

Scenario	**Bambe**	**Fever**	**Howdy**
±15-second-RTA-Error Scenarios			
Step-Descents with AMSTAR	3.46	4.30	3.97
3°-CDAs with AMSTAR	1.37	1.91	1.84
3°-CDAs with AMSTAR and Spoilers	1.42	2.22	2.06
2°-CDAs with AMSTAR	3.79	3.54	3.77
±60-second-RTA-Error Scenarios			
Step-Descents with AMSTAR	3.84	5.57	5.55
3°-CDAs with AMSTAR	3.00	4.01	4.22
3°-CDAs with AMSTAR and Spoilers	3.21	4.48	4.70
2°-CDAs with AMSTAR	4.07	5.06	5.57

The speed changes resulted in some significant transit-time differences, and these two metrics together affected fuel consumption. Larger RTA errors led to increased

fuel use, however the maximum fuel consumption was still less than the nominal step-descent fuel consumption for the all of the CDA simulations. The means and standard deviations, shown in parentheses, of the fuel consumption are shown in Table XXIX. In the ±15-second-RTA-error case, the variation in the step descent and 2°-CDA fuel consumption was comparable, and the 3°-CDA scenarios had smaller variations in fuel use. However, in the ±60-second-RTA-error case, the variation in the step-descent fuel consumption was greater than for any of the CDA cases.

Table XXIX. Comparison of Fuel Consumption Means and Standard Deviations.

Scenario	**Bambe (kg)**	**Fever (kg)**	**Howdy (kg)**
±15-second-RTA-Error Scenarios			
Step-Descents with AMSTAR	297.09 (1.31)	563.40 (2.62)	605.75 (1.35)
3°-CDAs with AMSTAR	266.70 (0.84)	513.49 (1.27)	550.55 (1.35)
3°-CDAs with AMSTAR and Spoilers	267.27 (0.99)	516.00 (1.80)	552.93 (1.64)
2°-CDAs with AMSTAR	225.43 (1.46)	466.65 (1.61)	501.14 (1.66)
±60-second-RTA-Error Scenarios			
Step-Descents with AMSTAR	297.41 (8.11)	564.63 (9.17)	608.24 (11.44)
3°-CDAs with AMSTAR	267.01 (2.83)	514.44 (4.26)	551.92 (4.99)
3°-CDAs with AMSTAR and Spoilers	269.42 (2.81)	518.70 (4.56)	556.27 (4.71)
2°-CDAs with AMSTAR	229.06 (4.02)	471.90 (4.07)	506.16 (4.63)

CHAPTER XII

CONCLUSIONS AND FUTURE WORK

Different approaches to combining AMSTAR, an APS tool, and CDA operations were evaluated to determine whether increased runway capacity could be achieved for CDAs. Step descents with AMSTAR were used as a baseline to determine the capacity that could be achieved using more traditional approach methods. Other baseline simulations showed that capacity is sacrificed when CDA routes are flown without the use of a precision spacing tool. The three approaches to combining APS and CDAs were: 3°-CDAs with AMSTAR, 3°-CDAs with AMSTAR and spoilers, and 2°-CDAs with AMSTAR. These baselines and research approaches were simulated in a fast-time environment, and the aircraft were subjected to ±15- and ±60-second metering errors.

The step-descent methods provided the best runway capacity as evidenced by the small variation in runway-threshold spacing errors. The decreased deceleration capabilities inherent to the CDA routes resulted in larger variability in the runway-threshold spacing. However, the approach using 3°-CDAs with AMSTAR and spoilers was able to achieve fewer separation losses than the other CDA methods. Further research into AMSTAR gains and filtering for CDA operations, may provide increased capacity over the results shown with this research.

Statistical results showed that the route design and the metering-fix sequence may affect AMSTAR performance by invoking periodic behavior, but no unstable results were observed over the 100-aircraft scenarios. AMSTAR was shown to be robust for both traditional step descents and noise- and fuel-efficient CDA methods.

The CDA routes provided a noise savings over the more traditional step-descent routes, where the 3°-CDA along the Fever route was 5,000 feet higher that the step-

descent route at a distance of 37 NM from the runway. The 3°-CDAs were approximately 9.5% more fuel efficient than the step descents, and the 2°-CDAs provided an even greater fuel savings. Although the 2°-CDAs were more fuel efficient, some noise efficiency is sacrificed with the shallower flight-path-angle routes. The use of the precision spacing system, AMSTAR, did not result in significant costs to the CDA fuel efficiency.

While further research is necessary, this research has shown that combining APS concepts and CDA operations is feasible and beneficial. Some planned and proposed future research topics are detailed below.

Proposed research includes a study to evaluate the AMSTAR filter and gain scheduling for CDA operations. Increasing the gains further from the runway threshold, where aircraft flying CDAs have more speed control, may have a significant effect on threshold-spacing-error variability. These gain changes may lead to higher numbers of speed changes, which may negatively impact pilot and airliner acceptability of the concept. Based upon these results, the approaches to combining AMSTAR and CDAs should be reevaluated.

AMSTAR-induced speed changes may negatively impact the noise benefits of CDA routes. Other proposed research will include evaluating AMSTAR's cost to the CDA noise efficiency using the FAA's Integrated Noise Model program.

Planned research includes integrating the LNG system into TMX for fast-time simulation capabilities. The integration of this system into TMX will permit real-time lateral route changes and the optimization of the vertical path for the most noise-efficient descent. Integration with AMSTAR may be impossible; therefore new APS tools may be developed and evaluated for the precision spacing of aircraft that are using the LNG system. System evaluation may include string-stability analysis.

REFERENCES

[1] U.S. Department of Transportation, Federal Aviation Administration, The MITRE Corporation, Center for Advanced Aviation System Development, "Capacity needs in the National Airspace System, an analysis of airport and metropolitan area demand and operational capacity in the future," Tech. Rep., June 2004. [Online]. Available: http://www.faa.gov/arp/publications/reports/capneedsnas.pdf

[2] M. S. Nolan, *Fundamentals of Air Traffic Control*, 3rd ed. Pacific Grove, CA: Brooks/Cole Publishing Company, 1999.

[3] J. Hull, B. Barmore, and T. Abbott, "Technology-enabled airborne spacing and merging," presented at the 23rd Digital Avionics and Systems Conference, Salt Lake City, UT, October 2004.

[4] Federal Aviation Administration, "ADS-B Home Page," January 2005, [Online]. Available: http://adsb.tc.faa.gov/ADS-B.htm.

[5] L. Credeur, "Basic analysis of terminal operation benefits resulting from reduced vortex separation minima," NASA Headquarters, Washington, D.C., Tech. Rep., October 1977, NASA TM-78624.

[6] T. S. Abbott, "Speed control law for precision terminal area in-trail self spacing," NASA Langley Research Center, Hampton, VA, Tech. Rep., July 2002, NASA/TM-2002-211742.

[7] R. M. Oseguera-Lohr, G. W. Lohr, T. S. Abbott, and T. M. Eischeid, "Evaluation of operational procedures for using a time-based airborne inter-arrival spacing

tool," presented at the AIAA Aircraft Technology, Integration, and Operations Conference, Los Angeles, CA, October 2002, AIAA-2002-5824.

[8] G. W. Lohr, R. M. Oseguera-Lohr, T. S. Abbott, and W. R. Capron, "Flight evaluation of a time-based airborne inter-arrival spacing tool," presented at the 5th USA/Europe ATM R&D Seminar, Budapest, Hungary, June 2003.

[9] B. Barmore, T. Abbott, and K. Krishnamurthy, "Airborne-managed spacing in multiple arrival streams," presented at the 24th International Congress of the Aeronautical Sciences, Yokohama, Japan, September 2004.

[10] T. S. Abbott, "Advanced Terminal Area Approach Spacing concept (ATAAS) including Airborne Merging and Spacing for Terminal Arrivals (AMSTAR)," March 2004, Unpublished NASA AATT Project document, Hampton, VA.

[11] K. Krishnamurthy, B. Barmore, F. Bussink, L. Weitz, and L. Dahlene, "Fast-time evaluations of an airborne merging and spacing concept for terminal arrival operations," to be presented at the 2005 AIAA Guidance, Navigation, and Control Conference, San Francisco, CA, August 2005 (Submitted).

[12] N. T. Ho and J.-P. Clarke, "Mitigating operational aircraft noise impact by leveraging on automation capability," presented at the 1st AIAA Aircraft Technology, Implementation, and Operations Forum, Los Angeles, CA, 2001, AIAA-2001-5239.

[13] L. Ren, J.-P. Clarke, and N. T. Ho, "Achieving low approach noise without sacrificing capacity," presented at the 22nd Digital Avionics and Systems Conference, Indianapolis, IN, October 2003.

[14] J.-P. B. Clarke, N. T. Ho, L. Ren, J. A. Brown, K. R. Elmer, K.-O. Tong, and

J. K. Wat, "Continuous descent approach: Design and flight test for Louisville International Airport," *Journal of Aircraft*, vol. 41, pp. 1054–1066, September-October 2004.

[15] A. Haraldsdottir, E. G. Schoemig, A. W. Warren, K.-O. Tong, and J. M. Crutchfield, "Analysis of arrival management performance with continuous descent trajectories using the regional traffic model," presented at the 23rd Digital Avionics and Systems Conference, Salt Lake City, UT, October 2004.

[16] D. H. Williams, R. M. Oseguera-Lohr, and E. T. Lewis, "Design and testing of a low noise flight guidance concept," NASA Langley Research Center, Hampton, VA, Tech. Rep., December 2004, NASA/TM-2004-213516.

[17] F. J. L. Bussink, N. A. Doble, B. E. Barmore, and S. Singer, "A fast-time simulation environment for airborne merging and spacing research," presented at the 23rd Digital Avionics and Systems Conference, Salt Lake City, UT, October 2004.

[18] A. Nuic, *User Manual for the Base of Aircraft Data (BADA) - Revision 3.4*, Eurocontrol Experimental Centre, Bretigny, France, June 2002. [Online]. Available: http://www.eurocontrol.fr/public/reports/eecnotes/2003/11.pdf

[19] M. T. Palmer, T. S. Abbott, and D. H. Williams, "Development of workstation-based flight management simulation capabilities within NASA Langley's flight dynamics and control division," presented at the Ninth International Symposium on Aviation Psychology, Columbus, OH, April 1997.

APPENDIX A

LIST OF ACRONYMS

Acronym	**Description**
ADS-B	Automatic Dependent Surveillance Broadcast
AMSTAR	Airborne Merging and Spacing for Terminal Arrivals
APS	Airborne Precision Spacing
ATAAS	Advanced Terminal Area Approach Spacing
ATC	Air Traffic Control
ATM	Air Traffic Management
CDA	Continuous Descent Approach
CNS	communication, navigation, and surveillance
DAG-TM	Distributed Air Ground Traffic Management
ETA	estimated time of arrival
FAA	Federal Aviation Administration
FMS	Flight Management System
ILS	Instrument Landing System
LaRC	NASA Langley Research Center
LNG	Low Noise Guidance
NASA	National Aeronautics and Space Administration
PDS	pair-dependent speed
QAT	Quiet Aircraft Technologies
RTA	required time of arrival
STAR	Standard Terminal Arrival Route
TCP	trajectory change point
TRACON	terminal radar approach control

APPENDIX B

TMX INPUT FILE EXAMPLE

This is an example of a TMX input file for the step descents with AMSTAR for the ±15-second-RTA-error case.

```
00:00:00.00>NOISE ON
00:00:00.00>RESONR 0
00:00:00.00>NAVDB JNT
00:00:00.00>DTLOOK 90
00:00:00.00>LABEL
00:00:00.00>VECTOR 1
00:00:00.00>+++++
00:00:00.00>PAN    KDFW
00:00:00.00>TRAFLOG ON
00:00:00.00>FF
00:00:00.00>RADARDT 1
00:00:00.00>DT .25

00:00:00.00>ADSB DEF MINRANGE TRANS 80
00:00:00.00>ADSB DEF MAXRANGE TRANS 90
00:00:00.00>ADSB DEF MINRANGE REC   80
00:00:00.00>ADSB DEF MAXRANGE REC   90

# AIRCRAFT SEQUENCE: 3, RTA ERROR: 0.62666 SECONDS
00:00:00.00>CRE     B757F003  ,B757 32.340261 -97.662275 45.2954 11000 280
00:00:00.00>ADDRTE  B757F003  _S_FEVER18R_ICKEL_CONVILS18R
00:00:00.00>ASAS    B757F003  ,ON
00:00:00.00>RESO    B757F003  ,OFF
00:00:00.00>DEST    B757F003  ,KDFW
00:00:00.00>LNAV    B757F003  ,ON
00:00:00.00>VNAV    B757F003  ,ON
00:00:00.00>SNAV    B757F003  ,ON
00:00:00.00>STAR    B757F003  _S_FEVER18R_ICKEL_CONVILS18R
00:00:00.00>MASS    B757F003   ,180
00:00:00.00>LABEL   B757F003  ,TOGGLE
00:00:00.00>PDS     B757F003  B757B002  100

# AIRCRAFT SEQUENCE: 4, RTA ERROR: 1.4384 SECONDS
00:00:16.00>CRE     B757H004  ,B757 32.381561 -96.449381 314.9836 11000 280
00:00:16.00>ADDRTE  B757H004  _S_HOWDY18R_ICKEL_CONVILS18R
00:00:16.00>ASAS    B757H004  ,ON
00:00:16.00>RESO    B757H004  ,OFF
00:00:16.00>DEST    B757H004  ,KDFW
```

```
00:00:16.00>LNAV    B757H004  ,ON
00:00:16.00>VNAV    B757H004  ,ON
00:00:16.00>SNAV    B757H004  ,ON
00:00:16.00>STAR    B757H004  _S_HOWDY18R_ICKEL_CONVILS18R
00:00:16.00>MASS    B757H004   ,180
00:00:16.00>LABEL   B757H004  ,TOGGLE
00:00:16.00>PDS     B757H004  B757F003  100

# AIRCRAFT SEQUENCE: 5, RTA ERROR: -5.7324 SECONDS
00:03:14.00>CRE     B757F005  ,B757 32.340261 -97.662275 45.2954 11000 280
00:03:14.00>ADDRTE  B757F005  _S_FEVER18R_ICKEL_CONVILS18R
00:03:14.00>ASAS    B757F005  ,ON
00:03:14.00>RESO    B757F005  ,OFF
00:03:14.00>DEST    B757F005  ,KDFW
00:03:14.00>LNAV    B757F005  ,ON
00:03:14.00>VNAV    B757F005  ,ON
00:03:14.00>SNAV    B757F005  ,ON
00:03:14.00>STAR    B757F005  _S_FEVER18R_ICKEL_CONVILS18R
00:03:14.00>MASS    B757F005   ,180
00:03:14.00>LABEL   B757F005  ,TOGGLE
00:03:14.00>PDS     B757F005  B757H004  100

# AIRCRAFT SEQUENCE: 1, RTA ERROR: -2.1628 SECONDS
00:03:20.00>CRE     B757B001  ,B757 33.356406 -97.679342 132.1447 11000 250
00:03:20.00>ADDRTE  B757B001  _S_BAMBE18R_ICKEL_CONVILS18R
00:03:20.00>ASAS    B757B001  ,ON
00:03:20.00>RESO    B757B001  ,OFF
00:03:20.00>DEST    B757B001  ,KDFW
00:03:20.00>LNAV    B757B001  ,ON
00:03:20.00>VNAV    B757B001  ,ON
00:03:20.00>SNAV    B757B001  ,ON
00:03:20.00>STAR    B757B001  _S_BAMBE18R_ICKEL_CONVILS18R
00:03:20.00>MASS    B757B001   ,180
00:03:20.00>LABEL   B757B001  ,TOGGLE
00:03:20.00>PDS     B757B001  ON

# AIRCRAFT SEQUENCE: 2, RTA ERROR: -8.3279 SECONDS
00:04:54.00>CRE     B757B002  ,B757 33.356406 -97.679342 132.1447 11000 250
00:04:54.00>ADDRTE  B757B002  _S_BAMBE18R_ICKEL_CONVILS18R
00:04:54.00>ASAS    B757B002  ,ON
00:04:54.00>RESO    B757B002  ,OFF
00:04:54.00>DEST    B757B002  ,KDFW
00:04:54.00>LNAV    B757B002  ,ON
00:04:54.00>VNAV    B757B002  ,ON
00:04:54.00>SNAV    B757B002  ,ON
00:04:54.00>STAR    B757B002  _S_BAMBE18R_ICKEL_CONVILS18R
00:04:54.00>MASS    B757B002   ,180
00:04:54.00>LABEL   B757B002  ,TOGGLE
00:04:54.00>PDS     B757B002  B757B001  100
```

VITA

Lesley Anne Weitz is the daughter of William and Debra Weitz of North Tonawanda, New York. Lesley graduated from the University at Buffalo with a Bachelor of Science degree in Mechanical Engineering in 2002. After working at Moog Inc. in East Aurora, NY, she entered the Aerospace Engineering department at Texas A&M University under the supervision of Dr. John E. Hurtado in 2003. Lesley has been awarded the National Science Foundation Graduate Research Fellowship, the Zonta International Amelia Earhart Fellowship, the Tau Beta Pi Fellowship, and the Texas Space Grant Consortium Fellowship. She will continue her graduate education in pursuit of a doctoral degree in the Fall of 2005.

Contact Address: Dr. John E. Hurtado; 3141 TAMU; College Station, TX 77843-3141